Essays on Quantitative Finance and Asset Pricing

Von der Mercator School of Management, Fakultät für Betriebswirtschaftslehre, der

Universität Duisburg-Essen

zur Erlangung des akademischen Grades

eines Doktors der Wirtschaftswissenschaft (Dr. rer. oec.)

genehmigte Dissertation

von

Daniel Zieling

aus

Duisburg

Referentin: Prof. Dr. Antje Mahayni

Korreferent: Prof. Dr. Rüdiger Kiesel

Tag der mündlichen Prüfung: 13.10.2015

Acknowledgments

First and foremost I would like to express my deepest gratitude to my supervisor Prof. Dr. Antje Mahayni for her support throughout the last years. I really appreciated the lovingly but scientifically intense atmosphere at her chair. Besides teaching and advising me as a co-author, she also gave me a lot of freedom to develop my own line of research.

Special thanks go to my co-authors and colleagues Dr. Sven Balder, Prof. Dr. Nicole Branger, Stefan Kaltepoth, Susanne Lucassen, Dr. Nikolaus Schweizer and Dr. Daniel Steuten. It was always inspiring and a great pleasure to work with you.

Finally, I would like to thank my family for supporting every step of my way. I am especially grateful to my wife Jenny for her deep love, patience and support.

Contents

List of Figures

List of Tables

CHAPTER 1

General introduction

Pricing, hedging and investment are arguably the three fundamental problems in quantitative finance and asset pricing. Naturally, the problems are closely connected. The present thesis consists of three chapters. Each chapter contributes to the literature dealing with aspects of the fundamental problems. Special emphasis is put on volatility and jump risk. According to the literature on empirical asset pricing we investigate the connection between market volatility and the risk premium. This connection crucially impacts the design of (near-)optimal investment strategies. Following the classical robustness definition that mother nature plays against the investor, we study robust strategies in market environments exposed to volatility and jump risk. Another interesting aspect is the joint influence of volatility and jumps on inter-temporal hedging demands. Accounting for the hedging demand, an investor protects herself against changes in the investment opportunity set. Volatility and jumps also play an important role in the literature on option pricing. The thesis contributes to the literature by introducing a pricing and hedging method for high-dimensional basket and basket spread options. The method applies to a very general class of continuous-time pricing models comprising stochastic volatility, stochastic correlation, or jump diffusion models. Methodically, the thesis contributes to the literature on econometric modeling (Chapter 2), numerical solutions of partial differential equations (Chapter 3), and Fourier analysis (Chapter 4).

Chapter 2 initiates the thesis with an empirical investigation of optimal investment strate-

gies.[1] Precisely, we use S&P 500 index return data for the time period 1985-2013 to evaluate the performance of portfolio insurance strategies. The chapter sheds light on the question if the performance of a constant proportion portfolio insurance (CPPI) strategy can be improved by means of a time-varying multiplier which depends on the estimated future volatility. Neglecting any inter-temporal hedging demand, the theoretical foundation of the strategies is given by maximizing the expected utility of an investor with hyperbolic absolute risk aversion (HARA) in a diffusion model setup. If the risk premium is assumed to be proportional to the variance, the optimal strategy is a CPPI strategy. Otherwise, the multiple is time-varying (PPI). Specifically, the optimal PPI-strategy is a stable volatility strategy if the risk premium is proportional to the square root of the local variance. In the context of portfolio insurance, stable volatility strategies link the multiple to the inverse of the local volatility. It turns out that even time-varying multiple strategies based on a rolling window of historical volatility estimates give a significant improvement of CPPI strategies. The out-performance is robust with respect to alternative performance measures and is also true for proportional transaction costs and adequate trigger trading.

Building on the empirical and theoretical insights of Chapter 2, Chapter 3 analyzes the robustness of stable volatility strategies. The chapter refers to stable volatility strategies in a slightly different way. Specifically, we refer to strategies in which the portfolio weight of the stock is inversely proportional to its local volatility.[2] These strategies are optimal for an investor with constant relative risk aversion (CRRA) if the stock follows a diffusion process, the expected excess return is proportional to its volatility, and the hedging demand is zero. We perform a simulation study to assess the performance of stable volatility strategies when these restrictive assumptions do not hold, but when the stock price is subject to jumps and when the risk premium is not proportional to volatility. We find that stable volatility strategies are indeed robust and outperform strategies that scale the portfolio weight by the variance or assume a constant portfolio weight. Furthermore, we show that (less model-dependent) myopic strategies often outperform (model-dependent) optimal strategies which account for the hedging demand.

1 The content of Chapter 2 is joint work with Antje Mahayni and Sven Balder published in the article Zieling et al. [Zie14].

2 The content of Chapter 3 is joint work with Nicole Branger and Antje Mahayni. A revised version is published in the article Branger et al. [Bra15].

Chapter 4 contributes to the literature on option pricing. The chapter introduces a new valuation method for basket options. The method can be applied to pricing and hedging problems in general semimartingale models with known joint characteristic functions. A main results is a theorem according to closed-form expressions of the Fourier transform of quadratic and piecewise linear approximations of the convex exercise boundary. A second contribution is a dimension reduction technique via (cross-)moment matching based on the characteristic function. Our method improves on a lower price bound recently introduced by Caldana et al. [Cal14], in two ways. First, moment matching allows to better approximate the unknown distribution of the arithmetic (sub-)baskets. The second improvement stems from accounting for the non-linearity of the exercise boundary. In the special case of two-asset basket or spread options, our lower price bound converges to the true price. Numerical experiments reveal that in higher dimensions the refinements significantly sharpen the lower price bound, particularly in the case of negative basket weights (basket spread options). The improvement due to moment matching comes at almost no additional cost. Accounting for non-linearity raises the dimension of the inverse Fourier transform from one to two, but the computational complexity remains quadratic in the number of assets. Therefore, the method does not suffer from the curse of dimensionality.

Finally, Chapter 5 summarizes the thesis and gives an outlook on further research.

CHAPTER 2

Performance evaluation of optimized portfolio insurance strategies

2.1 Introduction

The origin of portfolio insurance strategies dates back to Leland and Rubinstein (1976) and Brennan and Schwartz (1976). Leland and Rubinstein (1976) motivate the evolution of portfolio insurance with the observation that *'after the decline of 1973-74, many pension funds had withdrawn from the market only to miss the rally in 1975'* and their idea *'if only insurance were available, those funds could be attracted back to the market.'* Unsurprisingly, there are repeated revivals of portfolio insurance (PI) strategies observed on the institutional as well as the retail side of the asset management industry.[1] Along the lines of Grossman et al. [Gro89] and Basak [Bas02], PI strategies guarantee a minimum level of wealth (at a specified time horizon), but also participate in the potential gains of a reference portfolio. To obtain a protection mechanism, a risky portfolio (or benchmark index) can be combined with a risk-free asset and/or with a suitable financial derivative. This includes dynamic versions of option-based portfolio insurance (OBPI) strategies, stop-loss strategies, buy and hold strategies and constant proportion portfolio insurance (CPPI) strategies. In this chapter, we focus on the latter approach, the CPPI approach, but also account for proportional portfolio insurance (PPI) strategies with variable multiples. In both cases, the exposure in the risky asset is proportional to the cushion. While a CPPI strategy relies on a proportionality factor which is constant throughout the investment horizon, a variable

1 The practical implementation of the strategies benefits from progresses in the feasibility and effectiveness of dynamic portfolio insurance. Commercial feasibility is increased because of decreasing costs of trading and product innovations.

multiple strategy also allows for changes in the proportionality factor.[2]

Recently, there is a growing trend to implement a PPI trading rule where the multiplier is reduced in times of volatile markets and increased in less volatile times.[3] Our main aim is to shed light on the question if a time-varying multiple which is based on the estimated future volatility improves the risk and return profile if compared to a constant multiple. The answer depends on the assumptions which are posed on the dynamics of the underlying risky asset (or index), i.e. the true data generating process. In consequence, we rely on S&P 500 index return data for the time period 1985-2013 and conduct a performance evaluation of PI strategies with an exogenously given guarantee constraint. For the ranking of the strategies, we consider the certainty equivalent growth rate of a HARA investor as the main criterion. We also account for the expected value growth rate and common performance measures such as the Sharpe ratio, the adjusted for skewness Sharpe ratio, the Omega measure, the Sortino ratio and the upside potential ratio.

The strategies under consideration are justified by maximizing the expected utility of an investor with hyperbolic absolute risk aversion (HARA) in a diffusion model setup. Neglecting any inter-temporal hedging demand caused by deviating from log-utility or correlated asset prices and volatilities, the strategies are optimal within a class of models satisfying a specific assumption on the structure of the risk premium. From a practical point of view, a hedging demand is difficult to explain to the customer.[4] From a theoretical point of view, we omit the hedging demand because it is strongly model depending. In particular, we do not assume that the investor maximizes her expected utility in view of one specific model. Rather, she decides on the basis of a class of models satisfying a specific assumption on the risk premium structure. The certainty equivalent growth rate optimal strategies, i.e. their myopic part, are given in terms of the Merton solution, i.e. the multiple is equal to the fraction of the current excess return and the squared volatility. If the risk premium is assumed to be proportional to the variance, the optimal strategy is a constant proportion insurance (CPPI) strategy. Otherwise, the multiple is time-varying (PPI). To

2 The constant proportion portfolio insurance (CPPI) is introduced in Black et al. [Bla87]. For the basic procedure of the CPPI see also Merton [Mer71].

3 In practice, the decision if the market scenario is considered as excessive volatile is often based on a rolling window of historical volatility. In addition (or alternatively), the decision is also linked to macro economic variables.

4 We are not aware of PPI products which account for a hedging demand.

be more precise, the time-varying multiple strategies are motivated by two alternative assumptions: (A1) If the risk premium is proportional to the volatility, the optimal multiple is proportional to the inverse of the volatility. (A2) If the risk premium is constant, the optimal multiple is proportional to the inverse of the squared volatility. Expecting that for some cases (regimes, respectively) it is better to take a constant multiple and for other cases (depending on market conditions) to introduce a multiple which is a non increasing function of the volatility, we also account for strategies proportional to a power of the estimated volatility where the power itself depends on the market conditions. The optimality of the *optimized* strategies is impeded by (discrete time) jumps and other market frictions such as discrete time trading and transaction costs. We account for an additional gap control in form of upper bounds on the local multipliers. Trigger trading is used to mitigate the impacts of transaction costs.

First results are presented for the raw data, i.e. the strategies are evaluated on the daily returns of non-overlapping yearly and monthly investment horizons. The observations are in favor of the time-varying multiples where the multiplier is proportional to the inverse of the historically estimated volatility (or variance). However, in view of the high dispersion caused by leveraged strategies, it is not surprising that the results are not significant. We overcome the problem of too few path observations by introducing a simulation model. According to the intuition that the answer to the problem formulation may depend on different regimes, we select and infer a regime switching EGARCH model referred to Henry [Hen09].

Our contributions to the existing literature are as follows. We conduct an empirical comparison of *optimized* versions of proportional portfolio insurance (PPI) strategies. Along the lines of existing empirical comparison studies, we ensure the comparability of the strategies by implementing the same guarantee for all strategies. We add to the empirical literature by focusing on time-varying multipliers. To our knowledge, we are the first ones to compare the performance of constant and variable multiplier strategies which are maximizing the expected utility of a HARA investor under different model assumptions, in particular w.r.t. the risk premium. We shed light on the question if a variable multiple, motivated by deviations from the assumption that the risk premium is proportional to the squared volatility, is able to improve the risk and return profile of a constant multiple (CPPI) strategy. It turns out that our empirical findings are in favor of volatility based multiples, and are robust w.r.t. the investment horizon, the level of risk aversion of the HARA investor, and the choice of alternative performance measures.

Theoretically, the strategies can be further improved by accounting for regime switches, i.e. by strategies which are based on a power of the estimated volatility which itself depends on the market conditions. A further contribution stems from overcoming the shortcomings due to a limited number of return observations by means of a regime switching EGARCH model. We illustrate the maximal extent to which the myopic investor can benefit from the possibility to identify the regimes. In addition, the simulation model also allows to account for gap risk, and the impacts of transaction costs and trigger trading on the performance evaluation. We illustrate the potential of trigger trading rules that control for the high turnovers. In summary, we are able to justify the industry's approach to rely on a volatility based time-varying multiplier instead of the formerly predominant CPPI approach.

Related literature concerns the topics of portfolio insurance, portfolio optimization and the impacts of transaction costs. Without postulating completeness, we refer to the following literature. The properties of continuous-time CPPI strategies are e.g. studied by Bookstaber et al. [Boo00] and Black et al. [Bla92]. A comparison of OBPI and CPPI is given in Bertrand et al. [Ber02a]. The literature also deals with the effects of jump processes, stochastic volatility models and extreme value approaches on the CPPI method, cf. Bertrand and Prigent (2002b, 2003). Simulation and empirical studies which compare option based, zero plus underlying and constant proportion portfolio insurance (CPPI) strategies include the works of Cesari et al. [Ces03] and Do et al. [Do04]. Recent comparison studies by means of stochastic dominance criteria are Annaert et al. [Ann09] and Zagst et al. [Zag11]. Prospect theory is used in Dierkes et al. [Die10] and Dichtl et al. [Dic10]. Bertrand et al. [Ber11] rely on downside risk measures, in particular the Omega performance measure, to compare portfolio insurance strategies. Balder et al. [Bal12] point out some pitfalls of time invariant (TIPP) strategies immanent in index products and individual (iCPPI) strategies which are caused by horizon effects. An analysis of gap risk, i.e. the risk that the guarantee is violated, is provided in Cont et al. [Con09] and Balder et al. [Bal09]. Cont et al. [Con09] introduce the gap risk by considering jump-diffusion models. Balder et al. [Bal09] introduce the gap risk by adding trading restrictions such that the analysis also captures the effects of transaction costs. Accounting for gap risk can also motivate variable multiple strategies. Thus, our work is also linked to the literature focusing on additional constraints such as VaR and ES constraints, cf. Herold et al. [Her05], Hamidi et al. [Ham09a; Ham09b], Jiang et al. [Jia09], Ben Ameur et al. [BA11] and Ho et al. [Ho11]. In the context of portfolio insurance strategies, trigger trading is already suggested in Black et al. [Bla92] and Boulier et al. [Bou95]. Here,

the portfolio is rebalanced when the price of the risky asset exceeds an upper or lower return, i.e. the strategy is a buy and hold strategy as long as the asset price increment is not too extreme in terms of the trading filter. More recent literature poses the trigger on the implicit multiplier (or implicit exposure, respectively) of the CPPI, cf. Paulot et al. [Pau09], Hamidi et al. [Ham09a], MKaouar et al. [MKa07], Jessen [Jes09] and Khuman et al. [Khu09]. Concerning the literature on portfolio planning, references include Merton [Mer71] who solves the portfolio planning problem for a HARA investor with inter-temporal consumption. Amongst others, Kim et al. [Kim96] and Barberis [Bar00] consider optimal portfolios when the stock returns are predictable. Stochastic volatility and jumps are, for example, considered in Liu et al. [Liu03a], Branger et al. [Bra08] and Muck [Muc10]. Basak [Bas02] shows that adding a subsistence level to the problem leads to portfolio insurance strategies. Grossman et al. [Gro93] show that the time invariant portfolio insurance (TIPP) strategy is the optimal investment policy under drawdown constraints.

The outline of the chapter is as follows. Section 2 reviews some theoretical optimization results and defines benchmark assumptions on the risk premium. Along the ways, we introduce a regime switching model/strategy where the regimes correspond to the benchmark assumptions on the risk premium. In Section 3, we describe the data and discuss some rather descriptive results concerning the evaluation of constant proportion portfolio insurance strategies and the time-varying multiple strategies proportional to the inverse of the historically estimated volatility and variance, respectively. To overcome the shortcomings of the limited number of return observations, we select and infer a simulation model in Section 4. Using simulated paths, we evaluate and rank various CPPI and PPI strategies in Section 5. In particular, we also allow for switching strategies. In addition, we account for gap risk and transaction costs. Besides daily trading, we implement a trading filter which mitigates the negative effects caused by the transaction costs. Section 6 concludes the chapter.

2.2 Basic optimization results and strategies under consideration

The following section gives the foundations of our research question whether, when, and to what extent it is possible to improve CPPI strategies by means of dynamic (but simple) PPI strategies. In the first instance we recall the associated optimization problems which justify the strategies as optimal. Then, we account for deviations from these model assumptions and market frictions such as discrete time trading and transaction costs which impede the

optimality of the strategies. Along the ways, we discuss why it is important to concentrate on tractable and simple to implement strategies in favor of more sophisticated but strongly model dependent strategies.

2.2.1 The investment problem

Throughout the following, optimality is defined in terms of an investor with hyperbolic absolute risk aversion (HARA). The investor maximizes her (expected) utility u^{HARA} of terminal wealth where

$$u^{\text{HARA}}(x) = \begin{cases} \frac{(x-G)^{1-\gamma}}{1-\gamma} & \text{for } \gamma > 0 \text{ and } \gamma \neq 1 \\ \ln(x-G) & \text{for } \gamma = 1. \end{cases} \tag{2.1}$$

The guarantee G ($G \geq 0$) defines her subsistence level. A terminal wealth below the guarantee G is prohibitive. In addition to G, the risk aversion depends on γ. For $G = 0$, the level of relative risk aversion is equal to γ, i.e. utility functions with constant relative risk aversion (CRRA) also belong to the class of HARA utility functions. However, we consider portfolio insurers, i.e. we assume $G > 0$. The relative risk aversion is $\gamma x(x-G)^{-1}$. It is decreasing in wealth and converges to γ, i.e. $\lim_{x\to\infty} \gamma x(x-G)^{-1} = \gamma$. For $x > G$ it is larger than γ, i.e. holds $\gamma x(x-G)^{-1} > \gamma$. Ceteris paribus, the relative risk aversion is the higher the higher the guarantee G is.[5] There are two investment possibilities: a risky asset S and a (locally) risk-free money market account. For reasons of clarity and comprehensibility we restrict the discussion on excess returns such that the risk-free rate is zero. If not mentioned otherwise, all stochastic processes under consideration are continuous time semi-martingales defined on a stochastic basis $(\Omega,\mathcal{F},(\mathcal{F}_t)_{t\in[0,T^*]},P)$ which satisfies the usual hypotheses. A continuous-time investment strategy or saving plan for the interval $[0,T]$ can be represented by a predictable process $\left(\phi_t^{(S)},\phi_t^{(B)}\right)_{t\in[0,T]}$ such that $\phi^{(S)}$ is an admissible integrand for S and $\phi^{(B)}$ is an admissible integrand for all $t \in [0,T]$. At t, $\phi_t^{(S)}$ denotes the number which is invested in the risky asset S and $\phi_t^{(B)}$ denotes the amount which is put into the money market account. The corresponding value process is denoted

5 For a CRRA investor ($G = 0$), empirical research supports a level of risk aversion larger than one, i.e. $\gamma > 1$. Recently, Chiappori et al. [Chi11] use panel data to analyze how individuals' portfolio allocation between risky and riskless assets varies in response to changes in total financial wealth. Their result supports the CRRA assumption. In particular, the authors estimate a median level of risk aversion of $\gamma = 1.7$. For $G > 0$, it is difficult to give empirical support for the HARA assumption. However, assuming that the subsistence level G is exogenously given may well imply a rather low γ (e.g. $\gamma = 1$), i.e. if G is rather high compared to the initial investment, the drift and the time horizon under consideration.

by $(V_t)_{t\in[0,T]}$, i.e.

$$V_t = \phi_t^{(S)} S_t + \phi_t^{(B)}.$$

The strategy is self-financing if, after an initial investment $V_0 = v_0$, there are no further in- or outflows of funds, i.e.

$$dV_t = \phi_t^{(S)}\, dS_t + \phi_t^{(B)} dt \text{ where } V_0 = v_0.$$

The investor now seeks to optimize her expected utility over all self-financing strategies starting with her initial wealth v_0 and the terminal restriction posed by $V_T \geq G$ a.s.. Alternatively to the number of shares, the (self–financing) strategies can be stated in terms of the fraction $\tilde{m}_t$ of wealth invested in the risky asset S while the remaining portfolio fraction is left for the risk-free investment. In particular, $\tilde{m}_t = \frac{E_t}{V_t}$, where $E_t = \phi_t^{(S)} S_t$ denotes the time t asset exposure. An investment rule which states the asset exposure E_t proportionally to the portfolio value V_t is called a proportional strategy. The proportionality factor $\tilde{m}_t$ is called multiplier. A constant proportional strategy is implied by a constant multiplier $\tilde{m}_t = \tilde{m}$, for all $t \in [0,T]$. If there are no further restrictions than the usual integrability and predictability conditions, the class of proportional strategies is equal to the set of admissible strategies. If $\tilde{m}_t > 1$ (for all $t \in [0,T]$), the trading rule prescribes a reduction (increase) of the risky exposure in the case of downward (upward) moving markets. This is also called momentum strategy. The postulation of a subsistence level G ($G < V_0$) implies that the optimal strategy is a (proportional) portfolio insurance (PPI) strategy. Here, the proportionality factor m_t is applied to the difference of the portfolio value V_t and the floor (guarantee, respectively) G, i.e.[6]

$$E_t = m_t \times (V_t - G) = m_t \times C_t$$

where $C_t := V_t - G$ denotes the cushion at time t. The (initial) guarantee is given by a fraction $\alpha \in [0,1[$ of the initial portfolio value, i.e. $G = \alpha V_0$, ensuring $C_0 > 0$. In the following, it is convenient to represent the expected utility maximization problem in terms of the proportionality factor m, i.e.

6 A practical advantage of the CPPI (a constant multiplier m) or a simple rule based multiplier is the simplicity of the strategy. In this case, the PPI method is less demanding than synthesizing an option payoff, i.e. the dynamic version of option based portfolio protection (OBPI). More importantly, the PPI method can, theoretically, be applied to an arbitrary (in particular, an infinite) investment horizon T.

$$\begin{aligned} &\max_m \; E\left[u^{\mathrm{HARA}}(V_T)\right] \text{ s.t. } V_T \geq G \\ =&\max_m \; E\left[u^{\mathrm{CRRA}}(C_T)\right] \end{aligned} \tag{2.2}$$

where $(m_t)_{0\leq t\leq T}$ is restricted by the set of predictable and square integrable processes. u^{CRRA} denotes the CRRA utility function which is defined by u^{HARA} in combination with $G = 0$, cf. Equation (2.1). In particular, the maximization problem of the HARA investor is represented by the maximization problem of a CRRA investor who measures her utility in terms of the cushion C instead of the value V. Alternatively, the optimization problem can be stated in terms of the certainty equivalent (CE) growth rate comprising the same information as the expected utility. Since the CE growth rate is more convenient to interpret, the empirical evaluation results are stated in CE terms. The CE growth rate y^{CE} is defined by

$$\begin{aligned} u^{\mathrm{HARA}}\left(V_0 e^{y^{\mathrm{CE}}T}\right) = E\left[u^{\mathrm{HARA}}(V_T)\right] \Leftrightarrow \;\; u^{\mathrm{CRRA}}\left(C_0 e^{y^{\mathrm{CE}}T}\right) = E\left[u^{\mathrm{CRRA}}(C_T)\right], \\ \text{i.e. } y^{\mathrm{CE}} = \begin{cases} \frac{1}{T}\ln\left(E\left[\left(\frac{C_T}{C_0}\right)^{1-\gamma}\right]^{\frac{1}{1-\gamma}}\right) & \text{for } \gamma > 0 \text{ and } \gamma \neq 1 \\ \frac{1}{T}E\left[\ln\frac{C_T}{C_0}\right] & \text{for } \gamma = 1. \end{cases} \end{aligned} \tag{2.3}$$

2.2.2 Model dependent optimal investment policies

The solution of the optimization problem (2.2) is well known in a Black and Scholes model setup where the price dynamics of the risky asset are given by a geometric Brownian motion with constant drift μ (equity risk premium λ, respectively) and constant volatility σ, and which does not account for market frictions such as trading restrictions and transaction costs. Under the assumption of independent and identically distributed asset price increments it is straightforward to show that the optimal multiplier is given by $m^* = \lambda/(\gamma\sigma^2)$.[7] Obviously, the empirical data is not consistent with the assumption of the Black and Scholes model.

7 The above result is well known. Amongst other results, Merton [Mer71] showed that the optimal fraction of wealth m^* which is invested in the risky asset for a CRRA investor described by a utility function of the form $u(x) = \frac{x^{1-\gamma}}{1-\gamma}$ for $\gamma > 0$ and $\gamma \neq 1$, and $u(x) = \ln x$ for $\gamma = 1$, is given by $m^* = \frac{\lambda}{\gamma\sigma^2}$. The optimality of a CPPI with multiplier $m = \frac{\lambda}{\gamma\sigma^2}$ associated with the introduction of a subsistence level G into the utility function, i.e. a more general HARA utility function, is for example considered in Basak [Bas02].

Assume for now that the risky asset dynamics S are described by a diffusion setup for the risky asset and a diffusion setup for its volatility, i.e.

$$dS_t = S_t(\lambda_t\,dt + \sigma_t\,dW_t^S) \tag{2.4}$$

$$d\sigma_t = \alpha_t\,dt + \beta_t\,dW_t^\sigma \tag{2.5}$$

where $(W_t^S)_{0\le t\le T}$ and $(W_t^\sigma)_{0\le t\le T}$ each denote a one dimensional standard Brownian motion and λ_t denotes the (possibly stochastic) equity risk premium. It is assumed that all coefficients of the above SDEs are progressively measurable with respect to the filtration $(\mathcal{F}_t)_{0\le t\le T}$. Furthermore, the two Brownian motions may be correlated. For the sake of simplicity, we assume a constant correlation denoted by ρ, i.e. the quadratic variation at t ($t \in [0,T]$) is given by $[W^S,W^\sigma]_t = \rho t$.

For predictable and square integrable processes $(m_t)_{0\le t\le T}$, the cushion dynamics is given by

$$dC_t = C_t m_t \frac{dS_t}{S_t} = C_t\left(m_t\lambda_t\,dt + m_t\sigma_t\,dW_t^S\right).$$

In particular, it holds

$$\begin{aligned} u^{\text{CRRA}}(C_T) &= u^{\text{CRRA}}\left(C_0 e^{\int_0^T \left(m_u\lambda_u - \frac{1}{2}(m_u\sigma_u)^2\right)du + \int_0^T m_u\sigma_u\,dW_u^S}\right) \\ &= \begin{cases} \frac{1}{1-\gamma} C_0^{1-\gamma} e^{\int_0^T (1-\gamma)\left(m_u\lambda_u - \frac{1}{2}(m_u\sigma_u)^2\right)du + \int_0^T (1-\gamma)m_u\sigma_u\,dW_u^S} & \text{for } \gamma > 1 \\ \ln C_0 + \int_0^T \left(m_u\lambda_u - \frac{1}{2}(m_u\sigma_u)^2\right)du + \int_0^T m_u\sigma_u\,dW_u^S & \text{for } \gamma = 1. \end{cases} \end{aligned}$$

It is well known that the strategy for an expected-utility-maximizing investor is myopic for $\gamma = 1$ or for all $\gamma \ge 1$ in combination with $\rho = 0$.[8] The myopic investor maximizes her expected incremental utility $E[d\,u(C_t)]$. Using Itô's Lemma it is straightforward to show

$$\begin{aligned} E[d\,u(C_t)|\mathcal{F}_t] &= E\left[\frac{\partial u(C_t)}{\partial C_t}\,dC_t + \frac{1}{2}\frac{\partial^2 u(C_t)}{\partial C_t^2}\,d[C]_t\middle|\mathcal{F}_t\right] \\ &= C_t^{\gamma-1}\left(m_t\lambda_t dt - \frac{1}{2}\gamma m_t^2\sigma_t^2\right)dt. \end{aligned}$$

The first-order condition immediately implies that the optimal (myopic) multiplier $m_t^{*,\text{SV}}$ is

8 Cf. for example Merton [Mer73]. An optimal portfolio strategy is called myopic if the optimal decisions of a long-term investor and an otherwise identical short-term investor coincide. For a detailed discussion of myopic portfolio choices we refer to Campbell et al. [Cam02].

given by

$$m_t^{*,\mathrm{SV}} = \frac{\lambda_t}{\gamma\sigma_t^2} \quad \text{for all } t \in [0,T]. \tag{2.6}$$

In particular, the integrability conditions are satisfied if $\int_0^T |\lambda_t m_t^{*,\mathrm{SV}}| + (\sigma_t m_t^{*,\mathrm{SV}})^2 dt < \infty$, which corresponds to $\int_0^T \left(\frac{\lambda_t}{\sigma_t}\right)^2 dt$.[9]

In general, there is an inter-temporal hedging demand for non-logarithmic utility ($\gamma \neq 1$), i.e. if $\rho \neq 0$. In particular, a time depending hedging demand immediately implies that a time-varying multiplier is able to improve the performance of a constant multiple. However, the strategies under consideration only account for an optimized myopic part, i.e. we neglect the strongly model dependent hedging demand. We do not assume that the investor maximizes her expected utility in view of one specific model – based on an accurate specification of the volatility and correlation processes – but rather for a whole class of models.[10] To be more precise, we consider the question whether a time-varying multiple (myopic demand, respectively) is able to improve the results of a constant multiple immanent in a CPPI strategy. Neglecting any hedging demand, the answer only depends on the assumption on the link between the local risk premium λ_t of the risky asset and the local volatility σ_t. For example, the theoretical literature about portfolio planning often relies on the assumption that the risk premium is proportional to the variance, i.e.

$$\text{(A0)} \quad \lambda_t = \bar{\lambda}\sigma_t^2.$$

In particular, (A0) implies that the Sharpe ratio is increasing in the volatility. Alternative assumptions are that the risk premium is proportional to the volatility (A1) or is constant (A2), i.e.

$$\text{(A1)} \quad \lambda_t = \bar{\lambda}\sigma_t, \quad \text{(A2)} \quad \lambda_t = \bar{\lambda}.$$

In consequence, we obtain the following implications for the performance evaluation of

9 The above condition is usually satisfied for standard financial markets as defined by Karatzas et al. [Kar99]. For the empirical comparison study, the PPI strategies are based on the realized variance. Along the lines of Schied [Sch13], such strategies are also well-defined if the above condition is not met.

10 For a similar reasoning we also refer to Diris et al. [Dir14].

variable multiple strategies: PPI strategies can not outperform the optimal constant multiple under the assumption (A0). However, they can outperform the CPPI if either the Sharpe ratio is constant (A1) or if the risk premium is constant (A2). Since the answer may also depend on different regimes, we account for the possibility that there are (depending on the market conditions) regimes which may correspond to the above assumptions posed on the risk premium. Theoretically, this can be modeled by a finite state Markov chain $(X_t)_{0\leq t\leq T}$ (adapted to the information structure) with state space $\{1,\dots,N\}$. For $c = (c_1,\dots c_N)'$ and $\alpha = (\alpha_1,\dots \alpha_N)'$, we set

$$\lambda_t = c_{X_t}\sigma_t^{\alpha_{X_t}}.$$

For $N = 3$, $c = (c_1,c_2,c_3)'$, and $\alpha = (\alpha_1,\alpha_2,\alpha_3)' = (2,1,0)'$, the regimes are consistent with the three assumptions on the risk premium. In particular, regime 1 corresponds to the assumption (A0), regime 2 to (A1), and regime 3 to (A2). However, different values of α or other specifications of λ_t are able to capture more general regimes as well. If the Markov chain is observable it is straightforward to show that the myopic part of the multiplier satisfies

$$m_t^{*,\text{switch}} = c_{X_t}\sigma_t^{\alpha_{X_t}-2}. \tag{2.7}$$

2.2.3 Introduction of gap risk and gap risk control

The risk that the guarantee is not achieved by a dynamic portfolio insurance strategy is called gap risk. In contrast to the above theoretical model setup, gap risk is introduced by accounting for (discrete time) jumps in the asset price. Intuitively, it is clear that gap risk is linked to the inadequacy to omit the risky positions *fast enough* in downward moving markets. A formal proof that there are no other sources for gap risk apart from jumps in asset prices or discrete rebalancing is given in Schied [Sch13].

Obviously, the introduction of gap risk impedes the optimality of the above strategies.[11] Similar to the reasoning as with regard to the inter-temporal hedging demand caused by deviations from $\gamma = 1$ in combination with a non zero asset and volatility correlation, we view it beyond the scope of the investor to accurately specify a jump-diffusion process

11 Notice that jumps thus impede the concept of dynamic portfolio insurance. Accounting for a positive jump probability (without restrictions on the downside jump sizes and multipliers) introduces gap risk such that a dynamic PPI strategy is not optimal.

for the asset dynamics. In view of model risk and practical applications under market frictions, it is thus interesting to analyze if one of the above simple and tractable to implement strategies is preferred by the investor. Nevertheless, it important to account for a meaningful gap control and an adequate trigger design. We start with the gap risk and discuss the implications of transaction costs afterwards.

A first insight on the impact of gap risk can be obtained by considering the sensitivities of the strategies to the introduction of a gap risk control. Since the strategies are implemented in discrete time, we represent the gap event in a discrete time setup. At the same time this allows to account for (real) jumps, i.e. jumps which are not exclusively introduced by trading restrictions in form of discrete time trading. Therefore, let τ^n denote a sequence of equidistant refinements of the interval [0,T], i.e. $\tau^n = \left\{t_0^n = 0 < t_1^n < \cdots < t_{n-1}^n < t_n^n = T\right\}$, where $t_{k+1}^n - t_k^n = \frac{T}{n}$ for $k = 0, \cdots, n-1$. To simplify the notation, we drop the superscript n and denote the set of trading dates with τ instead of τ^n. The restriction that trading is only possible immediately after $t_k \in \tau$ implies that the number of shares held in the risky asset is constant on the intervals $]t_k,t_{k+1}]$ for $k = 0, \ldots, n-1$. However, the fractions of wealth which are invested in the assets change as assets prices fluctuate. Thus, it is necessary to consider the number of shares held in the risky asset $\phi^{(S)}$ and the number of bonds (position in the money account, respectively) $\phi^{(B)}$. Along the lines of Balder et al. [Bal09], we call a strategy $\phi^\tau = \left(\phi^{(S),\tau},\phi^{(B),\tau}\right)$ discrete-time PPI if for $t \in]t_k,t_{k+1}]$ and $k = 0, \ldots, n-1$

$$\phi_t^{(S),\tau} := \max\left\{\frac{m_{t_k} C_{t_k}^\tau}{S_{t_k}},0\right\}, \ \phi_t^{(B),\tau} := V_{t_k}^\tau - \eta_t^\tau S_{t_k}.$$

It is straightforward to show that the cushion dynamics are given by

$$C_{t_{k+1}}^\tau = C_{t_0}^\tau \prod_{i=1}^{\min\{\nu,k+1\}} \left(m_{t_{i-1}} \frac{S_{t_i}}{S_{t_{i-1}}} - (m_{t_{i-1}} - 1)\right),$$

where $\nu := \min\left\{t_k \in \tau | V_{t_k}^\tau(\alpha) - G \leq 0\right\}$, and $\nu = \infty$ if the minimum is not attained. Consistent with the perception of a myopic decision rule, we consider a local quantile

guarantee condition posed by[12]

$$P_{t_k}\left(C_{t_{k+1}} > 0 \middle| C_{t_k} > 0\right) \geq 1 - \varepsilon,$$

where ε denotes some exogenously specified upper bound on the local shortfall probability. Together with the observation that

$$P_{t_k}\left(C_{t_{k+1}} > 0 \middle| C_{t_k} > 0\right) = P_{t_k}\left(m_{t_k}\frac{S_{t_{k+1}}}{S_{t_k}} - (m_{t_k} - 1), > 0\right)$$

this implies an upper bound $\overline{m}_{t_k}$ on the admissible multiplier, i.e. a gap control affords to limit the multiplier at t_k by $\overline{m}_{t_k}$. Let $\tilde{F}_{t_k}$ denote the marginal distribution function of the standardized simple return $\frac{S_{t_{k+1}}}{S_{t_k}} - 1$. The upper bound is given by

$$\overline{m}_{t_k} = \left| E_{t_k}\left[\frac{S_{t_{k+1}}}{S_{t_k}}\right] - 1 + \sqrt{\mathrm{Var}_{t_k}\left[\frac{S_{t_{k+1}}}{S_{t_k}}\right]}\,\tilde{F}_{t_k}^{-1}(\alpha)\right|^{-1}.$$

For example, the above condition is used in Hamidi et al. [Ham14] who estimate the conditional (upper) multiplier by means of Dynamic AutoRegressive Expectile (DARE) models. In view of the *optimized* multiples, it is worth to emphasize that the upper limit implied by $\overline{m}_{t_k}$ is less binding for strategies which already reduce the multiple in times of higher volatility.

Finally, we comment on a further challenge on the implementation of CPPI and dynamic PPI strategies, i.e. transactions costs. Notice that because of the guarantee constraint, it is not possible to change the risk-free position of the PPI method (which is needed without transaction costs). Rather, the transaction costs are to be financed by a reduction of the asset exposure arising in the case without transaction costs.[13] Along the lines of Balder et al. [Bal09], the discrete time cushion process under proportional transaction costs with proportionality factor θ is given by

$$C_{t_k+} = C_{t_k} - \theta\left|m_{t_k}C_{t_k+} - m_{t_{k-1}}C_{(t_{k-1})+}\frac{S_{t_k}}{S_{t_{k-1}}}\right|, \tag{2.8}$$

12 Obviously, there are other meaningful criterions to control the gap risk, e.g. to control the expected shortfall as well as the global gap probability. However, besides contradicting the idea of a myopic investor this is beyond the scope of the present work.

13 Black et al. [Bla92] assume that rebalancing occurs *net of transaction costs*, too.

i.e. $m_{t_k} C_{t_k+}$ denotes the asset exposure immediately after a transaction cost adjustment. Obviously, accounting for transaction costs implies a further reduction of the upper bound on an admissible multiplier with regard to gap risk, cf. Balder et al. [Bal09]. From a practical point of view, the above reasoning emphasizes the importance to consider simple and rule based strategies which can be tractably adjusted to account for gap risk and transaction costs, i.e. to determine an adequate trading filter.

2.3 Performance evaluation

We consider a data set containing index return data of the S&P 500 (composite index) for the past 28 years and about 5 month. The data is provided by Thomson Reuters for the time period 2 January 1985 - 7 June 2013. The composite index is net of dividends. The loss of dividends is interpreted as the management fee for the PPI products.[14] The data contains daily simple returns. The number of observations is 7,418. This resembles approximatively 260 trading days per year. The daily simple return is denoted by r_t^S, i.e. $r_t^S = \frac{S_t}{S_{t-1}} - 1$. As a proxy for the (locally) risk-free rates, we use discount yields of T-Bills with 91 days to maturity. In particular, interest rate data congruent to the S&P 500 returns is used for the discounting. The whole analysis is then conducted w.r.t. the simple excess returns. To be more precise, let r_t^f denote the risk–free daily interest rate. The excess

Summary and test statistics of daily (yearly) excess returns

Mean excess return	0.000229	(0.061206)	
Standard deviation	0.011508	(0.185557)	
Skewness	-0.841247		
Kurtosis	24.962414		
Minimum	-0.204590		
Maximum	0.115778		
	t-statistic	critical value	p-value
Skewness	-29.5835	-3.2905	0.0000
Kurtosis	386.2201	3.2905	0.0000
Normality (Jarque-Bera)	149,940	14.6257	0.0000

Table 2.1: Summary statistics of the whole data set containing 7,418 observations. If convenient, the corresponding yearly values are included in brackets. In particular, $\overline{\lambda}_{\text{annual}} = (1+\overline{\lambda_{\text{daily}}})^{260}-1$ and $\sigma_{\text{annual}} = \sigma_{\text{daily}}\sqrt{260}$. Critical values are reported for $\alpha = 0.1\%$.

14 This assumption is e.g. also posed in Bertrand et al. [Ber11].

return is then given by $R_t = r_t^S - r_t^f$. A summary and test statistics accounting of the whole time period is provided in Table 2.1. The mean daily excess return is $\hat{\lambda} = 0.000229$ or about 0.0612 per year. The skewness is negative and significant. There is also significant excess kurtosis, i.e. extremes tend to be more pronounced than for a normally distributed random variable. A Jarque-Bera test confirms the departure from a normal distribution.

To get some first intuition about the performance of *optimized* CPPI and time-varying strategies, we consider a first set of benchmark strategies. The initial investment is $V_0 = 100$ and the guarantee is $G = 90$. The investment horizon is $T = 1$ ($T = \frac{1}{2}$, respectively). Recall that the guarantee also defines the subsistence level of the utility function u^{HARA}, cf. Equation (2.1). The investor can be assessed as highly risk averse because of the rather high guarantee such that a realistic choice of γ implies a rather low γ. If not mentioned otherwise, we use $\gamma = 1$. Since this resembles a log-utility measured on the cushion there is no inter-temporal hedging demand. Comparing the outcomes of PPI strategies which are solely based on a myopic component has the advantage that there are no distortion effects (utility losses, respectively) due to an inter-temporal hedging demand. However, since log-utility implies a very specific attitude towards risk we consider the impact of deviations from $\gamma = 1$ in the subsequent simulation study. For now, we evaluate the growth rates of some representative strategies for non-overlapping investment horizons. As a proxy for the optimal constant multiplier consistent with assumption (A0), we rely on the long term estimates for the risk premium $\hat{\lambda}$ and the volatility $\hat{\sigma}$, i.e.

$$m^{*,\text{const}} = \frac{\hat{\lambda}}{\hat{\sigma}^2} = \frac{0.000229}{0.011508^2} = 1.7256.$$

As additional benchmark strategies we also include a CPPI strategy with $m = 1$ (static portfolio insurance), $m = 4$ and $m = 6$. Motivated by the (alternative) assumptions (A1) and (A2), we also include strategies which are proportional to the inverse of a historically

Mean yearly growth rates of selected PPI strategies

Panel A: Investment horizon $T = 1$ year

	$\frac{1}{T}E[\ln \frac{C_T}{C_0}]$	$\frac{1}{T}E[\ln \frac{V_T}{V_0}]$	$E[V_T]$	min V_T	SR	$ASSR$	$\Omega - 1$	SoR	UPR
$m_{t,(\mathrm{A1})}$	0.075	0.014	101.496	95.454	0.332	0.391	1.710	0.876	1.389
	0.362	*0.043*	*4.502*						
$m_{t,(\mathrm{A2})}$	0.077	0.038	105.695	93.787	0.221	0.289	3.628	2.146	2.737
	0.700	*0.166*	*25.723*						
$m = 1$	0.032	0.004	100.457	96.313	0.290	0.268	1.062	0.461	0.896
	0.165	*0.016*	*1.574*						
$m^{*,\mathrm{const}}$	0.034	0.007	100.745	94.066	0.274	0.259	0.966	0.446	0.908
	0.299	*0.027*	*2.715*						
$m = 4$	-0.100	0.012	101.413	90.553	0.230	0.232	0.771	0.410	0.942
	0.839	*0.061*	*6.145*						
$m = 6$	(-0.278)	0.013	101.683	87.622	0.183	0.193	0.641	0.364	0.931
	1.401	*0.088*	*9.176*	**1**					

Panel B: Short investment horizon $T = 1/12$ year

$m_{t,(\mathrm{A1})}$	0.076	0.013	100.112	96.118	0.114	0.114	0.332	0.175	0.701
	0.344	*0.034*	*0.984*						
$m_{t,(\mathrm{A2})}$	0.085	0.026	100.230	94.698	0.126	0.130	0.425	0.221	0.742
	0.616	*0.063*	*1.834*						
$m = 1$	0.030	0.004	100.038	97.213	0.076	0.074	0.234	0.104	0.551
	0.176	*0.017*	*0.495*						
$m^{*,\mathrm{const}}$	0.031	0.007	100.064	95.377	0.075	0.074	0.230	0.105	0.560
	0.311	*0.030*	*0.852*						
$m = 4$	-0.098	0.015	100.148	91.045	0.075	0.076	0.229	0.111	0.595
	0.818	*0.068*	*1.955*						
$m = 6$	(-0.220)	0.022	100.226	89.074	0.075	0.079	0.235	0.120	0.630
	1.108	*0.100*	*2.907*	**1**					

Table 2.2: Mean performance *(and standard deviations)* for selected strategies over the past 28 years. For Panel A and B the investment horizon is $T = 1$ and $T = \frac{1}{12}$ year, respectively. The initial portfolio value is given by $V_0 = 100$. The initial guarantee is $G = 90$. The investment quote is bounded to a maximum of 200% of the current portfolio value V_t. The optimal constant multiplier is $m^{*,\mathrm{const}} = 1.7256$. The expected growth rates presented in the first column for the strategy $m = 6$ are given in brackets. This strategy failed to ensure the guarantee of 90 (also compare the 'min V_T' column). In this case the cushion is negative and the expected cushion growth rate is equal to $-\infty$. Since this result is less informative, the quantity in parentheses reports the expected cushion growth rate if the negative cushion years (month) are simply excluded. However, they cannot be compared to the other growth rates because of the introduced bias. The boldface number in the second line of the min V_T column counts the number of floor violations.

estimated volatility (variance).[15] According to the assumptions posed on the risk premium,

15 For the variable multiplier strategy m_t, we implement different methods for estimating the local volatility σ_t. Our main focus is on a non-parametric approach. We rely on historical volatility estimates $\hat{\sigma}_t = \sigma_{t,x\mathrm{M}}$, where $x \in \{1,2\}$ denotes the number of months of the estimation window. For example, $\sigma_{t,1\mathrm{M}}$ is calculated using a window of the latest 21 daily excess returns observed at days $(t, t-1,...,t-20)$. The results are only reported for the better performing strategies which are based on a one month window. It is worth mentioning that a further meaningful set of strategies can be based on implicit volatilities derived from observed option prices. Implicit volatilities are often considered as more informative. We omit such strategies because of the following reason. Unsurprisingly, the performance results obtained for the limited ob number of observations do not allow for a significant comparison. In a next step, we thus infer a simulation model, a regime switching EGARCH model, for the excess returns under the *real world* probability measure. A consistent modelling of the risk neutral dynamics is beyond the scope of this thesis.

we denote these strategies with $m_{t,A1}$ and $m_{t,A2}$ where

$$m_{t,A1} = \frac{\hat{\lambda}}{\hat{\sigma}} \frac{1}{\sigma_{t,1\mathrm{M}}}, \tag{2.9}$$

$$m_{t,A2} = \hat{\lambda} \frac{1}{\sigma^2_{t,1\mathrm{M}}}. \tag{2.10}$$

$\sigma_{t,1\mathrm{M}}$ is the volatility estimate calculated using a window of the latest 21 daily excess returns observed at days $(t, t-1,...,t-20)$. Theoretically, a PPI strategy may imply that the asset exposure is financed by an unlimited position in the risk-free asset. In contrast, traded PPI products include a cap on the investment fractions. Therefore, we focus on strategies with a capped investment fraction.[16]

The descriptive statistics w.r.t. yearly and monthly investment horizons are summarized in Table 2.2. All observations are based on non-overlapping investment periods such that the number of observations is 28 (28×12 plus 5 month in 2013) in the case of a yearly (monthly) investment horizon. In addition to the average cushion growth rates (certainty equivalent growth rates, respectively), Table 2.2 summarizes the average rate of return, the average payoff, the Sharpe ratio SR (cf. Sharpe [Sha66]), the adjusted for skewness Sharpe ratio $ASSR$ (cf. Zakamouline et al. [Zak09]), the Omega measure Ω (cf. Keating et al. [Kea02]), the Sortino ratio SR (cf. Sortino et al. [Sor94]), and the upside potential ratio UPR. The definitions of the performance measures are given in Table 2.3. Throughout the following, we use the standard versions of the performance measures which rely on the choice $K = V_0$.

First, consider Panel A which summarizes the evaluation of the strategies for a one year investment horizon. Notice that, for all strategies but the CPPI with $m = 6$, the minimum terminal value $\min V_T$ is higher than the guarantee ($G = 90$). For $m = 6$, the CPPI failed to ensure the guarantee exactly once, at Black Monday, October 19, 1987, with an excess return of -0.2046, i.e. a multiplier $m > |1/-0.2046| = 4.8876$ induces a negative cushion. Although the average value of the time–varying multiple $m_{t,\mathrm{A2}}$ is 4.49, and $m_{t,\mathrm{A2}}$ varies between 0.0668 and 29.45, the worst case terminal portfolio value is ($\min V_T = 93.79$).

16 Formally, the borrowing constraints are represented by an asset exposure $E_t = \min\{mC_t, wV_t\}$. $w-1$ denotes the maximal fraction of the portfolio which can be financed by borrowing. If not mentioned otherwise, we use $w = 2$.

Performance measures

Sharpe ratio (SR)	$\frac{E\left[V_T - V_0 e^{rT}\right]}{\sqrt{\mathrm{Var}[V_T]}}$
Adjusted Sharpe ratio ($ASSR$)	$SR\sqrt{1 + b_3 \frac{\mathrm{Skew}}{3} SR}$ where $b_3 = 2$
Omega measure (Ω)	$\frac{E[\max\{V_T - K, 0\}]}{E[\max\{K - V_T, 0\}]}$
Sortino ratio (SoR)	$\frac{E[V_T - K]}{\sqrt{E[(\max\{K - V_T, 0\})^2]}}$
Upside potential ratio (UPR)	$\frac{E[\max\{V_T - K, 0\}]}{\sqrt{E[(\max\{K - V_T, 0\})^2]}}$

Table 2.3: Summary of performance measures.

Among the constant multiple strategies, the strategy with multiple $m^{*,\mathrm{const}}$ indeed gives the highest average cushion growth rate. But, the growth rate is improved by all strategies with a time-varying multiple based on historical volatility estimates. The multiple $m_{t,\mathrm{A1}}$ yields a 120% higher average cushion growth rate, the one based on the multiple $m_{t,\mathrm{A2}}$ a 126% higher average cushion growth rate. This contradicts the assumption of a risk premium which is proportional to the squared volatility. At the same time, we conjecture that the time-varying multiple strategies are able to outperform the standard CPPI. Intuitively it is clear that the growth rates of leveraged strategies are highly volatile. This is also the case here. For example, the standard deviation of the cushion growth rates is 0.36 (0.70) for the strategy $m_{t,\mathrm{A1}}$ ($m_{t,\mathrm{A2}}$) which is proportional to the inverse of the historical volatility (variance) estimate. Unsurprisingly, it turns out that none of the comparative growth rate results is significant.

We now comment on the ranking which is implied by the other performance measures. The Sharpe ratio (SR) is a mean-variance-based performance measure. If the investor values skewness positively, a mean-variance based measure overrates the strategies which reduce skewness (value strategies) and underrates strategies, which buy skewness (momentum or portfolio insurance strategies). Ceteris paribus, the Sharpe ratio is the lower the higher the leverage is. This is also observed in Panel A where the SR is the lower the higher the multiplier is. However, a ranking of the strategies along the lines of the Sharpe ratio is not meaningful in the case of PI strategies. Relying on the adjusted for skewness Sharpe ratio ($ASSR$) confirms a better performance of the time-varying multiple strategies compared

to the optimal constant multiple strategy. This is also true for the omega measure.[17] In addition, the time-varying multiple strategy are also ranked higher than the CPPI strategies according to the Sortino ratio (SoR) measure.[18] Compared to the Sortino ratio, the so called upside potential ratio (UPR) uses as nominator the expected payoff of a call (with strike K) instead of the expected excess. However, the SoR also confirms the superiority of the strategies which rely on a time-varying volatility estimate. In summary, all performance measures indicate a superiority of the time-varying multipliers, excluding the Sharpe ratio.

Finally, it is worth to comment on the impact of the investment horizon on the performance measures. While Panel A refers to the performance evaluation w.r.t a yearly investment horizon, Panel B states the corresponding results assuming a monthly investment horizon. While a ranking according to the cushion growth rate is the same for both investment horizons, this is not true for the other performance measures. For example, in case of the Sortino ratio, the ranking of the constant multiplier strategies differs for the yearly and monthly horizon.

In summary, the results of Table 2.2 tend to favor the time-varying multiple strategies. The strategies which are based on the estimation of the daily forward volatility are promising candidates for outperforming the constant multiplier (CPPI) strategies w.r.t. the expected (cushion) growth rates as well as the other performance measures under consideration. However, as mentioned above, the descriptive results based on yearly non-overlapping historical return blocks do not allow the deduction of any significant performance results. With the exception of the benchmark static portfolio insurance strategy ($m = 1$), the strategies under consideration are leveraged strategies such that the standard deviation of the terminal values is rather high. In consequence, a significant answer to the research question if the performance of the optimal constant multiplier strategy can be improved by time–varying multiple strategies affords a sufficiently high number of observations (daily return paths, respectively). A meaningful solution is given in terms of a simulation model

17 The Omega measure accounts of the whole payoff distribution. According to a level K which defines the minimum acceptable payoff, the Omega measure divides the payoff into two parts. Note that we report $\Omega - 1$ throughout. This variation is proposed by Kazemi et al. [Kaz04], who show that $\Omega - 1$ is negative if the expected excess $E[V_T - K]$ is negative. This allows an interpretation similar to the Sharpe Ratio.

18 The SoR states the expected excess return (with respect to some level K) in relation to the square root of the second lower partial moment (semi-standard deviation, respectively). A theoretical foundation of this performance measure is given in Pedersen et al. [Ped02]. The authors show the relation of the performance measure and the maximum principle.

which mimics the empirical return distributions as close as possible.

2.4 Simulation Model

2.4.1 Model selection and estimation

Recall that our argumentation is, to a large extent, based on model risk. The *true* data generating process deviates from the assumed model. The investor is aware of this and optimizes her strategy in view of a whole model class instead of one particular model. However, the true data generating process is also not (perfectly) consistent with the benchmark assumptions on the relation between excess return and volatility, i.e. assumptions (A0), (A1), and (A2). It is also possible that the answer to the question of which of the assumptions on the risk premium is the most realistic one, depends to the market conditions itself, i.e. it can change over time. In order to be able to account of a rather complex interplay between expected excess return and volatility, we use a Markov Regime Switching Exponential GARCH-in-Mean (MRS-EGARCH-M) model. In addition, regime switching provides a feasible way to capture the observations of other empirical works which can be summarized as follows (cf. Whitelaw [Whi00]): Against the intuition the relation between conditional expected returns and conditional volatility is *(i)* often found to be weak or even negative, but *(ii)* this relation fluctuates significantly over time.[19]

In the following, we use a two-state Markov process and denote the regime indicator by $s_t = i$, $i = 1,2$. The information set I_{t-1} contains information about all observed variables, particularly the excess returns $(R_{t-1},R_{t-2},...)$, but it does not contain the unobservable regime path $(s_{t-1},s_{t-2},...)$. The transition probabilities $\Pr(s_t = j|s_{t-1} = i) = p_{ji}$ are assumed to be constant and specified by the matrix

$$\begin{bmatrix} p_{11} & p_{21} \\ p_{12} & p_{22} \end{bmatrix} = \begin{bmatrix} p & (1-q) \\ (1-p) & q \end{bmatrix}. \tag{2.11}$$

The conditional distribution of excess returns is modeled as a mixture of two normal

19 For a detailed information about regime-switching models with (E)GARCH volatility, we refer to the works of Gray [Gra96], Henry [Hen09], Klaassen [Kla02], Marcucci [Mar05], and Reher et al. [Reh11].

distributions, i.e.

$$R_t|I_{t-1} \sim \begin{cases} N(\lambda_{1,t},\sigma_{1,t}^2) & \text{with probability } p_{1,t} \\ N(\lambda_{2,t},\sigma_{2,t}^2) & \text{with probability } (1-p_{1,t}), \end{cases} \tag{2.12}$$

where $\lambda_{i,t}$ denotes the state-dependent conditional expected excess return (the conditional risk premium) and $\sigma_{i,t}^2$ the conditional variance. In the literature, the probability $p_{1,t} = \Pr(s_t = 1|I_{t-1})$ of being in regime 1 at time t is called *ex-ante* probability. The conditional variance $\sigma_{i,t}^2$ is given by an EGARCH model, cf. Nelson [Nel91]. One advantage is the possibility of asymmetric responses of the volatility to positive and negative shocks in the returns. In particular, the so-called *leverage effect* might differ over regimes. Furthermore, the exponential specification of σ_t^2 ensures a strictly positive volatility, i.e. without additional introduction of non-negativity constraints.

An important aspect concerns the dependence of the conditional excess returns on the volatility in each regime. For instance, we want to capture the possibility that $\lambda_{i,t}$ is constant in one regime but proportional to $\sigma_{i,t}$ or $\sigma_{i,t}^2$ in the other one. Comparing the goodness of fit of several specifications – also comprising variants proportional to $\ln \sigma_t^2$, i.e. variants which deviate from our three basic assumptions – it turns out that a combination of a constant c_i and a term proportional to volatility for both regimes, $\lambda_{i,t} = c_i + \theta_i \sigma_{i,t}$, gives the best description of the underlying data set.[20] For regime 1, the constant c_1 is negative and the volatility coefficient θ_1 is positive. In contrast, the opposite turns out for regime 2. In summary, we estimate the following model for the excess returns R_t by means of the ML-method:

$$\begin{aligned} R_t &= \lambda_{i,t} + \sigma_{i,t} z_t, \qquad z_t \sim N(0,1), \\ \lambda_{i,t} &= c_i + \theta_i \sigma_{i,t}, \\ \ln \sigma_{i,t}^2 &= \omega_i + \alpha_i \left(|\widetilde{z}_{i,t-1}| - \sqrt{2/\pi} \right) + \gamma_i \widetilde{z}_{i,t-1} + \beta_i \ln \widetilde{\sigma}_{i,t-1}^2. \end{aligned} \tag{2.13}$$

We specify the lagged variance $\widetilde{\sigma}_{i,t-1}^2$ and the lagged shock $\widetilde{z}_{i,t-1}$ entering the variance

20 This is consistent with the literature. For example, Engle et al. [Eng87] suggest this form of the expected risk premium in a single regime (G)ARCH-in-Mean model. More recently, Reher et al. [Reh11] observe similar results in a two-regime and more general GARCH-type model (nesting EGARCH as a special case).

equation for state $s_t = i$ following Klaassen's approach. KLAASSEN [Kla02] suggests to integrate out the unobservable state at time $t-1$ by taking expectation of $\sigma^2_{i,t-1}$, conditional on the information that the current state is $s_t = i$. The lagged quantities and Klaassen's conditional probabilites $\widetilde{p}_{ji,t-1}$ are computed as follows

$$\begin{aligned}
\widetilde{\sigma}^2_{i,t-1} &= \widetilde{p}_{ii,t-1}\sigma^2_{i,t-1} + \widetilde{p}_{ji,t-1}\sigma^2_{j,t-1} + \widetilde{p}_{ii,t-1}\widetilde{p}_{ji,t-1}\left[\lambda_{i,t-1} - \lambda_{j,t-1}\right]^2, \\
\widetilde{z}_{i,t-1} &= \widetilde{p}_{ii,t-1}\frac{R_{t-1} - \lambda_{i,t-1}}{\sigma_{i,t-1}} + \widetilde{p}_{ji,t-1}\frac{R_{t-1} - \lambda_{j,t-1}}{\sigma_{j,t-1}}, \\
\widetilde{p}_{ji,t-1} &= \Pr\left(s_{t-1} = j \middle| s_t = i, I_{t-1}\right) = \frac{p_{ji}\Pr\left(s_{t-1} = j | I_{t-1}\right)}{\Pr\left(s_t = i | I_{t-1}\right)} = \frac{p_{ji}p_{j,t-1}}{p_{i,t}},
\end{aligned}$$

with i,j = 1,2. The ex-ante probabilities are calculated using the transition probabilities p_{ij} as defined by Equation (2.11) and the conditional probability density function $f(r_t|I_{t-1})$ corresponding to the conditional mixed-normal distribution of returns, cf. Equation (2.12), as

$$p_{j,t} = \Pr(s_t = j|I_{t-1}) = \sum_{i=1}^{2} p_{ij}\left[\frac{f(R_{t-1}|s_{t-1} = i)p_{i,t-1}}{\sum_{k=1}^{2} f(R_{t-1}|s_{t-1} = k)p_{k,t-1}}\right]. \tag{2.14}$$

Table 2.4 summarizes the quasi-maximum likelihood estimates of the model parameters. The asymptotic standard errors imply that all parameters are significantly different from zero. The smallest t-statistics (in absolute terms) is observed for c_1 with a value of 2.850. In order to guarantee stationarity of the conditional variance, the persistence parameter must be restricted to $|\beta_i| < 1$ for both regimes. To obtain a stable simulation model with non-

Parameter estimates for the MRS-EGARCH-M model

	Regime 1	Asymp. SE		Regime 2	Asymp. SE
c_1	-0.001164	0.000409	c_2	0.002830	0.000278
θ_1	0.146237	0.049559	θ_2	-0.289444	0.041209
ω_1	-0.109877	0.012589	ω_2	-0.125000	0.036809
α_1	0.062288	0.006232	α_2	0.135578	0.016464
γ_1	-0.038539	0.005598	γ_2	-0.263822	0.012076
β_1	0.988012	0.001312	β_2	0.988012	0.003918
p	0.993919	0.001292	q	0.986645	0.002876

Table 2.4: Parameter estimates and asymptotic standard errors for the model along the lines of Equation (2.13). The transition probabilities $p = p_{11}$ and $q = p_{22}$ are defined by Equation (2.11).

explosive volatility, we slightly sharpen this restriction and set an upper bound at $\beta_i \leq \beta$, where $\beta = 0.988012$ is the persistence parameter estimate obtained for a single-regime EGARCH model, ceteris paribus. We observe that both β_i are set to this upper bound by the estimation routine, i.e. volatility is highly persistent in both regimes.[21] Also, the regimes are quite persistent as implied by the transition probabilities. Though, for regime 1 the estimated persistence is $1/(1-p) = 164.45$ trading days. Regime 2 is estimated to persist just $1/(1-q) = 74.88$ days. Accordingly, the unconditional probability of being in regime 1 (regime 2) is $(1-q)/(2-p-q) = 68.71\%$ (31.29%).

It is interesting to note that the simple notion of a high-mean, low volatility regime 1, and a low-mean, high volatility regime 2 is far from being true. In fact, for both regimes the conditional expected risk premium $\lambda_{i,t}$ can be positive or negative, depending on the level of conditional volatility. To be more precise, it holds $\lambda_{1,t} > 0$ if $\sigma_{1,t} > |c_1/\theta_1| = 0.00796$. In regime 2, the conditional mean $\lambda_{2,t}$ is positive if the volatility does not exceed the value 0.00978. The main difference in the variance equations across regimes concerns the response to shocks. Often, positive and negative shocks are interpreted in terms of good and bad news. In regime 1, the volatility $\sigma_{1,t}$ responses rather symmetrically to good and bad news, i.e. shocks of either sign increase the volatility.[22] However, the impact of news is small. In sharp contrast, in regime 2 the volatility $\sigma_{2,t}$ is strongly increased after bad news, while good news slightly reduce volatility.

2.4.2 Additional benchmark strategies

The simulation model provides additional information according to the actual state $s_t = i$, $i = 1,2$, and the actual volatility $\sigma_{i,t}$ and expected risk premium $\lambda_{i,t}$ that generate a return R_t at time t. Recall that the simulation model (data generating process) is not known to the investor. Nevertheless it is interesting to report the performance results of selected (visionary) strategies. Our first additional benchmark strategy $m_{t,\text{switch1}}$ is based on all information needed by a HARA investor to determine the myopic part of a strategy which is optimal in a diffusion setup (cf. Subsection 2.2) without the restriction to discrete time trading. In particular, the investor – which is from our point of view a visionary – knows the state s_t as well as the corresponding expected excess return $\lambda_{.,t}$ and the local volatility $\sigma_{.,t}$. For the special case that $\gamma = 1$, we denote the corresponding multiplier by $m_{t,\text{switch1}}$,

21 Further details on the model estimation, simulation and statistical tests are available from the authors on request.

22 This is because $|\alpha_1| > |\gamma_1|$, i.e. the magnitude effect dominates the leverage effect.

i.e.

$$m_{t,\text{switch1}} = \begin{cases} \frac{\lambda_{1,t}}{\sigma^2_{1,t}} & \text{if } s_t = 1, \\ \frac{\lambda_{2,t}}{\sigma^2_{2,t}} & \text{if } s_t = 2. \end{cases} \tag{2.15}$$

The second (additional) benchmark strategy $m_{t,\text{switch2}}$ also uses the information about the current state s_t. However, the (partially visionary) investor does not know the local volatility $\sigma_{.,t}$ and the expected excess return $\lambda_{.,t}$. However, w.r.t. the set of multipliers comprising constant multipliers and multipliers proportional to the inverse of volatility or squared volatility, i.e. multipliers consistent with the benchmark assumptions (A0), (A1), and (A2), she knows which of these strategies performs best, given the regime. In particular, this strategy corresponds to the optimized (myopic) multiplier in a regime switching diffusion model setup as given in Subsection 2.2 , cf. Equation (2.7). The corresponding strategy is denoted by $m_{t,\text{switch2}}$ where (for $\gamma = 1$) it turns out that

$$m_{t,\text{switch2}} = \begin{cases} 4 & \text{if } s_t = 1 \\ m_{t,A2} & \text{if } s_t = 2, \end{cases} \tag{2.16}$$

where $m_{t,A2}$ is defined as in Section 3, Equation (2.10), i.e. a multiplier proportional to the inverse of the simple rolling window estimate of conditional variance. Basically, this strategy (its performance results, respectively) sheds light on the question to what (maximal) extent a regime-dependent combination of the corner strategies corresponding to the basic assumptions on the risk premium can outperform the corner strategies themselves.

The third benchmark strategy is similar to $m_{t,\text{switch2}}$, but is not based on the knowledge of the regime/state. Instead, a Bayesian procedure is applied to infer the ex-ante probabilities $p_{i,t}$ (2.14) of the current state being 1 or 2. A similar Bayesian procedure is proposed in Hainaut et al. [Hai12]. The strategy $m_{t,\text{Bayes}}$ is defined in a similar manner as $m_{t,\text{switch2}}$, but the multiplier is averaged across $m = 4$ and $m_{t,A2}$ according to the regime probabilities,

i.e.[23]

$$m_{t,\text{Bayes}} = 4\, p_{1,t} + m_{t,A2}\, p_{2,t}. \tag{2.17}$$

It is worth mentioning that this strategy is yet not admissible, because the inference of the regime probabilities is based on the knowledge about the model specification of $\lambda_{i,t}$ and $\sigma_{i,t}$. In addition, it also relies on the knowledge which corner strategies are the most promising, i.e. depending on the regime.

2.5 Performance Evaluation – Simulation results

The simulation tool established in the above section allows for significant results concerning the comparison of time-varying and constant multiple strategies. In addition, we account for the impacts of transaction costs. We investigate time-varying multipliers as a function of the volatility. The corner functions are fixed. Besides a constant multiple, the multiples $m_{t,A1}$ and $m_{t,A2}$ are proportional to the inverse of first and second power of the historically estimated standard deviation, i.e. proportional to the inverse of the standard deviation or

Notation used for variable multiplier strategies

Corner strategy	**Variable m_t proportional to the inverse of the:**
$m_{t,A1}$	standard deviation of the latest 1 month (21 days) historical returns ($t, t-1,\ldots,t-20$)
$m_{t,A2}$	variance of the latest 1 month (21 days) historical returns
Switching strategy	**Information includes**
$m_{t,\text{switch1}}$	current regime, simulation model implied conditional expected excess return and volatility
$m_{t,\text{switch2}}$	current regime, best performing corner strategy (including constant mult.) given the regime
$m_{t,\text{Bayes}}$	best performing corner strategy (including const. mult.) given the regime, and ex-ante regime prob.'s

Table 2.5: Summary of the dynamic multiplier strategies. $m_{t,A1}$ and $m_{t,A2}$ are consistent with assumptions (A1) and (A2), respectively, cf. Equations (2.9) and (2.10). In addition, the switching strategies include additional information: The strategy $m_{t,\text{switch1}}$ is based on the regime and the regime dependent myopic part. $m_{t,\text{switch2}}$ and $m_{t,\text{Bayes}}$ are, along the lines of Equation (2.7), proportional to a regime dependent power of the estimated current volatility. In the case of $m_{t,\text{switch2}}$, the regime is known. In contrast, $m_{t,\text{Bayes}}$ is based on a Bayesian inference of the ex-ante regime probabilities. For the initialization, we additionally use a 3 month set of pre-sampled returns, i.e. each year.

23 Obviously, it is also possible to consider strategies that are not based on weighting the corner multipliers with the state probabilities. For example, an alternative and reasonable strategy is to base the decision on the most probable state. However, we restrict ourselves to the results of the strategy that performed best in our simulation setup.

variance, respectively, cf. Equations (2.9) and (2.10).[24] According to the intuition that for some cases it is better to take a constant multiple and for other cases (depending on market conditions) to introduce a multiple which is a non increasing function of the volatility, we also include switching strategies implied by the optimal multiplier of a regime switching diffusion setup, cf. Equation (2.7). In particular, the strategies are then proportional to the inverse of a power of the standard deviation where the power α_t itself depends on market conditions.

Recall that we do not assume that the true regime is known by the investor. The investor must thus decide how to estimate the probabilities of being in a certain regime. We consider a Bayesian approach giving rise to the strategy $m_{t,\text{Bayes}}$ where a detailed description is given in Subsection 4.1. Finally, we also include a visionary who knows the fraction of expected excess return and squared volatility in each regime. Along the lines of the degree of information, we denote the corresponding strategies by $m_{t,\text{switch1}}$ (regime and myopic multiplier is known) and $m_{t,\text{switch2}}$ (regime is known, but not the myopic multiplier). The basic features of the strategies are summarized in Table 2.5.

For expositional clarity, the simulation results are stated in two parts. In the first part, we abstract from transaction costs. We focus on the distribution of the variable multipliers, their daily changes and introduce some convenient key numbers which characterize the turnovers of the strategies. In the second part, we account for positive proportional transaction costs, introduce trigger trading (stochastic trading dates), and reconsider the evaluation of the PPI strategies for positive proportional transaction costs.

2.5.1 CPPI and PPI evaluation in the absence of transaction costs

Table 2.6 summarizes the statistics of the dynamic multipliers and their relative changes. Recall that the optimal constant multiplier is $m^{*,\text{const}} = 1.7256$. On average, the variable multipliers are much larger. We also observe a high standard deviation (10.465) and a mean daily change of 21,8 % for the multiplier $m_{t,\text{switch1}}$, which might be explained by the fact

24 Probably, the results can be improved by means of more advanced volatility estimates. For example, a conditional variance model could be estimated on each path, i.e. on a simulated historic pre-sample. This issue is beyond the scope of this thesis. It is left for further research. However, we conjecture that the gain of these strategies is rather small. The results which are generated by the strategies based on the simple estimates turn out to be quite close to those of the ones implied by the variance along the lines of the simulation model.

Summary statistics of variable multipliers m_t and the relative changes Δm_t

	Mean	Median	Stdev	Skewness	Kurtosis	Min
$m_{t,\text{A1}}$	2.857	2.228	2.307	4.617	36.809	0.066
$m_{t,\text{A2}}$	5.761	2.964	7.468	2.548	8.479	0.003
$m_{t,\text{switch1}}$	6.492	2.804	10.465	1.943	4.874	0.001
$m_{t,\text{switch2}}$	5.389	4.000	5.843	3.773	16.382	0.003
$m_{t,\text{Bayes}}$	5.504	3.907	5.548	3.797	16.696	0.010
$\Delta m_{t,\text{A1}}$	0.035	0.019	0.048	4.173	42.026	0
$\Delta m_{t,\text{A2}}$	0.067	0.035	0.099	6.444	137.653	0
$\Delta m_{t,\text{switch1}}$	0.218	0.008	1.787	27.459	894.201	0
$\Delta m_{t,\text{switch2}}$	0.032	0.000	0.231	34.719	967.030	0
$\Delta m_{t,\text{Bayes}}$	0.037	0.012	0.080	10.977	343.541	0

Table 2.6: Summary statistics of variable multipliers and absolute percentage daily changes $\Delta m_t = \left|\frac{m_t - m_{t-1}}{m_{t-1}}\right|$. The multipliers $m_{t,\cdot}$ are defined as in Table 2.5. According to a simple gap control, all multipliers are bounded by a maximum of $m_t = 32.3165$, which is equal to $|1/-0.0309|$, where -0.0309 is the 1 % quantile of the dataset of daily excess returns. The results are approximated by a simulation of 50,000 years, each with 260 trading days.

that these multipliers are proportional to the model implied conditional risk premium $\lambda_{i,t}$, while all other strategies rely on a constant nominator $\hat{\lambda}$. In order to analyze the turnovers which are implied by the time-varying and constant multiplier strategies, we consider the following measures. Based on the relative daily turnover δ_t^S, given by

$$\delta_t^S := \frac{\left| m_t C_t - m_{t-1} C_{t-1} \frac{S_t}{S_{t-1}} \right|}{V_t}, \tag{2.18}$$

we report the expected maximum relative daily turnovers $\mathit{Maxturn} = E[\max_{t\in\{1,\dots n-1\}} \delta_t^S]$, the expected total relative turnovers $\mathit{Totturn} = E[\sum_{t=1}^{n-1} \delta_t^S]$, and the expected number of trading days per year $\mathit{Trades} = E[\sum_{t=0}^{n-1} 1_{\delta_t^S>0}]$.[25] If not mentioned otherwise, the results are based on a one year investment horizon ($T = 1$). As before, we assume $n = 260$ asset prices per year (corresponding to 259 simulated excess returns per path).

The performance results are summarized in Table 2.7. Basically, the descriptive results of Section 3 are confirmed. $m^{*,\text{const}}$ gives the highest cushion growth rate amongst the

25 Notice that, for interpretability reasons, the key numbers *Maxturn* and *Totturn* do not account for the initial trading volume at $t = 0$. In contrast, this is the case for *Trades*. For example, the CPPI strategy with $m = 1$ and a positive initial cushion is a buy and hold strategy. It holds $\mathit{Maxturn} = 0$, $\mathit{Totturn} = 0$, and $\mathit{Trades} = 1$.

Performance results for dynamic and constant multiplier strategies

	$E[\ln \frac{C_T}{C_0}]$	$E[\ln \frac{V_T}{V0}]$	$E[V_T]$	min V_T	SR	$ASSR$	$\Omega - 1$	SoR	UPR	$Maxturn$	$Totturn$
$m_{t,\mathrm{A1}}$	0.219	0.047	105.751	91.202	0.337	0.493	7.793	3.739	4.219	0.156	3.228
	0.583	*0.124*	*17.062*							*0.134*	*2.024*
$m_{t,\mathrm{A2}}$	0.252	0.069	108.885	90.277	0.380	0.532	7.465	4.015	4.552	0.421	7.236
	0.787	*0.167*	*23.355*							*0.251*	*3.584*
$m = 1$	0.033	0.006	100.602	90.000	0.302	0.279	1.299	0.477	0.844	0.000	0.000
	0.265	*0.020*	*1.993*							*0.000*	*0.000*
$m^{*,\mathrm{const}}$	0.036	0.011	101.124	90.000	0.327	0.338	1.480	0.609	1.021	0.005	0.249
	0.481	*0.034*	*3.436*							*0.006*	*0.068*
$m = 4$	(-0.051)	0.028	103.237	83.030	0.313	0.402	1.971	1.021	1.540	0.044	2.350
	1.133	*0.090*	*10.331*	**48**						*0.024*	*0.733*
$m = 6$	(-0.225)	0.041	105.495	75.721	0.291	0.380	2.251	1.339	1.934	0.109	5.556
	1.622	*0.146*	*18.859*	**206**						*0.053*	*2.129*
$m = 8$	(-0.484)	0.047	106.800	69.196	0.281	0.357	2.079	1.375	2.036	0.189	8.874
	2.058	*0.181*	*24.172*	**461**						*0.089*	*3.861*
$m_{t,\mathrm{switch1}}$	(0.559)	0.127	115.976	89.721	0.574	0.832	20.288	8.006	8.400	1.403	14.464
	0.878	*0.195*	*27.808*	**2**						*0.714*	*9.358*
$m_{t,\mathrm{switch2}}$	(0.404)	0.090	111.212	88.009	0.464	0.717	13.161	6.142	6.609	0.514	5.228
	0.766	*0.170*	*24.153*	**4**						*0.422*	*2.802*
$m_{t,\mathrm{Bayes}}$	(0.267)	0.072	109.225	89.460	0.401	0.566	7.317	3.808	4.329	0.377	5.927
	0.821	*0.165*	*23.030*	**1**						*0.296*	*3.440*

Table 2.7: Mean performance *(and standard deviations)* of the PPI strategies in the absence of transaction costs. The results are based on 50,000 simulations. The maximum investment quote is bounded to 200% of the current portfolio value V_t. The investment horizon is $T = 1$ year. The initial portfolio value is given by $V_0 = 100$. The guarantee is $G = 90$. The optimal constant multiplier is $m^{*,\mathrm{const}} = 1.7256$. In line with with the descriptive results in Table 2.2, the expected growth rates reported in parentheses are those where negative cushion pathes are excluded. The boldface number in the second line of the min V_T column counts the number of floor violations that occurred within the 50,000 simulations.

constant multiplier strategies. This is not true for all of the other performance measures. In contrast to the descriptive results, the simulation model gives a better description of the gap risk. We observe a rather high number of gap events for $m = 4$, $m = 6$, and $m = 8$. While CPPI strategies give rise to a high degree of gap risk, this is not the case for the time-varying strategies. There are no floor/guarantee violations observed for the multiplier $m_{t,\mathrm{A1}}$ and $m_{t,\mathrm{A2}}$, i.e. the strategies which, independent from the current regime, reduce the multiple in times of volatile markets. In contrast, we observe some gap events for the switching strategies. Along the lines of reasoning given in Subsection 2.2.3, an additional gap control is needed for a final practical application of the strategies. However, in view of our main research question, it is worth mentioning that a gap control is more binding in the case of constant than time-varying multiples which reduce the multiplier in times of excess volatility. An additional gap risk control does not deteriorate the performance comparison presented here. An upper bound on the multiplier reduces the CE growth rates. The reduction is more severe if the gap control becomes binding more often. Next, it

is important to observe that we validate the conjecture that the time-varying strategies proportional to inverse of the historical standard deviation and variance perform much better than the optimal constant multiplier. The out-performance turns out to be robust w.r.t. all performance measures. Obviously, the exact information w.r.t to the different regimes as used by the not feasible multiplier $m_{t,\text{switch1}}$ gives, by far, the highest average cushion growth (at least if 2 negative cushion pathes are not taken into account for). Intuitively, it is clear that the Bayesian switching multiplier $m_{t,\text{Bayes}}$ is also able to improve the performance. However, its average cushion growth rate is (only) 0.267 compared to 0.252 already obtained by $m_{t,\text{A2}}$. Unfortunately, the time-varying multiple strategies, in particular the ones with the highest performance, afford high turnovers. Thus, it is necessary to reconsider the performance evaluation accounting for transaction costs and using adequate trigger designs.

Before we tackle the problem stemming from transaction costs, we reconsider the choice of $\gamma = 1$, i.e. the restrictions towards a log-utility in terms of the cushion. Recall that the guarantee component is rather high such that it is realistic to consider rather low values of γ. Table 2.8 depicts the certainty equivalent (CE) growth rates along the lines of Equation (2.3) for the benchmark strategies scaled according to $\gamma \in \{0.8,1.0,1.2,1.4\}$. We consider two different investment horizons $T = 1$ year and $T = 10$ years, respectively. The results are given for capped multipliers (with borrowing constraints) and the uncapped counterpart strategies. First of all notice that the CE growth rates are, independent of the investment horizon, decreasing in γ, i.e. for all strategies. The higher the risk aversion is the lower is the CE growth rate. Intuitively, it is also clear that the loss due to borrowing constraints is the higher the lower the risk aversion is. However, our major concern is the utility loss and the distortion caused by neglecting the inter-temporal hedging demand linked to $\gamma \neq 1$. Obviously, a negative CE growth rate is prohibitive, in particular for an *optimized* multiplier. Notice that, for $\gamma = 1.4$, a negative CE growth rate is observed in the case of the *optimized* constant multiplier. The investor is even better of without any risky investment. In contrast, this is not the case for the time-varying multiples which still perform reasonably well. One might argue that neglecting the hedging demand even gives worth results in the case of a constant multiplier than a dynamic multiplier, i.e. a multiplier which is decreasing in the (local) volatility. However, the interpretation is to be taken with caution. In summary, we can nevertheless observe that the ranking of the strategies under consideration is not distorted when deviating from the assumption of $\gamma = 1$.

Certainty equivalent growth rates for different levels of risk aversion γ and investment horizons T

	Capped investment quote				*Uncapped investment quote*			
y^{CE}	$\gamma = 0.8$	$\gamma = 1.0$	$\gamma = 1.2$	$\gamma = 1.4$	$\gamma = 0.8$	$\gamma = 1$	$\gamma = 1.2$	$\gamma = 1.4$
Panel A: 1 year horizon								
$m_{t,\text{A1}}$	0.275	0.219	0.178	0.148	0.477	0.283	0.202	0.158
$m_{t,\text{A2}}$	0.301	0.252	0.212	0.179	1.398	0.645	0.386	0.266
$m^{*,\text{const}}$	0.061	0.036	0.019	-0.006	0.061	0.036	0.019	-0.006
Panel B: 10 year horizon								
$m_{t,\text{A1}}$	0.206	0.180	0.155	0.134	0.533	0.282	0.196	0.151
$m_{t,\text{A2}}$	0.225	0.203	0.181	0.160	1.654	0.642	0.366	0.250
$m^{*,\text{const}}$	0.064	0.037	0.017	-0.002	0.064	0.037	0.017	-0.002

Table 2.8: Certainty equivalent (CE) growth rates of the benchmark PPI strategies in the absence of transaction costs. The results are based on 50,000 simulations. The CE growth rates on the left hand side of the table refer to the case where the maximum investment quote is bounded to 200% of the current portfolio value V_t. On the right hand side, the corresponding CE growth rates of the otherwise identical uncapped strategies are quoted. The investment horizon is $T = 1$ year ($T = 10$, respectively). The initial portfolio value is given by $V_0 = 100$. The guarantee (subsistence level) is $G = 90$. The HARA paramter γ varies. The optimal constant multiplier is $m^{*,\text{const}} = \frac{1.7256}{\gamma}$.

2.5.2 Performance of triggered CPPI and PPI strategies under transaction costs

As indicted by the high turnovers of the strategies, accounting for transaction costs is especially important in the context of PPI strategies. The strategies imply a reduction of the asset exposure in falling markets. Analogously, the asset exposure is increased in rising markets. The investor suffers from any round-turn in the asset prices. The effect is particularly severe if there are in addition transaction costs, i.e. the effect is even leveraged by the transaction costs. Throughout the following, we consider proportional transaction costs denoted by θ. For daily trading, the cushion dynamics are given by Equation (2.8). In practice, the high turnovers of a strategy are normally controlled by implementing a trading filter. The trigger design is described as follows: Let τ denote a sequence of stopping times where $\tau_k \in \{0,1,\ldots,n-1\}$, $\tau_0 = 0$ and $\tau_{k+1} > \tau_k$. Assume that $C_{\tau_k+} > 0$ where C_{τ_k+} denotes that the transaction cost are already deducted, cf. Equation (2.8). The number of risky assets (constantly held immediately after τ_k) is $\eta_{\tau_k+} = \frac{m_{\tau_k} C_{\tau_k+}}{S_{\tau_k}}$ such that at t

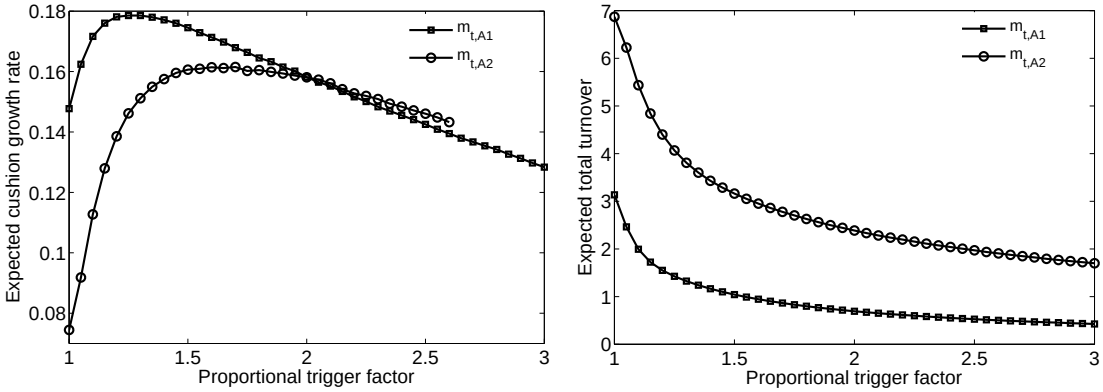

Figure 2.1: Left: Expected cushion growth rates for the dynamic multiplier strategies $m_{t,\mathrm{A1}}$ and $m_{t,\mathrm{A2}}$ and varying trigger levels specified by the proportional trigger factor φ and the trigger rule defined by Equation (2.19). The proportional transaction costs are given by $\theta = 0.25\%$. As the trigger factor φ increases from one (i.e. daily trading) to 3, the no–trade interval increases, too. For $m_{t,\mathrm{A2}}$, we omit the results for $\varphi > 2.6$ where floor violations occurred. Right: Expected total relative turnovers $Totturn = E[\sum_{t=1}^{n-1} \delta_t^S]$ where δ^S is defined by Equation (2.18) for the corresponding trigger levels. Results are based on 50,000 simulations.

$(\tau_{k+} < t < \tau_{k+1})$, the implicit multiplier is

$$m_t^{imp} = \frac{\eta_{\tau_k+} S_t}{C_t}.$$

In contrast, the target multiplier m_t is, at each trading date t, defined by the PPI rule. Along the lines of Paulot et al. [Pau09], Hamidi et al. [Ham09a], MKaouar et al. [MKa07], Jessen [Jes09] and Khuman et al. [Khu09], we only trigger the next rebalancing date if the deviations of the implicit multiplier and the target multiplier are sufficiently high. We define

$$\tau_k := \inf \left\{ t > \tau_{k-1} \,\middle|\, \{m_t^{imp} \leq \frac{1}{\varphi}\, m_t\} \cup \{m_t^{imp} \geq \varphi\, m_t\} \right\}, \tag{2.19}$$

where φ ($\varphi \geq 1$) denotes the proportional trigger factor. The special case that $\varphi = 1$ coincides with daily portfolio rebalancing.

Figure 2.1 illustrates the effects of varying trigger levels φ on the expected cushion growth rates. For illustrative purpose, we also depict the turnovers. Obviously, the expected total relative turnovers are the lower the higher the trigger level is. In contrast, the CE growth rate (expected cushion growth rate, respectively) is increasing in the trigger level for small trigger values but decreasing for high trigger values. The trade–off between more

frequent rebalancing, i.e. sticking to the *optimized* PPI rule, and the transaction costs of the turnovers implies an optimal trigger level. Intuitively, it is clear that the optimal trigger depends on the PPI rule, i.e. the rule defining the multiple (cf. BALDER et al. [Bal12]). Since our aim is the comparison of optimized PPI strategies, we use, for each strategy m, the (cushion growth rate) optimal level $\varphi^*(m)$.[26]

Table 2.9 restates the results of Table 2.7 under transaction costs of $\theta = 0.25\%$.[27] Each strategy is evaluated w.r.t. its optimal trigger level φ^*. Observe that, for the constant multiplier strategies, the optimal level $\varphi^*(m)$ is the higher, the higher the multiplier is. Nevertheless, the optimized trigger levels of the CPPI strategy $m^{*,\text{const}}$ is close to one which is rather close to daily trading. The optimized trigger levels of the time varying strategies range from $\varphi^* = 1.25$ for $m_{t,\text{A1}}$ to $\varphi^* = 4.75$ for $m_{t,\text{switch1}}$. Intuitively, it is clear that the optimal trigger level is the higher, the higher the dispersion of the multiplier values is. Compared to the multiplier $m_{t,\text{A1}}$ proportional to the inverse of the volatility, a higher trigger level is observed for the multiplier $m_{t,\text{A2}}$ proportional to the inverse of the estimated variance. Using the expected cumulated relative turnovers *Totturn* caused by daily trading, cf. Table 2.7, as a benchmark, the optimized trigger trading gives a reduction. This is especially true for the time-varying multiplier strategies. Here, the reduction is more than 50%. It is clear that the trigger induces: *(i)* fewer trades because small (and probably negligible) deviations of the target multiple m_t and the implied multiple m_t^{imp} are not taken into account, and *(ii)* less turnovers in total. However, the average and maximum turnover volume per trade *Maxturn* increases. In practice, maximal turnovers which are above 50% are often considered as prohibitive. The highest values of *Maxturn* are ca 131% for the (model based) switching strategy $m_{t,\text{switch1}}$ and ca 62% for the multiplier $m_{t,\text{A2}}$. This is a major drawback of a time-varying multiple $m_{t,\text{A2}}$ proportional to the historically estimated variance, in particular if compared to the time-varying multiple $m_{t,\text{A1}}$ proportional to the historically estimated standard deviation.

26 Thus, the optimal trigger levels are estimated in sample. The procedure is merely justified by the aim to avoid a distortion of the ranking by an inadequate trigger level, i.e. a trigger design which is in favor of some strategies.

27 Proportional transaction costs of $\theta = 0.25\%$ constitute a rather high estimate – even for private investors – and may be interpreted as already containing transaction taxes present in many countries (and currently discussed in others). For instance, JIANG et al. [Jia09] assume $\theta = 0.18\%$, composed of 0.08% commission fees and 0.1% taxes for Chinese investors.

Performance results for dynamic and constant multiplier strategies under transaction costs and optimized trigger trading

	$E[\ln \frac{C_T}{C_0}]$	$E[\ln \frac{V_T}{V0}]$	$E[V_T]$	min V_T	$ASSR$	$\Omega - 1$	SoR	UPR	$Maxturn$	$Totturn$	$Trades$
$m_{t,\text{A1}}$	0.179	0.041	105.034	91.099	0.449	5.922	2.984	3.487	0.204	1.426	19.769
$\varphi^* = 1.25$	*0.576*	*0.119*	*16.228*						*0.167*	*1.183*	*21.032*
$m_{t,\text{A2}}$	0.162	0.059	107.753	90.053	0.467	5.142	2.929	3.499	0.622	2.777	30.729
$\varphi^* = 1.70$	*0.832*	*0.164*	*22.731*						*0.348*	*1.702*	*43.186*
$m = 1$	0.031	0.006	100.576	90.000	0.269	1.225	0.454	0.825	0.000	0.000	1.000
$\varphi^* = 1$	*0.265*	*0.020*	*1.988*						*0.000*	*0.000*	*0.000*
$m^{*,\text{const}}$	0.034	0.010	101.091	90.000	0.330	1.436	0.590	1.000	0.010	0.038	5.440
$\varphi^* = 1.05$	*0.482*	*0.033*	*3.380*						*0.003*	*0.028*	*4.626*
$m = 4$	(-0.091)	0.023	102.756	82.537	0.350	1.581	0.844	1.378	0.052	1.211	48.690
$\varphi^* = 1.20$	*1.148*	*0.087*	*9.831*	**45**					*0.019*	*0.503*	*20.617*
$m = 6$	(-0.289)	0.034	104.546	73.547	0.328	1.745	1.069	1.682	0.135	2.428	42.260
$\varphi^* = 1.45$	*1.617*	*0.139*	*17.691*	**204**					*0.049*	*1.024*	*23.301*
$m = 8$	(-0.571)	0.037	105.549	60.559	0.301	1.586	1.076	1.754	0.246	3.682	48.882
$\varphi^* = 1.60$	*2.032*	*0.173*	*22.875*	**461**					*0.090*	*1.642*	*37.058*
$m_{t,\text{switch1}}$	(0.359)	0.089	111.260	87.255	0.651	11.098	5.030	5.483	1.309	7.850	49.701
$\varphi^* = 4.75$	*0.845*	*0.176*	*24.623*	**1**					*0.687*	*6.245*	*27.848*
$m_{t,\text{switch2}}$	(0.383)	0.082	110.174	81.748	0.682	13.423	6.046	6.496	0.549	2.489	50.504
$\varphi^* = 1.60$	*0.719*	*0.160*	*22.637*	**4**					*0.430*	*2.261*	*38.904*
$m_{t,\text{Bayes}}$	0.245	0.068	108.696	90.001	0.550	6.668	3.466	3.986	0.498	2.025	21.802
$\varphi^* = 1.55$	*0.819*	*0.161*	*22.336*						*0.350*	*1.902*	*34.302*

Table 2.9: Mean performance *(and standard deviations)* under proportional transaction costs of $\theta = 0{,}25\%$. The trigger design is described by Equation (2.19). The reported optimized proportional trigger factors φ^* are obtained numerically. To save space, the Sharpe ratio is not displayed. All other things (including the simulated set of paths) are identical to the setting of Table 2.7 in the above subsection. Note that *Trades* gives the expected number of trades per year, including the $t = 0$ trade for setting up the initial portfolio.

Concerning the performance evaluation under transaction costs and optimized trigger trading, we observe the following: Time-varying strategies which reduce the multiplier in times of volatile markets substantially outperform CPPI strategies. The result is robust for all performance measures under consideration. Finally, it is interesting to observe that the ranking of $m_{t,\text{A1}}$ and $m_{t,\text{A2}}$ is changed by the introduction of transaction costs. While $m_{t,\text{A1}}$ gives better results than $m_{t,\text{A2}}$ without transaction costs, the opposite is observed in the case of rather high transaction costs.

2.6 Conclusion

Recently, there is a growing trend to deviate from the concept of constant proportion portfolio insurance (CPPI) strategies. Instead of standardized constant multipliers, the industry relies on strategies with a rule based and time-varying multiple. We shed light on the question if the performance of constant proportion portfolio insurance (CPPI) strategies can be improved by means of such a time-varying multiplier.

Neglecting the inter-temporal hedging demand, the theoretical foundation of the strategies is given by maximizing the expected utility of a HARA investor in a diffusion model setup. Restricting the strategies to the myopic part of the multiplier implies the following distinction: If the risk premium is assumed to be proportional to the squared volatility, the optimal strategy is a constant proportion portfolio insurance (CPPI) strategy. Otherwise, the multiple is time–varying.

We use S&P 500 index return data for the time period 1985-2013 to evaluate the performance of *optimized* portfolio insurance strategies. In addition to an optimal constant multiplier, we consider multipliers which are either proportional to the inverse of the estimated future volatility or the inverse of the squared volatility. Also, we account for strategies proportional to the inverse of a power of the volatility where the power itself depends on the market conditions (regimes, respectively). The main focus is on historical volatility estimates. Performance comparisons directly based on the empirical return series are presented and discussed. We circumvent the problems caused by a limited number of observations by introducing a simulation model. A regime switching EGARCH model also helps to shed light on the performance of dynamic PPI strategies which can distinguish between different regimes. Furthermore, the simulation model allows to account for the impacts of transaction costs and trigger trading on the performance evaluation.

It turns out that the current industry approach of a rule based and time-varying multiplier which is linked to a rolling window of historical volatilities significantly outperforms the (optimal) constant proportion portfolio insurance strategies. The out-performance is robust w.r.t. alternative performance measures and levels of risk aversion of the HARA investor. The result is still valid accounting for proportional transaction costs and gap risk, if an adequate trigger trading and gap control is implemented. However, it also turns out that the time-varying multiplier strategies can further be improved by accounting for regime switching strategies, i.e. strategies proportional to a power of the volatility where the power itself depends on the market conditions.

CHAPTER 3

Robustness of stable volatility strategies

3.1 Introduction

The overall level of uncertainty in the market is time-varying. Dating back to Schwert [Sch89] and Campbell et al. [Cam92] it is a stylized fact that the volatilities of stock returns change substantially over time.[1] In general, this is also true for the volatility of portfolios. If an investor is interested in holding a portfolio with a (close to) constant volatility, she can rely on a stable volatility strategy in which the portfolio weight of the stock is inversely proportional to the volatility of the stock.[2]

The basic idea to achieve a constant volatility of the portfolio value is appealing. However, the question is whether this choice is also optimal, i.e. whether the portfolio value really should have a constant volatility. It can be shown that this is indeed the case if the investor has CRRA preferences and maximizes the expected utility of terminal wealth, there is no hedging demand, the stock price follows a diffusion process, and the expected excess stock return is proportional to the volatility of the stock. In reality, these restrictive conditions will most likely not be met, and the stable volatility strategy is suboptimal. The decisive question, however, is how good the strategy still is, or stated differently, how robust it is to model mis-specification. Indeed, recent empirical literature finds a rather good performance

1 Recent empirical studies about uncertainties in the market comprise e.g. Connolly et al. [Con05], Beber et al. [Beb09], Baele et al. [Bae10], Bollerslev et al. [Bol11] and Wachter [Wac13].

2 If the stock price follows a diffusion process, this strategy implies that the volatility of the resulting portfolio value is indeed constant. Scaling the portfolio to have constant volatility over time is widely applied in the asset management industry. Targeting an ex ante volatility is more common in practice than running constant leverage, cf. Barroso et al. [Bar15].

of stable volatility strategies.[3]

In this chapter we analyze whether stable volatility strategies are robust or close to optimal under model risk. It is well known that the solution to an optimization problem can lead to a very poor performance even if the true parameters differ only slightly from the parameters under which the optimal solution has been derived. This problem is highly relevant in portfolio optimization, as shown for example by DeMiguel et al. [DeM09] who find that optimal portfolios rarely outperform a naive benchmark. Since neither the true model nor the true parameters are known for sure, robust strategies which perform well in a whole class of models and/or for a whole set of parameters are particularly attractive.

The specification of a robust strategy starts with the set of models to take into account. In the present chapter, we rely on jump-diffusion models for the stock with stochastic volatility and stochastic jump intensity.[4] They capture both the risk of sudden large (usually downward) jumps and time-varying uncertainty. The models differ with respect to the assumptions on the expected excess return (constant, proportional to the diffusive return volatility, or proportional to the diffusive return variance) and on the jump intensity (zero, constant, proportional to the diffusive variance, or independent of the diffusive variance). The optimal strategies in the resulting twelve models follow by (numerically) solving the respective asset allocation problems. They are conditional on the specific models and thus subject to model risk.

One intuitive way to cope with model risk, that is, with the uncertainty about the true data-generating process, is robust portfolio optimization. In line with the classical robustness definition that mother nature plays against the investor, we rank the candidate strategies by the worst case certainty equivalent across all possible models. Our candidate strategies comprise the overall optimal strategies in the twelve models. In addition, we focus on simplified and easy-to-describe strategies. In a first step, we ignore the (highly model-dependent) hedging demand and rely on the (much less model-dependent) myopic demand only. The latter is based on the local risk-return trade-off, but no longer on the dynamics of the state variables. In a second step, we furthermore ignore the differences between jump

3 For example, Barroso et al. [Bar15] find that a stable volatility momentum strategy virtually eliminates crashes and nearly doubles the Sharpe ratio of the momentum strategy. Zieling et al. [Zie14] find that time-varying multiple portfolio insurance strategies based on a rolling window of historical volatility estimates give a significant improvement of CPPI strategies.

4 Empirical evidence supporting such a model setup comprises Bakshi et al. [Bak97], Bates [Bat00], Eraker et al. [Era03], and [Pan02].

and diffusion risk[5] and capture the risk by the local variance of the stock only. This results in an approximate myopic demand which is proportional to the ratio of the expected excess return and the local variance of the stock return. It can be interpreted as the 'common' component of the optimal strategies which they share across the different models. If the risk premium is proportional to the local volatility, the resulting strategy is indeed a stable volatility strategy. Taken together, our candidate strategies are given by the overall optimal strategies, the myopic strategies, and the approximate myopic strategies. We assess the performance of these strategies in all twelve reference models.

We take the characterization of the uncertainty set as given, i.e. we start with a given set of models. Our robust strategies depend on the choice of this set of models. They are thus subject to the same criticism as optimal strategies which depend on the choice of a specific model. A robust strategy may fail to be robust if the 'true' model is not included in this set of models. The question *'how robust is robustness?'* is highly relevant. To answer this question, we do not only assess the robustness of the strategies with respect to all models, but we also determine the strategies which are robust for some subsets of these models. This shows how robust the robust strategies are with respect to the specific choice of models.

The contribution of this chapter can be summarized as follows. We show that stable volatility strategies are indeed a robust portfolio choice w.r.t. a meaningful set of relevant models. We perform a simulation study to shed light on the importance of the (model dependent) hedging demand versus the exact (model dependent) myopic demand versus an approximate myopic demand which is based on the realized variance. In line with the empirical (out of sample and accounting for estimation risk) literature, the results provide a further justification for omitting the hedging demand.[6] The utility gain due to accounting for the hedging demand when the true model is known is very small and around 1 bp in our example. In case of model risk, the inclusion of the hedging demand can lead to a higher, but also to a lower utility, with potential gains and losses around 5-10 bp. There is thus no reason for the investor to include the (model-dependent) hedging demand, but she

5 [Liu03b] provide a detailed discussion of how jump and diffusion risk differ when it comes to finding the optimal strategy.

6 While, in sample, Sangvinatsos et al. [San05], Jurek et al. [Jur11], and Larsen et al. [Lar12], find utility gains resulting from accounting for the hedging demand, Diris et al. [Dir14] find the opposite in an out of sample analysis. Feldhütter et al. [Fel12] find that an investor with typical risk aversion is better off following a portfolio strategy implied by a misspecified but parsimonious model than a correctly specified but difficult to estimate model.

can rely on the myopic strategies.

The losses due to incorrect assumptions on the risk premium and the jump intensity can be much larger. When we rely on the expected utility in the respective worst case models, stable volatility strategies which are based on a risk premium that is proportional to volatility perform best. These strategies also minimize the maximal loss from model risk across all models that allow for jumps and nearly minimize it across all twelve models. When we turn to the approximate myopic strategy based on the realized variance, the argument for stable volatility strategies becomes even stronger. Again, they perform best in the respective worst case models. A direct comparison with strategies that scale the portfolio weight by the variance shows that the potential gains from stable volatility strategies by far exceed the potential losses.

The related literature deals in particular with topics linked to stable volatility strategies, portfolio planning, ambiguity/robustness, and robust portfolio optimization. Barroso et al. [Bar15] consider stable volatility strategies in form of risk-managed momentum and find that such strategies even give rise to a much greater puzzle than the original version. Zieling et al. [Zie14] give a performance evaluation of stable volatility strategies in the context of portfolio insurance. In particular, they find that time-varying multiple portfolio insurance strategies based on historical volatility estimates give a significant improvement of constant proportional portfolio insurance (CPPI) strategies. Ben Ameur et al. [BA14] use a quantile approach together with expected shortfall criteria. In particular, they provide explicit upper bounds on the multiple as functions of past asset returns and volatilities. Hamidi et al. [Ham14] also propose to use a conditional time-varying multiple and evaluate the use of a dynamic autoregressive expectile model for estimating the conditional multiple.

Concerning the literature on portfolio planning, references include Merton [Mer71] who solves the portfolio planning problem for a HARA investor with inter-temporal consumption. Amongst others, Kim et al. [Kim96] and Barberis [Bar00] consider optimal portfolios when the stock returns are predictable. Stochastic volatility and jumps are, for example, considered in Framstad et al. [Fra01], Liu et al. [Liu03b], Øksendal et al. [Øks05], Liu [Liu07], Branger et al. [Bra08] and Muck [Muc10]. More recently, Liu et al. [Liu13] propose a tractable and flexible portfolio choice model where market crashes can trigger switching into another regime with a different investment opportunity set. Elkamhi et al. [Elk14] analyze the portfolio choice problem in a model which allows for increased and asymmetric dependence between extreme return realizations.

Recognizing that the limitation of models is important for decision-making already dates

back to the seminal work of Gilboa and Schmeidler (1989). We also refer to the works of Hansen and Sargent ((2001), (2006), (2010)) and Cagetti et al. [Cag02].[7] An axiomatization of Hansen and Sargent's robustness preferences and the maxmin expected utility preferences of Gilboa et al. [Gil89] is given in Maccheroni et al. [Mac06] and Strzalecki [Str11].[8] Without postulating completeness, applications to portfolio optimization are analyzed by Chen et al. [Che02], Goldfarb et al. [Gol03], Epstein et al. [Eps03], Uppal et al. [Upp03], Maenhout [Mae04], Fabozzi et al. [Fab10], Buraschi et al. [Bur10], Ben Ameur et al. [BA13], and Ben-Tal et al. [BT13].[9]

The remainder of the chapter is organized as follows. Section 3.2 formulates the decision problem of a CRRA investor who faces model risk and introduces both the set of models and the set of candidate strategies. The (model dependent) portfolio planning problem of the investor is solved in Section 3.3. Section 3.4 reports the results of our simulation study in which we assess the performance of the overall optimal and approximate candidate strategies. Section 3.5 concludes.

3.2 The decision problem, strategies and models

In this section, we first describe the decision problem of a CRRA investor who faces model risk. In particular, we rely on a maxmin criterion. We then turn to the choice of a meaningful set of strategies. Recall that our research question goes beyond the determination of the robust strategy for one postulated model (confidence) set. Rather, we want to assess the robustness of easy-to-describe and tractable strategies. We focus on simplified versions of (model-dependent) overall optimal strategies and thus determine the candidate strategies simultaneously with the set of models. The models are given in the last part of this section.

3.2.1 The decision problem of the investor under model risk

Throughout the thesis, we consider a finite investment horizon T ($0 < T < \infty$). The investor has CRRA preferences and derives utility from terminal wealth Y_T only. If there

7 Much of the impetus also comes from the Hansen et al. [Han08] book titled Robustness.

8 In particular, Maccheroni et al. (2006) show that these robustness preferences are a specific subclass of variational preferences (VP). In addition, Strzalecki [Str11] establishes a link between the parameters of the multiplier criterion and the observable behavior of the agent.

9 An overview of developments in robust optimization since 2007 is given in Gabrel et al. [Gab14].

is no model risk, her optimization problem is

$$\begin{aligned} E[u(Y_T)] &\to \max \\ \text{where } u(x) &= \begin{cases} \frac{x^{1-\gamma}}{1-\gamma} & \text{for } \gamma > 0 \text{ and } \gamma \neq 1 \\ \ln(x) & \text{for } \gamma = 1. \end{cases} \end{aligned} \tag{3.1}$$

The optimization is done over all wealth distributions Y_T that result from admissible trading strategies, and the expectation is calculated w.r.t. one particular model setup.[10]

We use the certainty equivalent (CE) growth rate y^{CE} to describe the expected utility. The CE growth rate is defined by

$$\begin{aligned} u\left(Y_0 e^{y^{\text{CE}} T}\right) &= E\left[u(Y_T)\right], \\ \text{i.e. } y^{\text{CE}} &= \begin{cases} \frac{1}{T} \ln\left(E\left[\left(\frac{Y_T}{Y_0}\right)^{1-\gamma}\right]^{\frac{1}{1-\gamma}}\right) & \text{for } \gamma > 0 \text{ and } \gamma \neq 1 \\ \frac{1}{T} E\left[\ln \frac{Y_T}{Y_0}\right] & \text{for } \gamma = 1. \end{cases} \end{aligned} \tag{3.2}$$

It comprises the same information as the expected utility, but is the more convenient measure when we deal with model risk, since it allows for a comparison across different models.

The investor has neither a precise knowledge of the data generating process nor of its parameters. Hence, she is not able to implement the (model dependent) optimal strategy. For simplicity, assume that the investor commits herself to a finite set of strategies $\mathcal{A} = \{a_1, \dots a_n\}$ to choose from. For a finite discrete set of models $\mathcal{M} = \{m_1, \dots m_k\}$, her optimal strategy a^* is then given by

$$a^* = \text{argmax}_{a_i \in \mathcal{A}} \Phi\left(y_{i1}^{CE}, \dots, y_{ik}^{CE}\right),$$

where y_{ij}^{CE} denotes the certainty equivalent of strategy i $(i = 1, \dots, n)$ obtained w.r.t. model j $(j = 1, \dots, k)$, and Φ denotes some valuation function. In case of a worst case

10 For the sake of simplicity, we omit a concretization of models and admissible strategies for the moment.

valuation following the classical robustness approach, the function Φ is given by[11]

$$\Phi\left(y_{i1}^{CE}, \ldots, y_{ik}^{CE}\right) = \min\{y_{i1}^{CE}, \ldots, y_{ik}^{CE}\}.$$

The assumption of a finite set of models and strategies seems rather restrictive at a first glance but is in line with the objective of this chapter. Our main focus is on the robustness of strategies that are based on specific models with respect to the set of these models. The models represent opposing cases of assumptions on the risk premium and jump intensity. We next turn to the question of how to come up with sensible candidate portfolio strategies and models.

3.2.2 Motivation of model set $\mathcal{M}$ and strategy set $\mathcal{A}$

Our candidate strategies are based on a whole set of models instead of on one particular model. Furthermore, we do not rely on a set of models which includes the true model with a high confidence probability, but consider a finite (small) number of models which make rather different assumptions on the risk and return characteristics of the stock. We thus take a slightly different and more applied approach to portfolio choice under model risk than the one which is commonly used in the literature.[12] The idea behind our approach is to use the most representative strategy (which performs best across the whole set of models) instead of the most representative model (which best describes the data generating process), i.e. the strategy which embeds the common component of all model-dependent optimal strategies.

Intuitively, the most common component of the strategies is given by the myopic demand (some *robust* myopic demand, respectively).[13] Compared to the hedging demand the myopic demand is much less dependent on the specific model. The reason is that the myopic demand only depends on the local distribution of the stock return while the hedging demand relies on the stock price dynamics over the whole investment horizon and thus

11 An axiomatization of Hansen and Sargent's robustness preferences and the maxmin expected utility preferences of Gilboa et al. [Gil89] is given in Maccheroni et al. [Mac06] and Strzalecki [Str11].

12 To overcome the classical mean-variance portfolio optimization problems stemming from ignoring the estimation error, one strand of literature suggests to use Bayesian *shrinkage* estimators that incorporate a prior, or more recently multiple prior, cf. eg. Garlappi et al. [Gar07] and the literature mentioned herein.

13 A model dependent optimal portfolio strategy is called myopic if the optimal decisions of a long-term investor and an otherwise identical short-term investor coincide. For a detailed discussion of myopic portfolio choices we refer to Campbell et al. [Cam02].

also on the dynamics of the state variables.

In the following, we assume that the investor has access to a risky asset (the stock) and a risk-free asset. The myopic demand for the stock is driven by its risk-return trade-off and approximately given by

$$\text{myopic part} \approx \frac{\text{local expected excess return}}{\text{level of relative risk aversion} \times \text{local variance}}. \tag{3.3}$$

If there are no jumps in the stock price dynamics, Equation (3.3) is exact and gives the so-called Merton solution, cf. Merton [Mer73]. If the stock price can jump, Equation (3.3) becomes an approximation. More details are given in Section 3.3.

We assume that the stock price follows a jump-diffusion process (the exact dynamics are given in Section 3.2.3). The specific models in our model set and thus also the implied candidate strategies differ w.r.t. the assumptions on the expected excess return and the jump intensity. Estimating the expected excess return is notoriously difficult. An important distinction includes the relation between the local expected excess return $\mu_t - r$ and the local diffusion variance V_t. We distinguish the cases (RPV) $\mu_t - r = \mu_v V_t$, (RPσ) $\mu_t - r = \mu_\sigma \sqrt{V_t}$, and (RP0) $\mu_t - r = \mu_0$.[14] If the stock follows a diffusion process without any jumps, these assumptions imply a constant portfolio weight of the stock in the case (RPV), while the assumptions (RPσ) and (RP0) imply that the optimal strategy is inversely proportional to the volatility and the variance, respectively. Along the lines of Barroso et al. [Bar15] and the convention in the asset management industry, we call a strategy which is proportional to the inverse of the local volatility a stable volatility strategy.[15]

Jumps contribute to the overall uncertainty of the stock price, and one important question is whether the amount of jump risk varies over time or not.[16] The answer to this question has an impact on the local variance which comprises the diffusion variance and a jump risk component, where the latter is proportional to the jump intensity. If the jump intensity is a linear function of V (LV), the numerator of the approximate myopic demand is proportional

14 This in the line with the literature. While the theoretical literature on optimal portfolio planning often relies on the assumption (RPV) or (RP0) to obtain analytical tractability (cf. Liu [Liu07]), the assumption (RPσ) is consistent with a stable volatility strategy (cf. e.g. Barroso et al. [Bar15] and Zieling et al. [Zie14]). Chacko et al. [Cha05] allow the excess return to be an affine function of volatility.

15 If the stock price follows a diffusion process, this strategy implies that the volatility of the resulting portfolio value is indeed constant.

16 We follow the literature and assume that the jump intensity may be driven by state variables, while the distribution of the jump size is not.

to V. This is no longer true when the jump intensity is constant (L0) or when it is driven by some further state variable h (Lh). In addition, we also consider the case of no jumps (NJ).

In summary, our set of models is based on three different structural assumptions concerning the risk premium and four assumptions on the jump intensity, which are summarized in Table 3.1. The set of strategies is derived from this set of models and given in Table 3.2. In addition to the strategies which are optimal w.r.t. the respective models (and comprise the myopic part and the hedging demand), we consider strategies which only account for the myopic demand. For the latter, we look at the exact version and an approximative version (which is in addition based on the realized variance). Before we derive the first order condition which determines the strategies (Section 3.3), we give the general model setup which nests the twelve specific setups from above.

3.2.3 General jump diffusion model setup

We assume that the stock price S follows a general jump-diffusion process with stochastic volatility and stochastic jump intensity.[17] Uncertainty is introduced by a three dimensional Brownian motion $W = (W_S,W_V,W_h)$ and a Poisson process N. All processes are defined on a filtered probability space $(\Omega,(\mathcal{F}_t)_{0\leq t\leq T},P)$ satisfying the usual assumptions. The

Characterization of model set $\mathcal{M}$

Assumptions on risk premium $\mathcal{M}_1$	
$m_{1.}$ = RPV	risk premium proportional to local variance, i.e. $\mu_t - r = \mu_v V_t$
$m_{2.}$ = RPσ	risk premium proportional to local volatility, i.e. $\mu_t - r = \mu_\sigma \sqrt{V_t}$
$m_{3.}$ = RP0	constant risk premium, i.e. $\mu_t - r = \mu_0$
Assumptions on jump intensity $\mathcal{M}_2$	
$m_{.1}$ = L0	constant jump intensity, i.e. $l = l_0$
$m_{.2}$ = LV	jump intensity proportional to local variance, i.e. $l = l_v V$
$m_{.3}$ = Lh	jump intensity proportional to pure jump risk variable, i.e. $l = l_h h$
$m_{.4}$ = NJ	no jumps, i.e. $l = 0$

Table 3.1: The table gives our assumptions on the risk premia (upper panel) and on the jump intensity (lower panel) defining the model set $\mathcal{M} = \mathcal{M}_1 \times \mathcal{M}_2$.

17 Empirical evidence is e.g. given Bakshi et al. [Bak97], Bates [Bat00], Eraker et al. [Era03], and [Pan02]. For an analytical treatment of stochastic volatility and jumps we refer to [Duf00]

Characterization of strategy set ($\mathcal{A}$)

Assumptions on risk premium $\mathcal{A}_1$	
$a_{1..} = \text{RPV}$	risk premium proportional to local variance, i.e. $\mu - r = \mu_v V$
$a_{2..} = \text{RP}\sigma$	risk premium proportional to local volatility, i.e. $\mu - r = \mu_\sigma \sqrt{V}$
$a_{3..} = \text{RP0}$	constant risk premium, i.e. $\mu - r = \mu_0$
Assumptions on jump intensity $\mathcal{A}_2$	
$a_{.1.} = \text{L0}$	constant jump intensity, i.e. $l = l_0$
$a_{.2.} = \text{LV}$	jump intensity proportional to local variance, i.e. $l = l_v V$
$a_{.3.} = \text{Lh}$	jump intensity proportional to pure jump risk variable, i.e. $l = l_h h$
$a_{.4.} = \text{NJ}$	no jumps, i.e. $l = 0$
Distinction of myopic demand and hedging demand $\mathcal{A}_3$	
$a_{..1}$	(model dependent) myopic demand and hedging demand
$a_{..2}$	(model dependent) myopic demand
$a_{..2}$	approximative myopic demand (based on realized variance)

Table 3.2: The table characterizes our strategy set $\mathcal{A} = \mathcal{A}_1 \times \mathcal{A}_2 \times \mathcal{A}_3$.

dynamics of the stock price S and the diffusion variance V are given by

$$\begin{aligned} \frac{dS_t}{S_{t-}} &= \mu_t dt + \sqrt{V_t} dW_{t,S} + \left(e^{X_t} - 1\right) dN_t - E_{t-}\left[e^{X_t} - 1\right] l_t \, dt \\ dV_t &= \kappa_v \left(\theta_v - V_t\right) dt + \sigma_v \sqrt{V_t} \left(\rho \, dW_{t,S} + \sqrt{1-\rho^2} \, dW_{t,V}\right) \end{aligned} \tag{3.4}$$

where μ_t denotes the expected return on the stock, l_t denotes the intensity of N, and $e^{X_t} - 1$ is the jump size.

The stochastic diffusion variance V_t follows a square-root process with constant parameters θ_v (level of mean reversion), κ_v (speed of mean reversion), and volatility σ_v. The constant local correlation ρ between stock returns and the variance is usually negative and captures the leverage effect.

In line with the motivation above, we focus on the dependence of the expected return on the diffusion variance V_t and the diffusion volatility $\sqrt{V_t}$ such that we consider specifications given by[18]

$$\mu_t = r + \mu_0 + \mu_v V_t + \mu_\sigma \sqrt{V_t}$$

where r (risk-free interest rate), μ_0, μ_v, and μ_σ denote some non-negative constants. In

18 In particular, we do not consider an explicit dependence on pure jump intensity risk h.

the following, the main focus is on the three limiting cases of the risk premium, i.e. we rely on the assumptions (R0) $\mu_t - r = \mu_0$, (Rσ) $\mu_t - r = \mu_\sigma \sqrt{V_t}$, and (RV) $\mu_t - r = \mu_v V_t$ as summarized in the upper panel of Table 3.1.

N denotes a Poisson process with stochastic arrival intensity l_t. $\tilde{X}_t = e^{X_t} - 1$ is a random price-jump with mean $m_t = E_{t-}\left[\tilde{X}_t\right] < \infty$ and second central moment $m_t^{(2)} = E_{t-}[\tilde{X}_t^2] < \infty$ which is independent of the jump intensity l_t and across jump times. Since $\tilde{X}_t > -1$ by construction, positivity (limited liability) of S is guaranteed for arbitrary distributions of X_t. In line with the motivation above, the jump intensity can comprise a constant part, a part proportional to the diffusion variance V, and a part which is pure jump intensity risk, i.e. the jump intensity l_t is given by

$$\begin{aligned} l_t &= l_0 + l_v V_t + l_h h_t, \\ \text{where } dh_t &= \kappa_h \left(\theta_h - h_t\right) dt + \sigma_h \sqrt{h_t}\, dW_{t,h}. \end{aligned}$$

l_0, l_v, l_h are non-negative constants, i.e. $l_0, l_v, l_h \geq 0$.[19] In particular, $l_h > 0$ implies an additional randomness compared to $l_h = 0$. The dynamics of h are given by a square-root process with constat parameters θ_h (level of mean reversion), κ_h (speed of mean reversion), and volatility σ_h.[20] In summary, the above specification of the jump intensity nests our four different assumptions (L0) $l_t = l_0$, (LV) $l_t = l_v V_t$, (Lh) $l_t = l_h h_t$, or (NJ) $l_t = 0$ as summarized in the lower panel of Table 3.1.

3.3 Model dependent optimal portfolios

3.3.1 Portfolio planning problem – general setup

The objective of the investor is to maximize her expected utility of terminal wealth Y_T, i.e.

$$\max_{\{\phi_t, 0 \leq t \leq T\}} E[u(Y_T)], \tag{3.5}$$

where $(\phi_t)_{0 \leq t \leq T}$ is a previsible process and ϕ_t denotes the portfolio weight of the stock at time t. The utility function is given in Equation (3.1). For the stock price dynamics in Equation (3.4) and an initial wealth $Y_0 = y$, the dynamics $(Y_t)_{0 \leq t \leq T}$ of portfolio wealth

19 The HESTON [Hes93] stochastic-volatility model is obtained by the special case that $l_0 = l_v = l_h = 0$, i.e. in the case that jumps are not possible.

20 I particular, notice that we do not allow for any correlation between V and h here.

are given by

$$\frac{dY_t}{Y_{t-}} = (r + \phi_t(\mu_t - r))\,dt + \phi_t\sqrt{V_t}\;dW_{t,S} + \phi_t\tilde{X}_t dN_t - \phi_t m_t l_t\,dt. \tag{3.6}$$

Given our focus on stable volatility strategies, it is instructive to look at the impact of ϕ_t on the exposure of the portfolio to diffusion risk and jump risk. For a constant portfolio weight $\phi_t = \phi$ (for all $t \in [0,T]$), the diffusion variance of the portfolio wealth is increasing in V_t. The investor can reduce, offset or even reverse this increase by choosing a portfolio weight that is a decreasing function of V_t. In particular, a stable volatility strategy where ϕ_t is proportional to the inverse of the stock diffusion volatility $\sqrt{V_t}$ implies a constant exposure to diffusion risk. The impact on the jump risk exposure is more involved. Reducing the portfolio weight when the jump intensity of the stock increases does not reduce the intensity of jumps in the portfolio, but it reduces the size of these jumps. It is thus the average impact of jumps, given by the product of the jump intensity and the expected jump size, which the investor can control by changing the portfolio weight.

It is noteworthy that, unless there is no jump risk included ($l_0 = l_v = l_h = 0$), the investor has to deal with the risk of a large stock price change before she has the opportunity to adjust her portfolio weight. Because of this event-related *illiquidity* risk, the only way that the investor can guarantee that her wealth remains positive is by avoiding portfolio positions that are one jump away from ruin, cf. Liu et al. [Liu03b] and their Proposition 1. In the above context, where the support of X_t is not further restricted, the optimal portfolio weights ϕ_t^* are, if jumps are included, limited by the condition $0 < \phi_t^* < 1$.

Along the lines of Merton [Mer71], the indirect utility function of the investor denoted by $J = J(t,Y_t,V_t,h_t)$ is defined by

$$J(t,Y_t,V_t,h_t) = \max_{\{\phi_s, t \le t \le T\}} E[u(Y_T)].$$

Using the Martingale Principle of Optimal Control (MPOC), the HJB-equation for the

asset allocation problem is[21]

$$
\begin{aligned}
0 = \max_{\phi_t} \Bigg\{ & J_t + J_y Y_{t-} \left(r + \phi_t \left(\mu_t - r - m_t l_t\right)\right) + J_v \kappa_v \left(\theta_v - V_t\right) + J_h \kappa_h \left(\theta_h - h_t\right) \\
& + \frac{1}{2}\left(J_{yy} Y_{t-}^2 \phi_t^2 V_t + J_{vv} \sigma_v^2 V_t + J_{hh} \sigma_h^2 h_t\right) + J_{vy} Y_{t-} \phi_t \rho \sigma_v V_t \\
& + \left(E_{t-}\left[J\left(t, Y_{t-}\left(1 + \phi_t \tilde{X}_t\right), V_t, h_t\right)\right] - J\right) l_t \Bigg\},
\end{aligned}
$$

where J_t, J_Y, J_V, and J_h denote the partial derivatives of $J(t,Y_{t-},V_t,h_t)$ with respect to t, Y, V, and h. In addition, note that we have used the assumption that h is not correlated with the stock return and with the diffusion variance.

3.3.2 Portfolio planning problem – CRRA-investor

For a CRRA-investor with relative risk aversion $\gamma > 1$, we guess that the indirect utility function is

$$
J(t,Y_t,V_t,h_t) = \frac{Y_t^{1-\gamma}}{1-\gamma}\, g(t,V_t,h_t) \tag{3.7}
$$

with boundary condition $g(T,V,h) = 1$. Differentiating and inserting into the HJB equation gives

$$
\begin{aligned}
0 = \min_{\phi_t} \Bigg\{ & \frac{g_t}{g} + (1-\gamma)\left(r + \phi_t\left(\mu_t - r - m_t l_t\right)\right) + \frac{g_v}{g}\kappa_v\left(\theta_v - V_t\right) + \frac{g_h}{g}\kappa_h\left(\theta_h - h_t\right) \\
& - \frac{1}{2}\gamma(1-\gamma)\phi_t^2 V_t + \frac{1}{2}\frac{g_{vv}}{g}\sigma_v^2 V_t + \frac{1}{2}\frac{g_{hh}}{g}\sigma_h^2 h_t + (1-\gamma)\frac{g_v}{g}\phi_t \rho_{vs}\sigma_v V_t \\
& + \left(E_{t-}\left[\left(1 + \phi_t \tilde{X}_t\right)^{1-\gamma}\right] - 1\right) l_t \Bigg\}.
\end{aligned} \tag{3.8}
$$

Since the support of X_t is $\mathbb{R}$ in our subsequent numerical examples it follows that $\tilde{X}_t$ has support $]-1,\infty[$. With Proposition 1 of [Liu03b] the optimal portfolio weight is bounded by $]0,1[$ which means that, in the optimum, the investor does not take a short position or leveraged position in the risky asset. To guarantee the existence of an optimal portfolio weight we need to assume that the following mild regularity conditions are satisfied for all

21 For details, we refer e.g. to the textbook of Rogers [Rog13].

$\phi \in]0,1[$

$$M_t^{(1)} \equiv E_{t-}\left[\left(1+\phi\tilde{X}_t\right)^{-\gamma}\tilde{X}_t\right] < \infty \text{ and } M_t^{(2)} \equiv E_{t-}\left[\left(1+\phi\tilde{X}_t\right)^{1-\gamma}\right] < \infty.$$

Given the above regularity conditions there exists a solution of the portfolio planning problem posed by Equations (3.5) and (3.6). In particular, the value function is indeed of the form (3.7). The first-order condition for the optimal portfolio weight ϕ_t^* is given by

$$\mu_t - r - m_t l_t - \gamma\phi_t^* V_t + \frac{g_v}{g}\rho\sigma_v V_t + M_t^{*,(1)} l_t = 0 \tag{3.9}$$

such that

$$\phi_t^* = \frac{\mu_t - r}{\gamma V_t} + \frac{(M_t^{*,(1)} - m_t)l_t}{\gamma V_t} + \frac{\frac{g_v}{g}\rho\sigma_v}{\gamma}. \tag{3.10}$$

The optimal demand comprises the myopic demand and the hedging demand. The myopic demand follows from Equation (3.9) by setting g_v equal to zero. The hedging demand, which accounts for the difference between the optimal and the myopic demand, is driven by the dependence of the indirect utility function on the state variables, i.e. by g_v. It is equal to zero if the investor does not want to hedge variance risk (when $g_v = 0$) or is not able to hedge variance risk (when $\rho = 0$).[22]

To get an intuition about the structure of ϕ_t^*, we use a first order Taylor approximation[23]

$$\begin{aligned} M_t^{*,(1)} &\approx m_t - \gamma\phi_t^* m_t^{(2)} \\ \text{and } \phi_t^* &\approx \frac{\mu_t - r}{\gamma(V_t + m_t^{(2)} l_t)} + \frac{\frac{g_v}{g}\rho\sigma_v V_t}{\gamma(V_t + m_t^{(2)} l_t)}. \end{aligned} \tag{3.11}$$

The first term of the approximating ϕ_t^* is the myopic demand and the second term is the hedging demand. The approximate myopic demand is equal to the expected excess return on the stock, divided by the variance of the stock return, given by the sum of diffusion and jump variance, and the relative risk aversion.[24] Notice that w.r.t. the model set summarized by Table 3.1, the above approximation immediately implies a constant

22 There is no hedging demand for h, since the zero correlation between stock returns and h implies that the investor is not able to hedge h.

23 Using $f(x) = (1+x)^{-\gamma}$ and $x_0 = 0$ gives $f(x) \approx 1 - \gamma x$.

24 See also [Asc13] for approximating the jump components in portfolio planning problems and for an analysis of the resulting strategies.

myopic demand under model RPV/LV and model RPV/NJ. Intuitively, this motivates that closed-form solutions are possible in these special cases. In particular, in the case of no jumps a closed-form solution is derived in [Liu07]. [Liu03b] give a quasi-analytical solution for the model RPV/LV.

In general, the optimal portfolio weight ϕ_t^* depends on time t, the local diffusion variance V_t, and the jump intensity l_t such that the system of Equations (3.8) and (3.9) has to be solved numerically. A numerical approximation scheme is proposed in Appendix A.

3.4 Simulation Study

3.4.1 Simulation setup and implementation of strategies

The following numerical examples are based on independent and identically distributed X_t which are normally distributed $N(\mu_X,\sigma_X^2)$, i.e. we rely on a random jump size $\tilde{X}_t = e^{X_t} - 1$ with support $]-1,\infty[$. An investor who assumes a positive jump intensity will never take a leveraged or short position in the risky asset (see Section 3). As a consequence, we bound the portfolio weights to satisfy $\phi_t \in [0,1]$ for all $t \in [0,T]$ and for all strategies except the ones which explicitly do not account for jumps (NJ). In consequence, the approximate myopic strategies based on realized variance also account for (a part of) jump risk via the restriction $\phi_t \in [0,1]$.

For the model parameters we rely on the empirical results of [Era03]. The parameters for the risk premium and the jump intensity are set such that $\mu_0 = \mu_\sigma\sqrt{\theta_v} = \mu_v\theta_v$ and $l_0 = l_v\theta_v = l_h\theta_h$, respectively. The models thus give the same risk premium and the same jump intensity when the local diffusion variance V_t and jump intensity h_t are at their long run means. The parameters for the model with no jumps are chosen such that the local variance V_t is the same as in the other models when V_t is at its long-run mean, i.e. $\theta_v^{NJ} = \theta_v + E\left[\left(e^{X_t}-1\right)^2\right] l_v\theta_v$. The model parameters are summarized in Table 3.3.

We consider an investor with an investment horizon of two years ($T = 2$) and a relative risk aversion of $\gamma = 4$. The optimal strategies can either be solved for in closed form (for the case RPV/NJ), in semi-closed form (for the case RPV/LV) or have to determined numerically. In the latter case, we rely on a method detailed in Appendix A.

Benchmark parameter setup

Panel A: Assumptions on risk premium				
Param.	RP0	RPσ	RPV	
μ_0	0.08	—	—	
μ_σ	—	$\frac{0.08}{\sqrt{0.0205}}$	—	
μ_v	—	—	$\frac{0.08}{0.0205}$	
Panel B: Assumptions on stochastic volatility and jump intensity				
Param.	L0	LV	Lh	NJ
κ_v	3.2256	3.2256	3.2256	3.2256
θ_v	0.0205	0.0205	0.0205	0.0238
σ_v	0.2404	0.2404	0.2404	0.2404
ρ	-0.4668	-0.4668	-0.4668	-0.4668
κ_h	—	—	3.2256	—
θ_h	—	—	0.0205	—
σ_h	—	—	0.2404	—
μ_X	-0.0259	-0.0259	-0.0259	—
σ_X	0.0407	0.0407	0.0407	—
l_0	1.5170	—	—	—
l_v	—	$73.7463 = \frac{1.5170}{0.0205}$	—	—
l_h	—	—	$73.7463 = \frac{1.5170}{0.0205}$	—

Table 3.3: The table gives the parameters for the different models we look at. The base case (L0) is taken from [Era03]. We set $r = 0$ and $\mu_0 = \mu_\sigma\sqrt{\theta_v} = \mu_v\theta_v$ such that the risk premium is the same in all three models when V is at its long-run mean θ_v. We set $l_0 = l_v\theta_v = l_h\theta_h$ such that jump intensity is the same in all three models when V and h are at their long-run means θ_v and θ_h. The parameters for the model with no jumps are chosen such that the local variance is the same as in the other three models when V is at its long-run mean, i.e. $\theta_v^{NJ} = \theta_v + E\left[\left(e^X - 1\right)^2\right] l_v\theta_v$. Jumps in the log stock price follow a normal distribution with mean μ_X and variance σ_X^2.

3.4.2 Simulation results

The simulation results are summarized in Table 3.4.[25] It gives the certainty equivalent growth rates y_{ij}^{CE} defined in Equation (3.2) for each strategy $a_i \in \mathcal{A}$ and each model

25 We present lengthy tables at the end of this chapter.

$m_j \in \mathcal{M}$, cf. Table 3.2 and Table 3.1.[26] To simplify the exposition, we notate models by the assumptions on the risk premium and the jump intensity. The same holds true for the strategies, where the notation gives the assumptions for the reference model the strategy is based on.

We consider both the myopic strategies (upper panel of Table 3.4) and the overall optimal strategies (lower panel of Table 3.4) which comprise the myopic demand and the hedging demand. For the myopic strategies, we furthermore distinguish between the exact strategies and the approximate strategies, where the latter are based on an estimate of the realized variance[27]. The certainty equivalent (CE) growth rates for the approximate myopic strategies are given in the last two lines of the upper panel of Table 3.4.

In the following, we first compare the exact myopic strategies with the overall optimal strategies which also include a model-dependent hedging demand. We then focus on the myopic strategies only. We are interested in the robustness of the various strategies w.r.t. the whole model set and w.r.t. some relevant subsets of models. In particular, we are interested in the implications which both the assumptions on the risk premia and the assumptions on the jump intensity have.

Role of hedging demand

We first assess the importance of the hedging demand. Table 3.6 gives the gain in the CE growth rate from including the hedging demand for each strategy and in each model. Without model risk, the gain is of course positive or equal to zero. It is given on the diagonal. Economically, it is very small and amounts to 1.1 bp at most, so that the investor barely profits from the inclusion of the hedging demand.

When we turn to the cases with model risk, the CE growth rate can even drop due to the inclusion of the hedging demand, i.e. the investor may be better off with an (incorrect) myopic strategy than with an (incorrect) strategy that also includes the hedging demand. If the reference model relies on a risk premium which is proportional to the variance (RPV), the maximum loss from including the hedging demand is of the same order as the maximum gain (for L0, LV and Lh) or even exceeds it (for NJ). When the risk premium in

26 The results are based on 3 million simulations for each model. Simulation errors are provided in Table 3.5.

27 Along the lines of [Zie14], the realized variance RV_t is based on a simple rolling window of the latest 1 month (21 days) historical returns.

the reference model is proportional to the volatility (RPσ), the changes in the CE growth rate are very small and all well below 2 bp. If the reference model relies on a jump intensity proportional to h (RPσ/Lh), the gains are even non-negative across all models, but again negligible. In the case of a constant risk premium (RP0), potential profits cannot outweigh the possible losses from including the hedging demand if the reference model accounts for jumps (L0, LV and Lh). If the reference model does not account for jumps (RP0/NJ) and the true model does not include jumps either, the investor profits from including the hedging demand, and the maximum gain is 14.6 bp.

Overall, the potential gains and losses in the CE growth rate are below 20 bp.[28] As we will see in more detail in the following subsections, they are much smaller than the potential gains and losses due to model risk. The very small impact of the hedging demand is also confirmed by a comparison of the candidate strategies within the different models. The reference model which maximizes the CE growth rates is always the true model, which is obvious for strategies that include the hedging demand, but which needs not be the case for myopic strategies. The small gains and losses due to the omission of the hedging demand thus do not cause a change in the best strategy.

These results show that the hedging demand can basically be ignored. It leads to small gains only even if there is no model risk, and implies larger gains and losses when there is model risk. Put together, the small gains from its inclusion do not outweigh the potential losses when the reference model is not the true model. In the following, we thus focus on myopic strategies only.

Worst-case results

The myopic strategy is less dependent on the model than the hedging demand, but it still depends on the assumptions about the risk premium and the jump intensity. We now compare the performance of the (exact) myopic strategies over the whole model set $\mathcal{M}$. Table 3.7 gives the worst-case CE growth rates. It also states the worst-case model which gives rise to the worst CE growth rate.

The results show that the stable volatility strategy (RPσ) is indeed robust. While the worst-case CE growth rates of the strategies RPσ/L0, RPσ/LV and RPσ/Lh are 3.118%,

28 We back-tested the results for a longer investment horizon of $T = 10$ years. Qualitatively, we observe the same results as for the $T = 2$ year investment horizon. Potential gains and losses in the CE growth rate from including the hedging demand are below 25 bp.

3.11% and 3.09% respectively, the worst-case CE growth rates of the other strategies are all below 3%. To get the intuition, note that both the models and the strategies assume a risk premium that is constant (RP0), proportional to the volatility (RPσ), or proportional to the variance (RPV). The stable volatility strategy is based on the assumption RPσ and is thus a compromise between the three alternative specifications which avoids extreme implications for the scaling of the strategies.

In the following, we take a closer look at the impact which the assumptions on the risk premium and also on the jump intensity have. In particular, we want to find the robust assumptions.

Impact of assumptions on risk premium

To analyze the implications of mis-specification of the risk premium, we now focus on the opportunity cost which are defined as the difference between the maximal CE growth rate (when the myopic strategy from the correct reference model is used) and the CE growth rate of the strategy under consideration. Table 3.8 summarizes the opportunity costs of the exact and approximate myopic strategies for all models.

First, we consider the case in which the risk premium is proportional to V (RPV). If the jump intensity is proportional to V (LV), too, the optimal myopic portfolio weight is constant. The stable volatility strategy (RPσ/LV) scales the portfolio weight by the inverse of volatility and results in a utility loss of 0.222%. A scaling by $1/V$ which is based on the assumption of a constant risk premium (RP0) result in a bigger utility loss of 0.536%. The same picture holds true for other assumptions on the jump intensity in the reference model and/or the true model. Utility losses are smallest if the true assumption on the risk premium is used, moderate for stable volatility strategies, and increase significantly for strategies based on RP0.

Second, we turn to the case in which the true risk premium is proportional to the volatility (RPσ). For a jump intensity that is proportional to V (LV), the optimal portfolio weight is scaled by the inverse of volatility. The incorrect use of a constant portfolio weight (RPV/LV) results in a utility loss of 0.27%, while a scaling by the inverse of variance (RP0/LV) reduces the loss to 0.079%. A similar picture holds true for a jump intensity that is proportional to h (Lh) or constant (L0): utility losses are smaller for a reference model that incorrectly assumes a constant risk premium (RP0) than for a reference model that relies on a proportional risk premium (RPV). However, we observe the opposite effect if there are no jumps in the true model (NJ). Scaling by the inverse of variance (RP0/NJ)

results in a utility loss of 0.667%, while the use of a constant portfolio weight (RPV/NJ) results in a smaller utility loss of 0.459%.

Finally, we assume that the true risk premium is constant (RP0). For all strategies which account for jump risk (L0, LV and Lh), there is a clear ranking. Utility losses are smallest (below 0.022%) if the correct assumption on the risk premium is used (RP0), moderately increase to 0.059%-0.273% if the risk premium is assumed to be proportional to the volatility (RPσ), and are largest with values between 0.652% and 1.391% if the investor relies on a risk premium proportional to the variance (RPV). For strategies based on the assumption of no jump risk (NJ) the ranking is similar if the true data generating process does not include jumps (RP0/NJ). We observe a utility loss of 0.55% for the stable volatility strategy (RPσ/NJ), while the utility loss grows to 1.965% for the reference model proportional to the variance (RPV/NJ).

In summary, one can conclude that, as long as the investor accounts for jump risk, a scaling by $\frac{1}{\sqrt{V}}$ as immanent in the stable volatility strategies RPσ is rather robust to model mis-specification. Strategies based on either RPV or RP0 are more sensitive to model mis-specification and can induce larger opportunity costs. Furthermore, strategies based on RPσ outperform strategies based on RPV or RP0 in terms of the worst-case CE growth rate as well as in terms of the mean and medium CE growth rate. Stable volatility strategies thus perform best in case of uncertainty about the true risk premium.

Impact of assumptions on jump intensity

So far, we have mainly looked at the impact which the assumptions on the expected excess return have. These assumptions influence the nominator of the myopic demand. Now, we turn to the impact of the jump intensity and thus to the denominator of the (approximate) myopic demand.

Table 3.4 shows that the omission of jumps in the reference model (NJ) can result in prohibitively bad strategies. If the risk premium is assumed to be proportional to the level of volatility (RPσ) or constant (RP0), the expected utility can be equal to minus infinity if the true model allows for jumps, no matter whether the overall optimal strategy or the myopic strategy is used. Negative levels of terminal wealth are only avoided by the strategy based on a risk premium proportional to the local variance (RPV/NJ), which results in a constant portfolio weight. In our example this constant weight is smaller than one, so the investor does not take a leveraged position in the risky asset.

For a comparison of the strategies based on the assumptions of a constant (L0), proportional (LV), or independent (Lh) jump intensity, we again rely on the opportunity costs given in Table 3.8 and on the CE growth rates in Table 3.4. The differences between the strategies based on a jump intensity which is either constant or driven by some further risk factor h are small, with no clear ranking between these strategies. In contrast, the differences between these strategies and strategies based on a jump intensity which is proportional to V (LV) are a little more pronounced. However, there is still no clear ranking. The relative performance of the strategies depends on the assumed and the true risk premium.

In summary, opportunity costs are moderate if the investor relies on strategies which assume a positive jump intensity, while ignoring jumps can lead to infinity opportunity costs. The choice between a jump intensity which is proportional to V, proportional to h or constant depends on the assumptions on the risk premium.

Exact myopic part versus approximative solution

The last two lines of the upper panel of Table 3.4 give the CE growth rates for the approximate myopic strategies based on the realized variance. The realized variance RV_t is estimated using a rolling window of the returns over the last 21 days. The strategy RPσ/RV is defined by $\phi_t = \mu_\sigma/\gamma\sqrt{RV_t}$, and the strategy RP0/RV is given by $\phi_t = \mu_0/\gamma RV_t$, respectively. We thus scale the portfolio weight of the stock by the volatility and the variance, respectively.[29]

The CE growth rates show that the stable volatility strategy clearly outperforms the strategy that scales with 1/RV if the true model either assumes a risk premium proportional to the variance (RPV), or proportional to the volatility (RPσ). Utility gains are between 300 und 450 bp in the first case and between 80 and 140 bp in the second case. If the true model assumes a constant risk premium (RP0), then the strategy RP0/RV performs better than RPσ/RV. The utility losses from the use of the stable volatility strategy are all below 100 bp. Taken together, the potential gains outweigh the potential losses. We observe a worst-case CE growth rate of 2.994% for RPσ/RV, while the worst-case CE growth rate is 2.887% for the strategy that scales with 1/RV. The average CE growth rate of the approximative stable volatility strategy is 3.409%, while the average for the RP0/RV strategy is 3.275% (Table 3.7).

29 Notice that we need not consider the strategy RPV/LV based on the realized variance since the portfolio weight is constant and thus does not give rise to any scaling along the lines of the realized variance.

Finally, we compare the approximate myopic strategy RPσ/RV which is based on the realized variance to the exact myopic strategy RPσ/LV. The worst-case CE growth rate of the strategy RPσ/LV (3.118%) is slightly higher than the worst-case growth rate of the approximate strategy (2.994%). The strategy RPσ/LV also outperforms RPσ/RV if the risk premium is proportional to the volatility (RPσ) or constant (RP0). However, it performs worse if the true risk premium is proportional to the variance (RPV).

Robustness results

So far, we have looked at the performance of the strategies over the whole set $\mathcal{M}$ of models. Now, we turn to the question "how robust is robust?" and analyze the performance of the strategies in subsets of $\mathcal{M}$, too. Table 3.9 gives the worst-case CE growth rates for subsets of models.

If we only consider models with a proportional jump intensity (LV) or no jumps (NJ), stable volatility strategies that account for jump risk are even more robust. The worst case CE growth rate increases to 3.163% for the exact myopic strategies (and to 3.058% for the approximate myopic strategy RPσ/RV), while the other worst case CE growth rates are all smaller. Excluding only models without jumps does not change the ranking of the strategies either. The same holds true if we only consider models with a stochastic jump intensity. Stable volatility strategies based on RPσ/L0, RPσ/LV or RPσ/Lh are always superior to strategies that assume a constant risk premium (RP0) and thus scale with $1/V$ or strategies based on a proportional risk premium (RPV) which imply a constant myopic portfolio weight.

Only myopic demand

Strategy \ Model	RPV/L0	RPV/LV	RPV/Lh	RPV/NJ	RPσ/L0	RPσ/LV	RPσ/Lh	RPσ/NJ	RP0/L0	RP0/LV	RP0/Lh	RP0/NJ
RPV/L0	**3.600**	3.498	3.598	4.642	2.793	2.693	2.810	3.345	2.593	2.456	2.596	2.685
RPV/LV	3.555	**3.525**	3.554	4.614	2.972	2.945	2.991	3.547	3.068	3.005	3.071	3.130
RPV/Lh	3.573	3.476	**3.631**	4.634	2.771	2.674	2.846	3.337	2.582	2.447	2.645	2.683
RPV/NJ	3.504	3.452	3.503	**4.793**	2.740	2.685	2.762	3.443	2.770	2.661	2.771	2.858
RPσ/L0	3.288	3.369	3.288	4.285	**3.118**	3.206	3.139	3.717	3.604	3.664	3.609	3.720
RPσ/LV	3.204	3.302	3.205	4.178	3.110	**3.215**	3.131	3.706	3.660	3.739	3.665	3.783
RPσ/Lh	3.292	3.359	3.349	4.276	3.090	3.163	**3.166**	3.685	3.519	3.565	3.580	3.651
RPσ/NJ	$-\infty$	$-\infty$	$-\infty$	4.321	$-\infty$	$-\infty$	$-\infty$	**3.902**	$-\infty$	$-\infty$	$-\infty$	4.272
RP0/L0	2.930	3.057	2.931	3.783	3.029	3.162	3.049	3.568	**3.719**	3.832	3.725	3.830
RP0/LV	2.856	2.989	2.857	3.681	2.997	3.136	3.017	3.521	3.719	**3.838**	3.724	3.822
RP0/Lh	2.930	3.055	2.957	3.784	3.022	3.153	3.068	3.562	3.707	3.816	**3.738**	3.817
RP0/NJ	$-\infty$	$-\infty$	$-\infty$	2.747	$-\infty$	$-\infty$	$-\infty$	3.235	$-\infty$	$-\infty$	$-\infty$	**4.823**
RPσ RV	3.311	3.339	3.319	4.464	2.994	3.058	3.023	3.697	3.362	3.421	3.374	3.549
RP0 RV	2.967	3.016	2.978	4.003	2.887	2.977	2.915	3.557	3.416	3.518	3.430	3.638

Myopic and hedging demand

Strategy \ Model	RPV/L0	RPV/LV	RPV/Lh	RPV/NJ	RPσ/L0	RPσ/LV	RPσ/Lh	RPσ/NJ	RP0/L0	RP0/LV	RP0/Lh	RP0/NJ
RPV/L0	**3.608**	3.494	3.606	4.707	2.745	2.632	2.763	3.325	2.525	2.369	2.528	2.614
RPV/LV	3.565	**3.530**	3.564	4.680	2.939	2.906	2.959	3.545	3.020	2.947	3.023	3.090
RPV/Lh	3.577	3.470	**3.640**	4.695	2.721	2.612	2.801	3.315	2.513	2.360	2.579	2.612
RPV/NJ	3.443	3.383	3.442	**4.804**	2.617	2.551	2.640	3.361	2.619	2.491	2.620	2.717
RPσ/L0	3.292	3.373	3.291	4.298	**3.118**	3.206	3.139	3.725	3.602	3.663	3.607	3.724
RPσ/LV	3.206	3.304	3.207	4.182	3.110	**3.215**	3.132	3.708	3.659	3.738	3.664	3.783
RPσ/Lh	3.296	3.364	3.351	4.290	3.092	3.167	**3.166**	3.694	3.525	3.572	3.583	3.660
RPσ/NJ	$-\infty$	$-\infty$	$-\infty$	4.321	$-\infty$	$-\infty$	$-\infty$	**3.902**	$-\infty$	$-\infty$	$-\infty$	4.273
RP0/L0	2.893	3.023	2.894	3.721	3.014	3.149	3.034	3.533	**3.720**	3.836	3.726	3.815
RP0/LV	2.813	2.948	2.814	3.611	2.977	3.118	2.997	3.479	3.717	**3.839**	3.722	3.803
RP0/Lh	2.893	3.021	2.922	3.721	3.007	3.140	3.053	3.526	3.707	3.820	**3.739**	3.801
RP0/NJ	$-\infty$	$-\infty$	$-\infty$	2.894	$-\infty$	$-\infty$	$-\infty$	3.341	$-\infty$	$-\infty$	$-\infty$	**4.834**

Table 3.4: The table gives the certainty equivalent growth rates y^{CE} (in percent per year) defined by Equation (3.2). The investment horizon is $T = 2$ years, and the portfolio is rebalanced daily. The results are based on 3 million simulations for each simulation model (in columns). Each row reports results for a chosen investment strategy. The bold numbers correspond to a strategy that is correctly chosen according to the data generating process. The last two lines in the upper panel contain additional results for the strategies based on an estimate of the realized variance RV_t which is estimated from a simple rolling window of the latest 1 month (21 days) historical returns. Strategy RPσ RV is defined by $\phi_t = \mu_\sigma/\gamma\sqrt{RV_t}$, and strategy RP0 RV is defined by $\phi_t = \mu_0/\gamma RV_t$. The lower panel reports results for strategies that also account for the hedging demand.

Only myopic demand

Strategy \ Model	RPV/L0	RPV/LV	RPV/Lh	RPV/NJ	RPσ/L0	RPσ/LV	RPσ/Lh	RPσ/NJ	RP0/L0	RP0/LV	RP0/Lh	RP0/NJ
RPV/L0	**0.005**	0.005	0.004	0.004	0.006	0.007	0.005	0.007	0.008	0.008	0.007	0.008
RPV/LV	0.005	**0.005**	0.004	0.004	0.006	0.006	0.005	0.007	0.007	0.007	0.007	0.007
RPV/Lh	0.005	0.005	**0.004**	0.004	0.006	0.007	0.005	0.007	0.008	0.008	0.007	0.008
RPV/NJ	0.006	0.006	0.005	**0.005**	0.008	0.008	0.006	0.008	0.009	0.010	0.009	0.010
RPσ/L0	0.004	0.004	0.004	0.004	**0.005**	0.005	0.005	0.005	0.006	0.006	0.006	0.005
RPσ/LV	0.004	0.004	0.004	0.004	0.005	**0.005**	0.005	0.005	0.006	0.006	0.006	0.005
RPσ/Lh	0.004	0.004	0.004	0.004	0.005	0.005	**0.005**	0.006	0.006	0.006	0.006	0.005
RPσ/NJ	–	–	–	0.005	–	–	–	**0.007**	–	–	–	0.006
RP0/L0	0.004	0.004	0.004	0.004	0.005	0.005	0.004	0.005	**0.006**	0.005	0.006	0.004
RP0/LV	0.004	0.004	0.004	0.004	0.005	0.005	0.004	0.005	0.005	**0.005**	0.005	0.004
RP0/Lh	0.004	0.004	0.004	0.004	0.005	0.005	0.004	0.005	0.006	0.005	**0.006**	0.004
RP0/NJ	–	–	–	0.006	–	–	–	0.008	–	–	–	**0.006**
RPσ RV	0.005	0.004	0.005	0.004	0.006	0.006	0.005	0.006	0.007	0.006	0.007	0.006
RP0 RV	0.005	0.004	0.004	0.004	0.005	0.005	0.005	0.006	0.006	0.006	0.006	0.005

Myopic and hedging demand

Strategy \ Model	RPV/L0	RPV/LV	RPV/Lh	RPV/NJ	RPσ/L0	RPσ/LV	RPσ/Lh	RPσ/NJ	RP0/L0	RP0/LV	RP0/Lh	RP0/NJ
RPV/L0	**0.006**	0.006	0.005	0.004	0.007	0.007	0.006	0.008	0.008	0.008	0.008	0.009
RPV/LV	0.005	**0.005**	0.004	0.004	0.006	0.007	0.005	0.007	0.008	0.008	0.007	0.008
RPV/Lh	0.006	0.006	**0.005**	0.005	0.007	0.007	0.006	0.008	0.008	0.008	0.008	0.009
RPV/NJ	0.007	0.007	0.005	**0.005**	0.008	0.009	0.006	0.009	0.010	0.011	0.010	0.011
RPσ/L0	0.004	0.004	0.004	0.004	**0.005**	0.005	0.005	0.006	0.006	0.006	0.006	0.005
RPσ/LV	0.004	0.004	0.004	0.004	0.005	**0.005**	0.005	0.005	0.006	0.006	0.006	0.005
RPσ/Lh	0.004	0.004	0.004	0.004	0.005	0.005	**0.005**	0.006	0.006	0.006	0.006	0.005
RPσ/NJ	–	–	–	0.005	–	–	–	**0.007**	–	–	–	0.006
RP0/L0	0.004	0.004	0.004	0.004	0.005	0.005	0.004	0.005	**0.005**	0.005	0.005	0.004
RP0/LV	0.004	0.004	0.004	0.004	0.005	0.004	0.004	0.005	0.005	**0.005**	0.005	0.004
RP0/Lh	0.004	0.004	0.004	0.004	0.005	0.005	0.004	0.005	0.005	0.005	**0.006**	0.004
RP0/NJ	–	–	–	0.005	–	–	–	0.007	–	–	–	**0.005**

Table 3.5: The table gives the standard errors ($\times 10^2$) of the CE growth rates in Table 3.4.

Gain in CE growth rates from including the hedging demand

Strategy \ Model	RPV/L0	RPV/LV	RPV/Lh	RPV/NJ	RPσ/L0	RPσ/LV	RPσ/Lh	RPσ/NJ	RP0/L0	RP0/LV	RP0/Lh	RP0/NJ
RPV/L0	**0.008**	-0.003	0.008	0.065	-0.048	-0.061	-0.047	-0.021	-0.068	-0.087	-0.069	-0.071
RPV/LV	0.010	**0.005**	0.010	0.066	-0.033	-0.039	-0.032	-0.001	-0.047	-0.057	-0.048	-0.040
RPV/Lh	0.004	-0.006	**0.008**	0.061	-0.050	-0.062	-0.045	-0.022	-0.069	-0.087	-0.066	-0.070
RPV/NJ	-0.061	-0.069	-0.061	**0.011**	-0.123	-0.134	-0.122	-0.082	-0.150	-0.169	-0.152	-0.141
RPσ/L0	0.004	0.004	0.004	0.013	**0.000**	0.000	0.000	0.008	-0.001	-0.001	-0.001	0.005
RPσ/LV	0.002	0.002	0.002	0.004	0.000	**0.000**	0.000	0.002	-0.001	-0.001	-0.001	0.000
RPσ/Lh	0.004	0.005	0.002	0.013	0.003	0.004	**0.000**	0.009	0.006	0.006	0.004	0.009
RPσ/NJ	–	–	–	0.000	–	–	–	**0.000**	–	–	–	0.000
RP0/L0	-0.037	-0.034	-0.037	-0.062	-0.015	-0.013	-0.016	-0.035	**0.001**	0.004	0.001	-0.015
RP0/LV	-0.043	-0.040	-0.043	-0.070	-0.020	-0.017	-0.020	-0.041	-0.002	**0.001**	-0.002	-0.019
RP0/Lh	-0.037	-0.035	-0.036	-0.063	-0.016	-0.014	-0.015	-0.036	0.000	0.003	**0.001**	-0.015
RP0/NJ	–	–	–	0.146	–	–	–	0.106	–	–	–	**0.011**

Table 3.6: The table gives the gain in the CE growth rates from the inclusion of the hedging demand in percentage points.

Worst case certainty equivalent rates (whole model set $\mathcal{M}$)

strategy	worst case	best case	mean	median
RPV/L0	2.456 (RP0/LV)	4.642 (RPV/NJ)	3.109	2.802
RPV/LV	2.945 (RPσ/LV)	4.614 (RPV/NJ)	3.331	3.100
RPV/Lh	2.447 (RP0/LV)	4.634 (RPV/NJ)	3.108	2.809
RPV/NJ	2.661 (RP0/LV)	4.793 (RPV/NJ)	3.162	2.814
RPσ/L0	3.118 (RPσ/L0)	4.285 (RPV/NJ)	3.500	3.486
RPσ/LV	3.110 (RPσ/L0)	4.178 (RPV/NJ)	3.492	3.481
RPσ/Lh	3.090 (RPσ/L0)	4.276 (RPV/NJ)	3.475	3.439
RPσ/NJ	$-\infty$	4.321 (RPV/NJ)	$-\infty$	$-\infty$
RP0/L0	2.930 (RPV/L0)	3.832 (RP0/LV)	3.385	3.365
RP0/LV	2.856 (RPV/L0)	3.838 (RP0/LV)	3.346	3.328
RP0/Lh	2.930 (RPV/L0)	3.817 (RP0/NJ)	3.384	3.357
RP0/NJ	$-\infty$	4.823 (RP0/NJ)	$-\infty$	$-\infty$
RPσ RV	2.994 (RPσ/L0)	4.464 (RPV/NJ)	3.409	3.350
RP0 RV	2.887 (RPσ/L0)	4.003 (RPV/NJ)	3.275	3.216

Table 3.7: The table summarizes the worst case certainty equivalent rates. The corresponding models generating the worst cases are added in brackets.

Opportunity costs

Strategy \ Model	RPV/L0	RPV/LV	RPV/Lh	RPV/NJ	RPσ/L0	RPσ/LV	RPσ/Lh	RPσ/NJ	RP0/L0	RP0/LV	RP0/Lh	RP0/NJ
RPV/L0	**0.000**	0.027	0.033	0.151	0.324	0.522	0.356	0.557	1.126	1.382	1.142	2.137
RPV/LV	0.045	**0.000**	0.078	0.180	0.146	0.270	0.175	0.356	0.652	0.833	0.667	1.693
RPV/Lh	0.027	0.048	**0.000**	0.160	0.346	0.540	0.320	0.565	1.138	1.391	1.093	2.140
RPV/NJ	0.096	0.072	0.128	**0.000**	0.378	0.530	0.404	0.459	0.950	1.177	0.967	1.965
RPσ/L0	0.312	0.155	0.343	0.508	**0.000**	0.009	0.027	0.185	0.116	0.174	0.129	1.103
RPσ/LV	0.396	0.222	0.427	0.616	0.007	**0.000**	0.035	0.196	0.059	0.099	0.073	1.040
RPσ/Lh	0.308	0.166	0.282	0.517	0.028	0.052	**0.000**	0.217	0.200	0.273	0.158	1.172
RPσ/NJ	∞	∞	∞	0.473	∞	∞	∞	**0.000**	∞	∞	∞	0.550
RP0/L0	0.670	0.468	0.701	1.010	0.089	0.053	0.117	0.334	**0.000**	0.006	0.013	0.993
RP0/LV	0.744	0.536	0.774	1.113	0.120	0.079	0.149	0.381	0.001	**0.000**	0.014	1.000
RP0/Lh	0.670	0.469	0.674	1.010	0.095	0.061	0.098	0.340	0.013	0.022	**0.000**	1.006
RP0/NJ	∞	∞	∞	2.046	∞	∞	∞	0.667	∞	∞	∞	**0.000**
RPσ RV	0.289	0.186	0.313	0.329	0.123	0.156	0.143	0.205	0.357	0.417	0.364	1.273
RP0 RV	0.633	0.508	0.653	0.790	0.231	0.237	0.251	0.345	0.303	0.320	0.308	1.185

Table 3.8: The table gives the opportunity costs, i.e. the difference between the CE growth rate when the correct reference model is used and the CE growth rates when another model is used.

Worst case certainty equivalent rates (subsets of models)

model subset	**LV, NJ**		**L0, LV, Lh**		**LV, Lh**	
strategy	worst case	best case	worst case	best case	worst case	best case
RPV/L0	2.456 (RP0/LV)	4.642 (RPV/NJ)	2.456 (RP0/LV)	3.600 (RPV/L0)	2.456 (RP0/LV)	3.598 (RPV/Lh)
RPV/LV	2.945 (RPσ/LV)	4.614 (RPV/NJ)	2.945 (RPσ/LV)	3.555 (RPV/L0)	2.945 (RPσ/LV)	3.554 (RPV/Lh)
RPV/Lh	2.447 (RP0/LV)	4.634 (RPV/NJ)	2.447 (RP0/LV)	3.631 (RPV/Lh)	2.447 (RP0/LV)	3.631 (RPV/Lh)
RPV/NJ	2.661 (RP0/LV)	4.793 (RPV/NJ)	2.661 (RP0/LV)	3.504 (RPV/L0)	2.661 (RP0/LV)	3.503 (RPV/Lh)
RPσ/L0	3.206 (RPσ/LV)	4.285 (RPV/NJ)	3.118 (RPσ/L0)	3.664 (RP0/LV)	3.139 (RPσ/Lh)	3.664 (RP0/LV)
RPσ/LV	3.215 (RPσ/LV)	4.178 (RPV/NJ)	3.110 (RPσ/L0)	3.739 (RP0/LV)	3.131 (RPσ/Lh)	3.739 (RP0/LV)
RPσ/Lh	3.163 (RPσ/LV)	4.276 (RPV/NJ)	3.090 (RPσ/L0)	3.580 (RP0/Lh)	3.163 (RPσ/LV)	3.580 (RP0/Lh)
RPσ/NJ	$-\infty$	4.321 (RPV/NJ)	$-\infty$	$-\infty$	$-\infty$	$-\infty$
RP0/L0	3.057 (RPV/LV)	3.832 (RP0/LV)	2.930 (RPV/L0)	3.832 (RP0/LV)	2.931 (RPV/Lh)	3.832 (RP0/LV)
RP0/LV	2.989 (RPV/LV)	3.838 (RP0/LV)	2.856 (RPV/L0)	3.838 (RP0/LV)	2.857 (RPV/Lh)	3.838 (RP0/LV)
RP0/Lh	3.055 (RPV/LV)	3.817 (RP0/NJ)	2.930 (RPV/L0)	3.816 (RP0/LV)	2.957 (RPV/Lh)	3.816 (RP0/LV)
RP0/NJ	$-\infty$	4.823 (RP0/NJ)	$-\infty$	$-\infty$	$-\infty$	$-\infty$
RPσ RV	3.058 (RPσ/LV)	4.464 (RPV/NJ)	2.994 (RPσ/L0)	3.421 (RP0/LV)	3.023 (RPσ/Lh)	3.421 (RP0/LV)
RP0 RV	2.977 (RPσ/LV)	4.003 (RPV/NJ)	2.887 (RPσ/L0)	3.518 (RP0/LV)	2.915 (RPσ/Lh)	3.518 (RP0/LV)

Table 3.9: The table summarizes the worst case certainty equivalent rates. The corresponding models generating the worst cases are added in brackets.

3.5 Conclusion

Stable volatility strategies scale the portfolio weight of the stock by the local volatility of the stock return. If the stock price follows a diffusion process, this results in portfolios with a constant 'stable' volatility. In this chapter, we have analyzed the performance and robustness of these strategies in a more general jump-diffusion model.

The investor is exposed to model risk and neither knows the structure of the risk premium (which may be constant, proportional to the volatility, or proportional to the variance) nor the structure of the jump intensity (which may be constant, proportional to the diffusive variance, or be driven by some factor which is uncorrelated with diffusive variance). She considers a set of strategies which are given by the optimal strategies as well as simplified versions of the optimal strategies which only account for the myopic demand.

We first find that the investor can safely ignore the hedging demand. While utility losses in the true model are small, ignoring the hedging demand may even be beneficial under model risk. Secondly, we find that the robust strategy is indeed based on the assumptions of a risk premium that is proportional to volatility, which implies that the investor should scale the portfolio weight (approximately) by the volatility. Thirdly, we show that the stable volatility strategy is also the most robust one when the optimal portfolio weight is based on some rolling-window estimate for the realized variance instead of the true local variance.

CHAPTER 4

A general Fourier transform method for basket option pricing

4.1 Introduction

Pricing and hedging multivariate contingent claims in general continuous-time financial models is a numerically intensive task. In most cases, closed-form solutions are not available. Simulation methods can always be used to approximate prices and sensitivities. However, in most models which account for stochastic volatility or stochastic correlation, discretization schemes must be applied. With a growing number of assets and increasing time to maturity, simulations can be very time consuming. In a recent paper, Caldana et al. [Cal14] introduce a method to compute lower and upper price bounds of basket options. Prices are obtained by one-dimensional Fourier transform inversion. Most notably, their method is applicable to all models with known joint characteristic functions. The approach is not limited to a certain class of pricing models, like the affine class. The authors study a lower price bound based on replacing the optimal exercise set by an approximating set. They define the approximating set by the event of the corresponding log-geometric basket exceeding some trigger constant. Since this approach implies sub-optimal exercising, it guarantees a valid lower pricing bound. As such, the trigger can be freely chosen. Caldana et al. [Cal14] invert the Fourier Transform according to some initial guess of the constant and then maximize the lower price bound w.r.t. the trigger level. The method is closely related to earlier work of Curran [Cur94], Rogers et al. [Rog95a] and other authors, but extends it to general model setup. The overall complexity of the method is quadratic in

the number of assets in the basket.[1]

Despite of being general and efficient, the method can be quite inaccurate, especially if some of the basket weights are negative. Basket options with positive and negative asset-weights are termed *basket spread* or *multi-asset spread* options. Basket spread options comprise the commonly known two-asset spread options as a special case. Spread and basket spread options are important hedging instruments in equity, fixed income, foreign exchange and commodity markets. Carmona et al. [Car03] give examples of basket spread options in energy and agricultural markets. A typical energy basket is the so-called *crack spread*, a spread between crude oil and one ore more petroleum products. Options on crack spreads, like a 3:2:1 spread on the difference between crude oil, heating oil and gasoline prices, trade over-the-counter as well as on organized exchanges. Oil refineries and other energy market participants use these options to hedge against price risk. A frequently traded commodity basket in the agricultural sector is the *soybean crush spread*, which is the difference between soy, soy oil and soy meal. Besides traded products, Li et al. [Li10] relate basket spread option valuation to the valuation of physical assets in the energy sector. As examples, they give the valuation of *fossil fuel electric power plants*, *transmission assets* and *natural gas storage facilities*. Alos et al. [Alo11] also mention the valuation of *tolling contracts*, the financial equivalents of physical power plants. Let us briefly review one example. According to Li et al. [Li10], one reasonable way to evaluate a fossil fuel power plant is to approximate its value by a portfolio of basket spread options with different maturities. The ultimate maturity should match the life span of the plant, say 15-20 years. Throughout the (discretized) life span, the owner receives a payoff equal to that of a basket spread call option written on the difference between electricity price and fuel price, emission permit prices, operating and maintenance costs. The total number of basket spread options to be priced easily exceeds 5000, if the life span of the plant is discretized on a fine (e.g. daily) basis. This example emphasizes the need for an accurate and efficient method to price a large number of basket spread options, particularly in models with non-standard price dynamics.

In this chapter we introduce two ways to sharpen the lower price bound of Caldana

1 Generalizing the work of Vorst [Vor92], Caldana et al. [Cal14] also present a method based on the arithmetic-geometric mean inequality. This method yields another lower bound, an upper bound, and a price approximation in between the bounds. It is even faster because the complexity is linear in the number of assets. However, this method is found to be less accurate than the method relying on an approximating exercise set.

et al. [Cal14], by refining the approximating set. The European arithmetic basket option is exercised if the price of the basket exceeds the strike level. Though, an arithmetic basket is hard to handle analytically even in basic financial models. Neither the distribution of this (weighted) sum is known, nor its characteristic function. In order to maximize the lower price bound we proceed by selecting an approximating set that is close to the optimal one. Caldana et al. [Cal14] approximate the exercise set by replacing the arithmetic basket by its geometric counterpart. First, we notice that choosing the asset weights of the geometric basket equal to those of the original arithmetic one, is surely a reasonable guess to define an approximating set. This guess is applied by Caldana et al. [Cal14]. However, at least theoretically, one could directly improve the accuracy of their method by maximizing the lower price bound over the trigger constant *and* the geometric basket weights. For a general n-asset basket this implies an $(n+1)$-dimensional maximization over the inverse Fourier integral. Mentioning that the geometric and arithmetic baskets can have substantially different distributional characteristics, we go another way and apply moment matching to find suitable weights for the geometric basket.

Regarding to the literature on moment matching, our method has a common ground with a hybrid method of Deelstra et al. [Dee10]. Working in the geometric Brownian motion framework, the authors fit two correlated log-normal random variables to the means, variances and the correlation of the positive and negative sub-baskets (both of which having strictly positive support). The sub-baskets are chosen according to the sign of the asset weights of the basket spread. Replacing the sub-baskets by the moment-matched variables, the multivariate problem collapses to that of a two-asset spread option. With regard to this much simpler pricing problem the exact Fourier transform solution of Hurd et al. [Hur10] applies, as well as a number of closed-form approximations. In particular, Deelstra et al. [Dee10] use either the spread option approximation of Li et al. [Li08], or an approximation based on comonotonicity theory. As mentioned above, the authors assume a geometric Brownian motion (GBM) model. Asset prices are distributed according to the log-normal law. Even though the sum of log-normal random variables is not log-normal distributed, this distribution is known to approximate the unknown distribution quite well. This holds at least if the dimension of the problem is not too high, cf. Borovkova et al. [Bor07]. Moreover, the approximation is the better the more homogeneous the (marginal) distributions of the assets are. This fact is demonstrated in a two-dimensional log-normal setting by Brigo et al. [Bri04]. At least in case of basket spread options, it motivates

the separation of the basket into a positive and a negative sub-basket.[2] In line with our argumentation, numerical results in Deelstra et al. [Dee10] indicate that the methods based on splitting the basket outperform methods who treat the basket as a whole. However, beyond the GBM case, in models with skewed and leptokurtic asset return distributions, replacing each sub-basket by a *single* (log-normal) random variable can lead to substantial pricing errors. As an alternative, we study the use of moment matching to select suitable weights for the approximating geometric sub-baskets.

The second improvement to the lower price bound of Caldana et al. [Cal14] comes from accounting for the non-linearity of the boundary of the exercise set. Convexity of the exercise set arises through the split of the basket. In Section 4.4 we graphically analyze the shape of the exercise bound for basket spread options. Due to numerical feasibility we constrain the method to deal with an exercise boundary between only two sub-baskets. Accounting for the non-linear boundary between more than two aggregates is generally possible, and could further contribute to the precision of the approach. But the dimension of the inverse Fourier integral grows according to the number of sub-baskets. This results in an exponentially increasing computational effort. Caldana et al. [Cal14] do not split the approximating log-geometric basket into a positive and a sub-basket, which is equivalent to a linear approximation of the convex exercise boundary (in logarithmic variables). Against, our method captures the convex boundary explicitly. In Theorem 1 we derive the two-dimensional Fourier Transform of piecewise linear and quadratic approximations of the exercise boundary. We also derive the conditions for these transforms to exist. The theorem builds on the work of Hurd et al. [Hur10], who derive an exact two-asset spread option pricing formula. We review their method in Section 4.3.2. Capturing non-linearity requires a two-dimensional Fourier inversion. The dimension of the inverse integral in our method is independent of the number of assets n. If non-linearity is not accounted for (or we price an option with zero strike), then only a one-dimensional inversion is required. The computational complexity in both cases is (at most) quadratic in the number of assets. If we denote by N the number of integration points (assuming an equal number of points in each direction for the double integral) then the complexity stemming from dimension n is $O(n^2N^2)$ for the nonlinear, and $O(n^2N)$ for the linear approximation. As a consequence,

2 Though, also a strictly positive basket option pricing problem can be refined by splitting the basket. Building on the results of Brigo et al. [Bri04], splitting is particularly valuable in the presence of negative correlation. For instance, an equity of a gold-mining company – typically negatively correlated to other shares – should be separated into a sub-basket to homogenize distributions.

both approaches do not suffer from the curse of dimensionality. As a result we find that the two-dimensional inversion is quite efficient. Applying a measure correction introduced in Section 4.6, we actually observe a linear increase of CPU times. In a jump diffusion model with correlated diffusive parts and correlated jump size distributions, it takes just about two seconds to price a basket spread option on $n = 200$ assets, cf. Table 4.9.

The contribution of this chapter can be summarized as follows. Two-dimensional Fourier transforms of piecewise linear and quadratic approximations of the exercise boundary between two sub-baskets are derived in closed-form. The transforms are generalized Fourier transforms, and we derive the appropriate integration contours in the complex hyperplane. The transforms allow us to capture the nonlinear nature of the exercise boundary within the framework of integral transforms. In contrast to the method of Caldana et al. [Cal14], we arrive at a lower price bound that converges to the true price in the special case of *two*-asset basket or spread options. For higher-dimensional pricing problems we introduce a moment matching method based on the characteristic function. For the two particular multivariate pricing models studied in the numerical section, we provide explicit formulas for the relevant moments. We introduce a simple and efficient regression- and moment-based procedure to fit the approximating exercise boundary to the true boundary. We finally show that the resulting hybrid pricing method significantly sharpens the lower price bound of Caldana et al. [Cal14].

The remainder of this chapter is organized as follows. Section 4.2 summarizes general assumption on the model set. Section 4.3 reviews the related literature. Since our method shares some features with both, the approach of Caldana et al. [Cal14] and the spread option formula of Hurd et al. [Hur10], we summarize (and partly extend) the methods in Section 4.3.1 and Section 4.3.2, respectively. Section 4.4 first illustrates the convexity of the exercise boundary. Building on the insights, Theorem 1 presents the Fourier transforms of piecewise linear and quadratic approximations of the exercise boundary. Section 4.5 details the proposed moment matching procedure. The resulting pricing formula and a measure correction approach, useful to efficient implement the formula, can be found in Section 4.6. Section 4.7 details two exemplary pricing models which are used for the numerical experiments in Section 4.8. Section 4.9 concludes.

4.2 General assumptions and basic notation

Throughout the chapter we assume that asset prices are modeled as exponential semi-martingales. Following Eberlein et al. [Ebe09], semi-martingales are the most general processes in the framework of arbitrage theory. Examples include general diffusions, (time-changed) Lévy prossesses, or affine processes. The processes are assumed to be defined on a probability space $(\Omega,\mathcal{F},P)$ equipped with a filtration $(\mathcal{F}_t)_{0\leq t\leq T<\infty}$, satisfying the usual conditions, cf. Jacod et al. [Jac03]. We assume that the joint characteristic function of the state variables is known, at least up to the (numerical) solution of a system of Riccati ordinary differential equations.

Denoting by n the dimension of the basket, we further assume that certain moments of the asset price vector $\mathbf{S}(T) \in \mathbb{R}^n_{\geq 0}$ exist. We will state the precise moment conditions, which are closely related to suitable integration contours in the complex (hyper-)plane, in the respective propositions and lemmas explicitly. Though, in order to guarantee that moment matching applies in general models combined with arbitrary finite maturities T, we need to impose the following conditions throughout. Let Φ_{X_T} and M_{X_T} denote the characteristic function and the moment generating function, respectively, of the $\mathbb{R}^n$-valued random vector $\mathbf{X}(T) = (X_1(T),...,X_n(T))'$ of logarithmic asset prices $\mathbf{S}(T)$. The characteristic and the moment generating function are simply related through $M_{X_T}(\mathbf{u}) = E[\exp\{\mathbf{u}'\mathbf{X}_T\}] = \Phi_{X_T}(-\mathrm{i}\mathbf{u})$. Let $\mathbf{e}_k$ denote the k-th element of the canonical basis in $\mathbb{R}^n$, i.e. the k-th column of an n-dimensional identity matrix. For $k,j = 1,...,n$, we assume that the first (two) (cross-)moments exist:

$$\mathbb{E}[S_k] \Leftrightarrow M_{X_T}(\mathbf{e}_k) \Leftrightarrow \Phi_{X_T}(-\mathrm{i}\mathbf{e}_k) < \infty$$
$$\mathbb{E}[S_j S_k] \Leftrightarrow M_{X_T}(\mathbf{e}_j + \mathbf{e}_k) \Leftrightarrow \Phi_{X_T}(-\mathrm{i}(\mathbf{e}_j + \mathbf{e}_k)) < \infty.$$

This chapter examines the pricing of European-type options. We assume that pricing takes place at time $t = 0$. The basket option has a finite maturity $t = T > 0$. Dealing with just two points in time, we skip the argument $t = T$, if ambiguity about it is ruled out. Vectors and matrices are labeled by bold symbols. To make lengthy formulas better readable, we use the free sub-index to denote $\mathbf{X}_T = (X_1(T),...,X_n(T))'$ instead of $\mathbf{X}(T)$.

Matrix notation is used quite inconsistently in the literature. To avoid ambiguity, it seems reasonable to fix some notation beforehand. Working with complex valued numbers, it is important to note that we use notation $\mathbf{x}'$ to denote *nonconjugated* matrix transpose. '$\circ$' denotes element-wise multiplication. The square of a matrix is also understood in an

element-wise sense, i.e. $\mathbf{x}^2 = \mathbf{x} \circ \mathbf{x}$. The same holds true for matrix powers other than two. Sums or differences of a scalar and a matrix are also element-wise, i.e. $x + \mathbf{y} = x\mathbf{1} + \mathbf{y}$, where the dimensions of $\mathbf{1}$ and $\mathbf{y}$ agree. For an $n \times n$ matrix $\mathbf{x}$, we denote by $diag(\mathbf{x})$ the $n \times 1$ column vector comprising diagonal elements of $\mathbf{x}$. If not stated otherwise, all vectors are defined as column vectors.

Throughout, the Fourier transform of a function f is denoted by $\widehat{f}$. Moment matched random variables X are characterized as $\widetilde{X}$.

4.3 Review of related methods

Closely related literature on basket and spread option pricing deals in particular with topics linked to *(i)* lower price bounds based on approximating sets, *(ii)* moment matching methods and *(iii)* nonlinear approximations of the exercise boundary. For a comprehensive review of the literature concerning *(i)*, *(ii)* and beyond, we refer to Caldana et al. [Cal14].[3] A detailed review on spread options pricing is provided by Carmona et al. [Car03]. Let us briefly review some recent papers not listed in the mentioned surveys. Brigo et al. [Bri04] analyze the precision of two moment matching methods. They use measures for the distance between the densities of the (simulated) arithmetic basket, and those of distributions used to approximate it. In their study, the arithmetic basket consists of two correlated log-normal random variables and the moment matching methods are based on log-normal and the shifted log-normal random variables, respectively. We will review some of their results on appropriate moment matching in Section 4.5. Very recently, Korn et al. [Kor13] improve on a method of Gentle [Gen93] based on replacing the arithmetic average by the geometric average. The improvement builds on the idea that, adding a large constant to each element of the basket, the arithmetic and geometric averages coincide asymptotically. Korn et al. [Kor13] focus on the log-normal framework, though the main result is model-independent. In the log-normal model the shifted asset prices follow shifted log-normal processes. The authors finally use moment matching to approximate the shifted log-normal by log-normal random variables. Through this approximation they obtain a closed-form pricing formula. Their method is however restricted to strictly positive baskets. Linders et al. [Lin14] generalize the method of Korn et al. [Kor13] to Lévy copula models. Additionally, they propose a generalization of the moment matching method of Brigo

3 The authors also list basket option pricing approaches that we did not mention yet. For instance, there are analytical methods for model free pricing bounds, n-dimensional FFT methods converging to the true price (but suffering from the curse of dimensionality), and finite-difference methods.

et al. [Bri04], where the first three moments of the arithmetic basket are used to fit an approximating random variable. Basket option prices are obtained by one-dimensional Fourier transform inversion. However, they also restrict both methods to baskets with only positive weights. Finally, PALETTA et al. [Pal14] assume a model where asset prices follow shifted log-normal processes with jumps. Using a Hermite polynomial expansion of the density function, they show how to match a (possibly higher) number of moments exactly. Their method is also applicable to baskets with negative weights. Though appealing, the method cannot directly be used in general models (stochastic volatility models, for example).

With respect to nonlinear approximation of the exercise boundary *(iii)*, we emphasize the papers of LI et al. [Li08] on two-asset spread option pricing, generalized to the multi-asset case in LI et al. [Li10]. The idea in LI et al. [Li08] is to approximate the exercise boundary by a quadratic function. Interestingly, they point out that the widely used spread option formula of KIRK [Kir95] implicitly involves a *linear* approximation of the exercise boundary. They show that accounting for the non-linearity considerably increases the accuracy of the result. according to the calculation of greeks, the improvement is even more pronounced. The coefficients of the quadratic function are determined by a Taylor expansion of the exercise boundary. The resulting pricing formula is obtained in closed-form. Their method, however, is restricted to the class of jointly normal return models.

With regard to generality and efficiency the method proposed by CALDANA et al. [Cal14] constitutes a remarkable exception. In the following we first review their lower price bound. Afterwards we turn to the exact spread option formula of HURD et al. [Hur10], and extend it in two ways. A review of both methods is a good starting point to develop our improved lower bound in Sections 4.4 – 4.6.

4.3.1 The Caldana et al. (2014) lower price bound

We basically follow the notation of CALDANA et al. [Cal14] and denote by $\mathbf{w} = (w_1,...,w_n)' \in \mathbb{R}^n_{\neq 0}$ a vector of fixed basket weights. At maturity T the arithmetic basket, consisting of n assets with time-t price vector $\mathbf{S}_t = (S_1(t),...,S_n(t))'$, is simply defined as the weighted sum:

$$A(T) = \sum_{k=1}^{n} w_k S_k(T).$$

If $\mathbf{w}$ consists of positive and negative weights, the basket is also referred to as a *basket spread*. The European basket call option with maturity T and strike price $K > 0$ is defined by the payoff $(A(T) - K)^+$, and the corresponding put option by $(K - A(T))^+$. To simplify the exposition, we focus on basket call options. Prices of basket put options can be obtained similarly, or by applying the put-call parity. The exercise set of the arithmetic basket call is defined as $\mathcal{A} = \{\omega \in \Omega \colon A(T) > K\}$. Assuming a constant instantaneous interest rate r, the basket option value at time $t = 0$ is expressed as the discounted expected value

$$C_K = e^{-rT}\mathbb{E}\left[(A(T) - K)^+\right] = e^{-rT}\mathbb{E}\left[(A(T) - K)I(\mathcal{A})\right],$$

where $I(.)$ is the indicator function, and $\mathbb{E} = \mathbb{E}^Q_{\mathcal{F}_0}$, is short notation to denote $\mathcal{F}_0$-conditional expectation subject to a (pricing) measure Q, under which the discounted price process $(e^{-rt}\mathbf{S}_t)_{t\in[0,T]}$ is a martingale. For $n > 1$, the exercise set $\mathcal{A}$ depends on a (weighted) sum of exponential semimartingales. Due to the generally unknown distribution of the sum, it is difficult to handle analytically. Hence, replacing $\mathcal{A}$ by a suitable approximating set defined through an analytically tractable random variable greatly simplifies the pricing problem.[4] A natural candidate is the geometric average

$$G(T) = \prod_{k=1}^{n} S_k(T)^{w_k}.$$

Caldana et al. [Cal14] denote the approximating set by $\mathcal{G}$. Replacing the true set $\mathcal{A}$ by *any* approximating set $\mathcal{G} \subset \Omega$, it holds

$$\mathbb{E}\left[(A(T) - K)I(\mathcal{G})\right] \leq \mathbb{E}\left[(A(T) - K)^+ I(\mathcal{G})\right] \leq \mathbb{E}\left[(A(T) - K)^+\right].$$

As a result, the expectation on the very left can even be negative. As we will show, this is actually relevant, if the convex boundary of set $\mathcal{A}$ is not appropriately captured by the boundary of set $\mathcal{G}$. To rule out negative option prices the authors suggest to take the maximum part. The lower price bound follows by discounting:

$$C^{\mathcal{G}}_K = e^{-rT}\mathbb{E}\left[(A_n(T) - K)I(\mathcal{G})\right]^+ \leq C_K. \tag{4.1}$$

4 We refer to Caldana et al. [Cal14] for a list of references applying this technique to basket, Asian and spread option pricing problems.

Concretely, CALDANA et al. [Cal14] define the approximating set as $\mathcal{G} = \{\omega : Y(T) > \varkappa\}$, where $Y(T) = \log G(T) = \mathbf{w}' \log \mathbf{S}_T$ denotes the log-geometric basket, and $\varkappa$ is a trigger level used to maximize the lower price bound. Denote $\mathbf{X}_t = (X_1(t),...,X_n(t))'$ the vector of logarithmic asset prices with elements $X_k(T) = \log S_k(T)$, $k = 1,...,n$. Similarly, let $\mathbf{X}_T^R$ denote the vector of log-returns with elements $X_k^R(T) = \log(S_k(T)/S_k(0))$. The characteristic function of the log-returns is defined as

$$\Phi_{X_T^R}(\mathbf{u}) = \mathbb{E}\left[e^{\mathrm{i}\mathbf{u}'\mathbf{X}_T^R}\right],$$

$\mathbf{u} = (u_1,...,u_n)'$. Using $Y(T) = Y(0) + \mathbf{w}'\mathbf{X}_T^R$, the joint characteristic function of $\mathbf{X}_T^R$ and $Y(T)$ is given by

$$\begin{aligned}\Phi_{(X_T^R,Y_T)}(\mathbf{u},u_0) &= \mathbb{E}\left[e^{\mathrm{i}\mathbf{u}'\mathbf{X}_T^R + \mathrm{i}u_0 Y(T)}\right] \\ &= \mathbb{E}\left[e^{\mathrm{i}(\mathbf{u}+u_0\mathbf{w})'\mathbf{X}_T^R + \mathrm{i}u_0 Y(0)}\right] \\ &= e^{\mathrm{i}u_0 Y(0)}\Phi_{X_T^R}(\mathbf{u}+u_0\mathbf{w}),\end{aligned} \tag{4.2}$$

where u_0 is a scalar argument. We recall the lower pricing bound of CALDANA et al. [Cal14] in the following lemma.

Lemma 1 *Choose a damping factor $\delta \in \mathbb{R}_{>0}$, and assume that $\mathbb{E}\left[e^{\delta\mathbf{w}'\mathbf{X}^R(T)}\right] < \infty$ as well as $\mathbb{E}\left[e^{(\delta\mathbf{w}+\mathbf{e}_k)'\mathbf{X}^R(T)}\right] < \infty$, $\forall k = 1,...,n$, where $\mathbf{e}_k$ denotes the k-th element of the canonical basis in $\mathbb{R}^n$. A lower bound for the basket (spread) option price is given by*

$$C_K^{\mathcal{G}} = \max_{\varkappa\in\mathbb{R}} C_K^{\mathcal{G}}(\varkappa),$$

$$C_K^{\mathcal{G}}(\varkappa) = \left(e^{-\delta\varkappa - rT}\frac{1}{\pi}\int_0^{+\infty} e^{-\mathrm{i}u\varkappa}\Psi_{(X_T^R,Y_T)}(u;\delta)du\right)^+,$$

$$\Psi_{(X_T^R,Y_T)}(u;\delta) = \frac{1}{\mathrm{i}u+\delta}\left[\sum_{k=1}^n w_k S_k(0)\Phi_{(X_T^R,Y_T)}(-\mathrm{i}\mathbf{e}_k, u-\mathrm{i}\delta) - K\Phi_{(X_T^R,Y_T)}(\mathbf{0}, u-\mathrm{i}\delta)\right].$$

The Fourier Transform is taken with respect to the trigger level $\varkappa$. This is similar to the European vanilla option pricing method of CARR et al. [Car99], who take the transform w.r.t. the log-strike. According to the optimization routine, it is instructive to note that the numerically costly part of the integrand, $\Psi_{(X_T^R,Y_T)}(u;\delta)$, does not depend on $\varkappa$. In order to

find the value of $\varkappa^*$ which maximizes the lower price bound, $\Psi_{(X_T^R,Y_T)}$ must be computed only once.

4.3.2 The Hurd & Zhou (2010) formula and extensions

The spread option pricing formula of HURD et al. [Hur10] is conceptually different. The authors separately treat the Fourier transform of the options' payoff, and the Fourier transform of the underlying distribution (i.e. the characteristic function). The payoff transform of a basic spread option, $P(x_1,x_2) = (e^{x_1} - e^{x_2} - 1)^+$, is derived in closed-form. The more general case $K \neq 0$ can be easily handled by scaling and interchange of S_1 and S_2.[5] We review their two-dimensional Fourier transform $\widehat{P}(\mathbf{u})$, $\mathbf{u} = (u_1,u_2)' \in \mathbb{C}^2$, of the payoff function $P(\mathbf{x})$, $\mathbf{x} = (x_1,x_2)' \in \mathbb{R}^2$, and the resulting pricing formula in the following lemma.

Lemma 2 *Selecting any real numbers $\boldsymbol{\varepsilon} = (\varepsilon_1,\varepsilon_2)'$ with $\varepsilon_2 > 0$ and $\varepsilon_1+\varepsilon_2 < -1$ guarantees that the dampened payoff $e^{\boldsymbol{\varepsilon}'\mathbf{x}}P(\mathbf{x})$ is in $L^1(\mathbb{R}^2) \cap L^2(\mathbb{R}^2)$, and its Fourier transform $\widehat{P}(\mathbf{u})$ exists. The payoff function can be recovered as a generalized inverse Fourier transform*

$$P(\mathbf{x}) = (2\pi)^{-2} \iint_{\mathbb{R}^2+\mathrm{i}\boldsymbol{\varepsilon}} e^{\mathrm{i}\mathbf{u}'\mathbf{x}}\widehat{P}(\mathbf{u})d^2\mathbf{u}, \quad \widehat{P}(\mathbf{u}) = \frac{\Gamma(\mathrm{i}(u_1+u_2)-1)\Gamma(-\mathrm{i}u_2)}{\Gamma(\mathrm{i}u_1+1)}, \tag{4.3}$$

where Γ denotes the complex gamma function. Assume that the process $\mathbf{X}_t = \log \mathbf{S}_t$ has independent increments (PII) denoted by $\mathbf{X}_t^R = \mathbf{X}_t - \mathbf{X}_0$, such that the characteristic function factorizes as

$$\Phi_{X_T}(\mathbf{u}) = \mathbb{E}\left[e^{\mathrm{i}\mathbf{u}'\mathbf{X}_T}\right] \overset{PII}{=} e^{\mathrm{i}\mathbf{u}'\mathbf{X}_0}\Phi_{X_T^R}^{PII}(\mathbf{u}), \quad \Phi_{X_T^R}^{PII}(\mathbf{u}) = \mathbb{E}\left[e^{\mathrm{i}\mathbf{u}'\mathbf{X}_T^R}\right], \tag{4.4}$$

where $\Phi_{X_T^R}^{PII}$ does not depend on $\mathbf{X}_0$. Further assume that $\mathbb{E}\left[e^{\boldsymbol{\varepsilon}'\mathbf{X}^R(T)}\right] < \infty$. The exact time-0 price of a two-asset spread option follows by two-dimensional Fourier transform inversion

$$Spr(\mathbf{X}_0) = e^{-rT}(2\pi)^{-2} \iint_{\mathbb{R}^2+\mathrm{i}\boldsymbol{\varepsilon}} e^{\mathrm{i}\mathbf{u}'\mathbf{X}_0}\Phi_{X_T^R}^{PII}(\mathbf{u})\widehat{P}(\mathbf{u})d^2\mathbf{u}. \tag{4.5}$$

5 For the special case $K = 0$ (i.e. an *exchange* or *Margrabe* option), one can define $Z(T) = X_1(T) - X_2(T)$, and the two-dimensional problem collapses to a one-dimensional call option pricing problem with $\log K = 0$. The characteristic function of $Z(T)$ is simply $\Phi_{Z_T}(u_z) = \Phi_{X_T}(u_z, -u_z)$, and any Fourier-based one-dimensional call price formula applies. $\Phi_{X_T}(\mathbf{u})$ is defined in Lemma 2.

Remark 1 *The factorization* (4.4) *allows to apply inverse 2d-FFT to obtain approximate spread option prices by discretizing the double-integral in* (4.5)*. This is because* $\mathbf{X}_0$ *only appears in the phase factor* $\exp(\mathrm{i}\mathbf{u}'\mathbf{X}_0)$*, while the rest of the integrand does not depend on the initial state. For a discretization with* $N \times N$ *steps, one call of the FFT yields an* $N \times N$ *grid of spread option prices corresponding to different initial log-spot prices* $\mathbf{X}_0$*. The use of FFT implies a complexity of order* $O(N \log N)$*.* Hurd *et al. [Hur10] however state that the pre-computations of the (costly) part of the integrand in* (4.5)*, are however of order* $O(N^2)$*. Our numerical experiments confirm this. Due to the overall quadratic effort, it is advisable to choose a fast converging quadrature rule to keep* N *as small as possible. The FFT requires equally spaced (Newton-Cotes) quadrature schemes. Often, the basic trapezoidal rule with slow (but smooth) convergence is applied. We refer to* Lord *et al. [Lor08] for a discussion of suitable FFT-quadrature schemes. As an alternative, we propose to use higher-order direct integration schemes instead of the FFT. As it is for the FFT, the order is* $O(N^2)$*. But* N *can be chosen considerably smaller. Through non-equally spacing, the Gaussian quadrature rules (amongst others) typically allow for faster convergence. If spread option prices have to be computed for more than one of the triples* $(S_1(0),S_2(0),K)$ *and the factorization in* (4.4) *applies, then the costly part of the integrand,* $\Phi^{PII}_{X^R_T}(\mathbf{u})\widehat{P}(\mathbf{u})$*, should be computed only once for all instances of* $\mathbf{u}$*. The integration step finally executes very fast, even for a high number of option prices.*[6] *But more importantly, the direct integration method can also be applied if the dynamics of* $\mathbf{X}_t$ *is non-homogenous. A (trivial) generalization of the Hurd & Zhou inversion method, applicable also to the non-independent increment class of models, reads*

$$Spr(\mathbf{X}_0) = e^{-rT}(2\pi)^{-2} \iint_{\mathbb{R}^2+\mathrm{i}\varepsilon} \Phi_{X_T}(\mathbf{u})\widehat{P}(\mathbf{u})d^2\mathbf{u}, \tag{4.6}$$

with $\Phi_{X_T}(\mathbf{u}) = \mathbb{E}\left[e^{\mathrm{i}\mathbf{u}'\mathbf{X}_T}\right] = e^{\mathrm{i}\mathbf{u}'\mathbf{X}_0}\Phi_{X^R_T}(\mathbf{u})$*, where* $\Phi_{X^R_T}(\mathbf{u})$ *is allowed to depend on* $\mathbf{X}_0$*. In particular, this generalization allows to apply the method in the case of models with mean-reverting price processes. Those processes are common in energy and commodity markets, where spread options are most frequently traded.*

6 For a detailed comparison of direct integration (DI), FFT and *fractional* FFT schemes applied to European vanilla options pricing, we refer to Kilin [Kil06]

Next, we show that it is straightforward to extend the Hurd & Zhou formula to the 2-asset basket option case with payoff $(S_1(T) + S_2(T) - K)^+$, $K > 0$.[7]

Proposition 1 *Consider the (modified) payoff function* $P(\mathbf{x}) = (e^{x_1} + e^{x_2} - 1)^-$, *where* $(.)^-$ *denotes the negative part. For any real numbers* $\boldsymbol{\varepsilon} = (\varepsilon_1,\varepsilon_2)'$ *with* $\varepsilon_1 > 0$ *and* $\varepsilon_2 > 0$, *the dampened payoff function* $e^{\boldsymbol{\varepsilon}'\mathbf{x}}P(\mathbf{x})$ *is in* $L^1(\mathbb{R}^2) \cap L^2(\mathbb{R}^2)$, *and its Fourier transform* $\widehat{P}(\mathbf{u})$, $\mathbf{u} = (u_1,u_2)' \in \mathbb{C}^2$, *is defined by*

$$\widehat{P}(\mathbf{u}) = -\frac{\Gamma(-\mathrm{i}u_1)\Gamma(-\mathrm{i}u_2)}{\Gamma(2 - \mathrm{i}(u_1 + u_2))}. \tag{4.7}$$

Assume that $\mathbb{E}\left[e^{\boldsymbol{\varepsilon}'\mathbf{X}(T)}\right] < \infty$ *and* $\mathbb{E}\left[e^{\mathbf{e}_k'\mathbf{X}(T)}\right] < \infty$, $k = 1,2$, *where* $\mathbf{e}_1 = (1,0)'$ *and* $\mathbf{e}_2 = (0,1)'$. *The exact time-0 price of an European two-asset basket call option is given by*

$$C(\mathbf{X}_0) = e^{-rT}\left(\sum_{k=1}^{2}\Phi_{X_T}(-\mathrm{i}\mathbf{e}_k) - 1 - (2\pi)^{-2}\iint_{\mathbb{R}^2+\mathrm{i}\boldsymbol{\varepsilon}}\Phi_{X_T}(\mathbf{u})\widehat{P}(\mathbf{u})d^2\mathbf{u}\right). \tag{4.8}$$

In the special case of processes with independent increments (PII), the factorization in equation (4.4) *applies and the pricing formula can be restated as*

$$C(\mathbf{X}_0) = e^{-rT}\left(\sum_{k=1}^{2}S_k(0)\Phi^{PII}_{X^R_T}(-\mathrm{i}\mathbf{e}_k) - 1 - (2\pi)^{-2}\iint_{\mathbb{R}^2+\mathrm{i}\boldsymbol{\varepsilon}}e^{\mathrm{i}\mathbf{u}'\mathbf{X}(0)}\Phi^{PII}_{X^R_T}(\mathbf{u})\widehat{P}(\mathbf{u})d^2\mathbf{u}\right),$$

where the double integral is now in a form that can be computed using the FFT.

Proof: The basket call option payoff function can be rewritten as

$$(e^{x_1} + e^{x_2} - 1)^+ = (e^{x_1} + e^{x_2} - 1) - (e^{x_1} + e^{x_2} - 1)^-.$$

The expectation of the first part on the right follows simply as $\sum_{k=1}^{2}\Phi_{X_T}(-\mathrm{i}\mathbf{e}_k) - 1$, by linearity of expectations and noting that $\mathbb{E}\left[e^{X_k(T)}\right] = \Phi_{X_T}(-\mathrm{i}\mathbf{e}_k)$, $k = 1,2$. Note that the second part $P(\mathbf{x}) = (e^{x_1}+e^{x_2}-1)^-$ is not integrable on $\mathbb{R}^2$, because it tends to the constant -1 for small values of $\mathbf{x}$. Though, the dampened payoff function $e^{\boldsymbol{\varepsilon}'\mathbf{x}}P(\mathbf{x})$, converges to zero if $\mathbf{x}$ approaches negative infinity, provided that both $\varepsilon_1 > 0$ and $\varepsilon_2 > 0$. Hence, $e^{\boldsymbol{\varepsilon}'\mathbf{x}}P(\mathbf{x})$

7 If $K \leq 0$, the maximum operator $(.)^+$ vanishes, and the option price collapses to a discounted sum of expectations.

is in $L^1(\mathbb{R}^2)$. Obviously, this also holds for the squared dampened payoff, and $L^2(\mathbb{R}^2)$-integrability is provided. By the Parseval-Plancherel theorem, $L^1(\mathbb{R}^2) \cap L^2(\mathbb{R}^2)$-integrability of the dampened payoff insures $L^2(\mathbb{R}^2)$-integrability of its dampened Fourier transform $e^{\boldsymbol{\varepsilon}'\mathbf{x}}\widehat{P}(\mathbf{u}) = \widehat{P}(\mathbf{u} - \mathrm{i}\boldsymbol{\varepsilon})$. Following Eberlein et al. [Ebe10], we define $g(\mathbf{x}) := e^{-\boldsymbol{\varepsilon}'\mathbf{x}}P(\mathbf{x})$, $\bar{g}(\mathbf{x}) := g(-\mathbf{x})$, $\bar{\mathbf{x}} := -\mathbf{X}(0)$, and $\varrho(d^2\mathbf{x}) := e^{\boldsymbol{\varepsilon}'\mathbf{x}}Q_{X_T^R}(d^2\mathbf{x})$, where $Q_{X_T^R}$ is the law of the vector of log-returns $\mathbf{X}_T^R$. In terms of the negative initial log-asset price vector $\bar{\mathbf{x}}$, the option price at time $t = 0$ reads

$$\begin{aligned} C(\bar{\mathbf{x}}) &= e^{-rT}\mathbb{E}\left[P(\mathbf{X}_T^R - \bar{\mathbf{x}})\right] \\ &= e^{-rT-\boldsymbol{\varepsilon}'\bar{\mathbf{x}}} \iint_{\mathbb{R}^2} e^{\boldsymbol{\varepsilon}'\mathbf{x}} g(\mathbf{x} - \bar{\mathbf{x}}) Q_{X_T^R}(d^2\mathbf{x}) \\ &= e^{-rT-\boldsymbol{\varepsilon}'\bar{\mathbf{x}}} \iint_{\mathbb{R}^2} e^{\boldsymbol{\varepsilon}'\mathbf{x}} \bar{g}(\bar{\mathbf{x}} - \mathbf{x}) \varrho(d^2\mathbf{x}) \\ &= e^{-rT-\boldsymbol{\varepsilon}'\bar{\mathbf{x}}} \bar{g} * \varrho(\bar{\mathbf{x}}), \end{aligned}$$

where $\bar{g} * \varrho(.)$ is the (two-dimensional) convolution of $\bar{g}$ and the measure ϱ. The convolution theorem states that the Fourier transform $\widehat{\bar{g} * \varrho}(\mathbf{u})$ of an absolutely integrable convolution $\bar{g} * \varrho$, is equal to the product of the Fourier transforms $\widehat{\bar{g}}(\mathbf{u})\widehat{\varrho}(\mathbf{u})$ $\forall \mathbf{u} \in \mathbb{R}^2$. Using assumption $\mathbb{E}\left[e^{\boldsymbol{\varepsilon}'\mathbf{X}(T)}\right] < \infty$, we have $\varrho(\mathbb{R}^2) = \int \varrho(d^2\mathbf{x}) < \infty$. Since $g \in L^1(\mathbb{R}^2)$, also $\bar{g} \in L^1(\mathbb{R}^2)$, and as a consequence of Young's inequality $\bar{g} * \varrho \in L^1(\mathbb{R}^2)$. Hence, the convolution theorem applies.

According to Eberlein et al. [Ebe10] the inverse Fourier integral is a Lebesgue integral, since g (and $\bar{g}$) is continuous. This holds even if the joint distribution does not posses a Lebesgue density. The option price is recovered as

$$\begin{aligned} C(\bar{\mathbf{x}}) &= \frac{e^{-rT}}{(2\pi)^2} \iint_{\mathbb{R}^2} e^{-(\mathrm{i}\mathbf{u}+\boldsymbol{\varepsilon})'\bar{\mathbf{x}}}\, \widehat{\bar{g}}(\mathbf{u})\widehat{\varrho}(\mathbf{u}) d^2\mathbf{u} \\ &= \frac{e^{-rT}}{(2\pi)^2} \iint_{\mathbb{R}^2} e^{-(\mathrm{i}\mathbf{u}+\boldsymbol{\varepsilon})'\bar{\mathbf{x}}} \widehat{P}(\mathrm{i}\boldsymbol{\varepsilon} - \mathbf{u}) \Phi_{X_T^R}(\mathbf{u} - \mathrm{i}\boldsymbol{\varepsilon}) d^2\mathbf{u}. \end{aligned}$$

Rewriting the option price in the conventional form, i.e. as a function of the log-initial asset prices $\mathbf{X}_0 = -\bar{\mathbf{x}}$, we get

$$\begin{aligned} C(\mathbf{X}_0) &= \frac{e^{-rT}}{(2\pi)^2} \iint_{\mathbb{R}^2} e^{(\mathrm{i}\mathbf{u}+\boldsymbol{\varepsilon})'\mathbf{X}_0} \widehat{P}(\mathbf{u} - \mathrm{i}\boldsymbol{\varepsilon}) \Phi_{X_T^R}(\mathbf{u} - \mathrm{i}\boldsymbol{\varepsilon}) d^2\mathbf{u} \\ &= \frac{e^{-rT}}{(2\pi)^2} \iint_{\mathbb{R}^2 + \mathrm{i}\boldsymbol{\varepsilon}} e^{\mathrm{i}\mathbf{u}'\mathbf{X}_0} \Phi_{X_T^R}(\mathbf{u}) \widehat{P}(\mathbf{u}) d^2\mathbf{u}. \end{aligned}$$

It remains to proof the payoff transform in equation (4.7), given by

$$\widehat{P}(\mathbf{u}) = \iint_{\mathbb{R}^2} e^{-\mathrm{i}\mathbf{u}'\mathbf{x}} P(\mathbf{x}) d^2\mathbf{x}, \qquad \mathbf{u} \in \mathbb{C}^2.$$

According to the modified payoff $P(\mathbf{x}) = (e^{x_1} + e^{x_2} - 1)^-$, we restrict the domain of integration to $\{\mathbf{x} \ : \ x_1 < 0, e^{x_2} < 1 - e^{x_1}\}$. Since the dampened payoff is absolutely integrable if the imaginary part $\Im(\mathbf{u}) = \boldsymbol{\varepsilon} > 0$, an application of Fubini's theorem gives

$$\begin{aligned}
\widehat{P}(\mathbf{u}) &= \int_{-\infty}^{0} e^{-\mathrm{i}u_1 x_1} \left[\int_{-\infty}^{\log(1-e^{x_1})} e^{-\mathrm{i}u_2 x_2} \left(e^{x_1} + e^{x_2} - 1\right) dx_2 \right] dx_1 \\
&= \int_{-\infty}^{0} e^{-\mathrm{i}u_1 x_1} \left[\frac{(1 - e^{x_1})^{1-\mathrm{i}u_2}}{\mathrm{i}u_2 + {u_2}^2} \right] dx_1 \\
&= -\frac{\Gamma(-\mathrm{i}u_1)\Gamma(-\mathrm{i}u_2)}{\Gamma(2 - \mathrm{i}(u_1 + u_2))}.
\end{aligned}$$

□

Hurd et al. [Hur10] also prove a multidimensional extension of the spread option pricing formula. It is applicable to basket spread options with payoff $(S_1(T) - S_2(T) - ... - S_n(T) - K)^+$, which is actually the special case of a basket spread option where the positive sub-basket consists of only *one* asset. To price such an option using the extended formula, however, n-dimensional Fourier inversion is required. The computational cost increases exponentially in n. The two-asset basket option pricing formula (4.8) can also be extended to general n-dimensional positive basket options with (scaled) payoff $(e^{x_1} + ... + e^{x_n} - 1)^+$. The proof for the payoff transform $\widehat{P}$ is based on induction and widely analog to the one in Hurd et al. [Hur10]. The resulting pricing formula requires n-dimensional integration and suffers from the curse of dimensionality. We briefly summarize our results for completeness.

Lemma 3 *Select any $\boldsymbol{\varepsilon} = (\varepsilon_1,...,\varepsilon_n)' \in I\!R^n_{>0}$, and assume that $\mathbb{E}\left[e^{\boldsymbol{\varepsilon}'\mathbf{X}(T)}\right] < \infty$. The exact price of an n-asset basket call option with payoff $(e^{x_1} + ... + e^{x_n} - 1)^+$ is given by*

$$C(\mathbf{X}(0)) = e^{-rT} \left(\sum_{k=1}^{n} \Phi_{X_T}(-\mathrm{i}\mathbf{e}_k) - 1 - (2\pi)^{-n} \int_{I\!R^n + \mathrm{i}\boldsymbol{\varepsilon}} \Phi_{X_T}(\mathbf{u}) \widehat{P}(\mathbf{u}) d^n\mathbf{u} \right),$$

with

$$\widehat{P}(\mathbf{u}) = -\frac{\prod_{k=1}^{n} \Gamma(-\mathrm{i}u_k)}{\Gamma(2 - \mathrm{i}\sum_{k=1}^{n} u_k)}.$$

4.4 Nonlinear exercise boundary transforms

After introducing some notation, this section illustrates the typical shape of the exercise boundary of a (basket) spread option. Then, Theorem 1 presents the Fourier transforms of piecewise linear and quadratic approximations of the exercise boundary. We study two different approximations because the piecewise linear approximation converges to the true convex boundary, while the quadratic one is numerically more efficient. As before, the maturity value of an arithmetic basket consisting of n assets is denoted by $A(T)$. $\mathbf{w}$ denotes the vector of asset weights. In the following, we focus on basket spread options. At least one asset weight is presumed to be strictly positive, and at least on is strictly negative. In consequence, the basket has support $A(T) \in \mathbb{R}$. Building on the insights of Brigo et al. [Bri04] and Borovkova et al. [Bor07], we split the basket into two sub-baskets according to the signs of the weights. We define

$$\mathbf{w}^+ := \mathbf{w} \circ I(\mathbf{w} > \mathbf{0}) \in \mathbb{R}^n_{\geq 0}, \qquad \mathbf{w}^- := |\mathbf{w}| \circ I(\mathbf{w} < \mathbf{0}) \in \mathbb{R}^n_{\geq 0}, \tag{4.9}$$

where $I(.)$ denotes the indicator function (operating element-wise), and '$\circ$' an element-wise product. We choose to define $\mathbf{w}^+$ and $\mathbf{w}^-$ as full-length $n \times 1$-vectors (filled with zeros at obvious instances) mainly because it considerably facilitates the notation. Following the definition, it holds $\mathbf{w} = \mathbf{w}^+ - \mathbf{w}^-$. We define two sub-baskets, both with positive support, by

$$A^+(T) := (\mathbf{w}^+)'\mathbf{S}(T) \in \mathbb{R}_{>0}, \qquad A^-(T) := (\mathbf{w}^-)'\mathbf{S}(T) \in \mathbb{R}_{>0}, \tag{4.10}$$

where $\mathbf{S}(T) \in \mathbb{R}^n_{>0}$ is the vector of terminal asset prices. In consequence, it holds $A(T) = A^+(T) - A^-(T)$.

Figure 4.1 illustrates the convex boundary of the exercise set $\mathcal{A} = \{\omega \ : \ \log A^+(T) > \log(A^-(T) + K)\}$ of a basket spread call option. Graphically, the option is exercises for all tuples $(\log A^+, \log A^-)$ located above the black line. Suppose that the true convex boundary is approximated by a linear one. First, think of the linear approximation to be a tangent to the true boundary. According to the two subsets where the real boundary lies above the

Figure 4.1: Exercise boundary of a basket spread call option in logarithmic coordinates

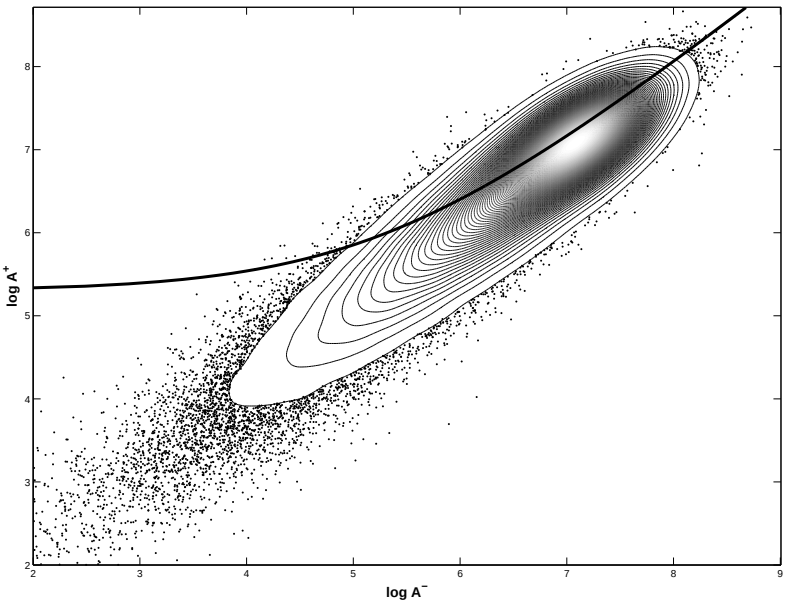

The black line depicts the boundary of the convex exercise set $\mathcal{A} = \{\omega : \log A^+(T) > \log(A^-(T) + K)\}$, where A^+ and A^- are the positive and the negative arithmetic sub-baskets, respectively. The joint distribution of asset prices follows from the jump-diffusion model described in Section 4.7.2. Parameters and basket weights are as in Table 4.7. Each sub-basket consists of 10 assets. Contract parameters are set according to $A^+(0) = 1000$, $A^-(0) = 900$ and $K = 200$ ($\log K \approx 5.3$), so the option is (slightly) out of the money. The unknown distribution of the arithmetic basket is approximated by 200,000 simulations. The outermost ellipse of the contour plot encases 99% of the simulated probability mass. As a smoothed contour plot is not useful to illustrate extreme realizations, we illustrate (most of) the bivariate 1% outliers by dots.

tangent, the true option payoff is zero, while the approximated one is negative. Alternatively, one can choose a straight line approximation which intersects the true boundary at two points. For this choice, there arises a third set enclosed by the linear and the real boundary. With regard to this set the true option payoff is positive, while the approximate one is zero. Of course, choosing the level and slope of a linear approximation in order to maximize the resulting lower price bound (due to suboptimal exercising) gives rise to an optimization problem.

Maximizing the lower price bound with respect to a (parametric) approximating exercise bound might also be interpreted as minimizing the probability-weighted absolute distance

between the true and the approximate boundary.[8] In fact, the slope of true boundary converges to zero for $\log A^- \to -\infty$, and to one for $\log A^- \to +\infty$, i.e. it approaches linearity in both directions. However, we add a contour plot (as a proxy for the bivariate density) to Figure 4.1, which illustrates that the true boundary in the relevant region (where probability mass is concentrated), is substantially non-linear.

Figure 4.2: Exercise boundary for different strike levels K

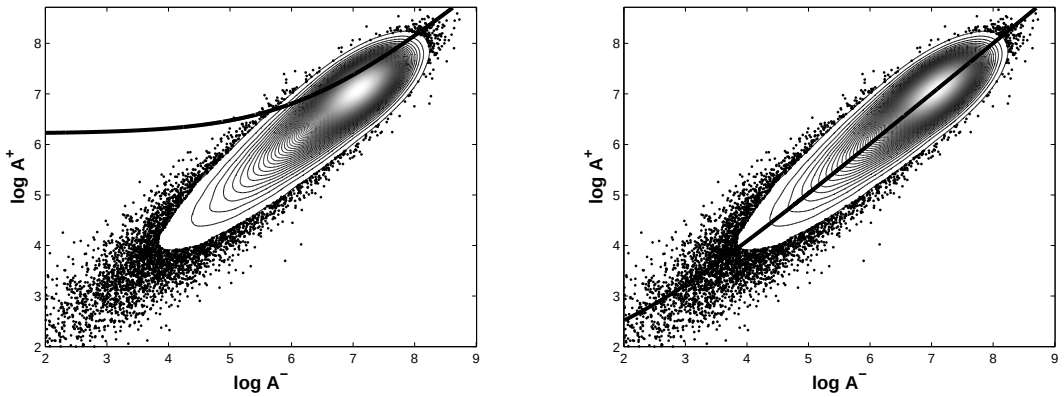

(a) Strike $K = 500$ (b) Strike $K = 5$

Setup as in Figure 4.1, but strike levels corresponding to deep out of the money and in the money options.

Figure 4.2 illustrates the effect of varying the strike level K on the convexity of the exercise boundary in the relevant region of the bivariate density. The left plot (a) corresponds to a deep out of the money (basket) spread call option with $K = 500$. In this case, it will obviously not be possible to find a linear approximation which yields a sharp lower price bound. Against, the plot on the right of Figure 4.2 corresponds to an in the money option with $K = 5$. Notice that in the special case $K = 0$ the true boundary is just the bisection line. In the most relevant part, the boundary for $K = 5$ is almost linear. Though, for $\log A^- \to -\infty$ the boundary approaches $\log K \approx 1.6$, i.e. convexity matters. However, by noting that the probability mass represented by the black 'outlier' dots is just 1% of the total mass, approximating the boundary by the bisection line (or something close to it) will yield a sharp lower price bound.

8 This interpretation holds at least if we do not take into account the second source of error which stems from approximating $(\log A^+, \log A^-)$ by appropriately chosen random variables.

As mentioned earlier, it is advisable to also separate a strictly positive basket into (two) more homogeneous positive sub-baskets. This turns out to be most relevant in the case of negative asset correlation. When splitting strictly positive baskets, the exercise boundary is concave rather than convex. An illustration can be found in Appendix B, Figure B.1. We focus on basket spread options in the following.

The approximate bivariate densities of $(\log A^+(T), \log A^-(T))$ in Figures 4.1 and 4.2 are based on Monte Carlo simulations. Unless applying time-consuming simulations, arithmetic baskets (and their log equivalents) are not feasible to work with. We rather approximate $(\log A^+(T), \log A^-(T))$ by some random variables $(Y^+(T),Y^-(T))$, which have a known joint characteristic function. Selecting appropriate random variables Y is the subject of Section 4.5. Actually, we will choose the variables to equal some modified log-geometric baskets. Let us for the moment assume that either $(Y^+(T),Y^-(T))$ are given, or the basket dimension is $n = 2$. In this special case of a 2-asset spread option, $(\log A^+(T), \log A^-(T))$ and $(Y^+(T),Y^-(T))$ agree, if the latter are chosen as the log-geometric sub-baskets (weighted asset prices, respectively).

Let us shorten the notation as $Y^+ = Y^+(T) \in \mathbb{R}$ and $Y^- = Y^-(T) \in \mathbb{R}$. According to an appropriately chosen parameter vector $\mathbf{c} = (c_0,c_1,c_2)'$, we define the quadratic approximation of the convex exercise set as

$$\mathcal{G}^{quad}(\mathbf{c}) := \{\omega \,:\, Y^+ > c_2(Y^-)^2 + c_1 Y^- + c_0\}. \tag{4.11}$$

The piecewise linear approximation is defined by a sum of event sets, where each subset is given by the event that Y^+ exceeds a linear function of Y^-, while at the same time Y^- is in an interval (b_j^l,b_j^u), $b_j^u > b_j^l$, $j = 1,...,M$, where $M > 1$ denotes the total number of intervals. Since Y^- takes values along the whole real line, the outermost intervals are chosen as $(-\infty,b_1^u)$ and (b_M^l,∞). Therefore, the approximation does not posses a *truncation error*. For $M \to \infty$, the approximation converges to the true continuous and monotone exercise boundary.[9] Denote $\mathbf{c} = (\mathbf{c}_0,\mathbf{c}_1)$ a $M \times 2$-matrix consisting of coefficient-vectors $\mathbf{c}_0 = (c_{0,1},...,c_{0,M})'$ and $\mathbf{c}_1 = (c_{1,1},...,c_{1,M})'$, fitted to match the exercise boundary at M

9 The total width of the interval of fitted straight line segments is given by (b_1^l,b_M^u), partitioned into M sub-intervals. Convergence is more precisely provided if $b_1^l \to -\infty$, $b_M^u \to \infty$ and $M \to \infty$. The slope of the true exercise boundary, however, converges to 0 for $A^-(T) \downarrow 0$, and it converges to 1 for $A^-(T) \to \infty$, respectively. It therefore suffices to choose the total width *large*, and then replace b_1^l by $-\infty$, and b_M^u by ∞. We provide explicit formulas to handle both, the lower and the upper sub-intervals of infinite length, hence avoiding a truncation error.

given sub-intervals (b_j^l,b_j^u) with $b_j^u > b_j^l$, and $b_j^u = b_{j+1}^l$. We define the approximate exercise set according to a piecewise linear boundary as

$$\mathcal{G}^{plin}(\mathbf{c}) := \begin{cases} \mathcal{G}^{plin}(\mathbf{c}_1, -\infty,b_1^u) + \mathcal{G}^{plin}(\mathbf{c}_2,b_2^l,\infty), & \text{if } M = 2 \\ \mathcal{G}^{plin}(\mathbf{c}_1, -\infty,b_1^u) + \sum_{j=2}^{M-1} \mathcal{G}^{plin}(\mathbf{c}_j,b_j^l,b_j^u) + \mathcal{G}^{plin}(\mathbf{c}_M,b_M^l,\infty), & \text{if } M > 2 \end{cases}$$

$$\text{where} \quad \mathcal{G}^{plin}(\mathbf{c}_j,b_j^l,b_j^u) = \left\{\omega \,:\, Y^+ > c_{1,j}Y^- + c_{0,j},\ Y^- \in (b_j^l,b_j^u)\right\},\ j = 1,...,M. \tag{4.12}$$

In the numerical Section 4.8 we comment on appropriate methods to fit the quadratic and the piecewise linear approximation.

The exercise set may be interpreted in terms of payoffs of digital options. The following theorem gives the Fourier transforms of the payoffs $I(\mathcal{G}^{quad})$ and $I(\mathcal{G}^{plin})$. In accordance to the last Section 4.3.2, we will denote the digital payoff transforms by $\widehat{P}(\mathbf{u};\mathbf{c})$. These transforms are the basis to derive pricing formulas according to payoffs $(A(T)-K)I(\mathcal{G}^x)$, $x \in \{quad,plin\}$, in Section 4.6. We explicitly write the coefficient vectors or matrices $\mathbf{c}$ as a second argument of $\widehat{P}$, since we will use them in Section 4.6 to numerically maximize the lower price bound.

Theorem 1 *According to the exercise sets $\mathcal{G}^{quad}$ and $\mathcal{G}^{plin}$ in (4.11) and (4.12), we follow the notion of payoffs of digital options, and denote by P^x, $x \in \{quad,plin\}$*

$$P^{quad}(\mathbf{y}) = I(y_1 > c_2y_2^2 + c_1y_2 + c_0) \tag{4.13}$$

$$P^{plin}_{-\infty,b^u}(\mathbf{y}) = I(y_1 > c_1y_2 + c_0,\ y_2 \in (-\infty,b^u)) \tag{4.14}$$

$$P^{plin}_{b^l,b^u}(\mathbf{y}) = I(y_1 > c_1y_2 + c_0,\ y_2 \in (b^l,b^u)) \tag{4.15}$$

$$P^{plin}_{b^l,\infty}(\mathbf{y}) = I(y_1 > c_1y_2 + c_0,\ y_2 \in (b^l,\infty)), \tag{4.16}$$

where $I(.)$ denotes the indicator function, $\mathbf{y} = (y_1,y_2)' \in \mathbb{R}^2$, $c_0,c_1,c_2,b^l,b^u \in \mathbb{R}$, $b^u > b^l$ and $-\infty < b^l,b^u < \infty$. The payoffs (4.13)–(4.16) can each be recovered by two-dimensional inverse Fourier transforms

$$P^x(\mathbf{y}) = (2\pi)^{-2} \iint_{\mathbb{R}^2+\mathrm{i}\varepsilon} e^{\mathrm{i}\mathbf{u}'\mathbf{y}} \widehat{P}^x(\mathbf{u};\mathbf{c}) d^2\mathbf{u}, \qquad x \in \{quad,plin\}, \tag{4.17}$$

under the following case-specific restrictions on $\boldsymbol{\varepsilon} = (\varepsilon_1,\varepsilon_2)'$ *and coefficients* $\mathbf{c}$

$$\widehat{P}^{quad}(\mathbf{u};\mathbf{c}) = -\frac{\mathrm{i}\sqrt{\pi}}{u_1\sqrt{\mathrm{i}u_1c_2}}\exp\left\{\frac{\mathrm{i}\left(u_1^2(c_1^2-4c_0c_2)+2u_1u_2c_1+u_2^2\right)}{4u_1c_2}\right\}$$
$$\text{with } \varepsilon_1<0 \text{ and } c_2>0, \tag{4.18}$$

$$\widehat{P}^{plin}_{-\infty,b^u}(\mathbf{u};\mathbf{c}) = \frac{1}{u_1(u_1c_1+u_2)}\exp\left\{-\mathrm{i}\left(u_1c_0+b^u(u_1c_1+u_2)\right)\right\}$$
$$\text{with } \varepsilon_1<0 \text{ and } \varepsilon_1c_1+\varepsilon_2>0, \tag{4.19}$$

$$\widehat{P}^{plin}_{b^l,b^u}(\mathbf{u};\mathbf{c}) = \frac{1}{u_1(u_1c_1+u_2)}\exp\left\{-\mathrm{i}\left(u_1c_0+(b^l+b^u)(u_1c_1+u_2)\right)\right\}$$
$$\times\left(\exp\left\{\mathrm{i}b^l(u_1c_1+u_2)\right\}-\exp\left\{\mathrm{i}b^u(u_1c_1+u_2)\right\}\right)$$
$$\text{with } \varepsilon_1<0, \tag{4.20}$$

$$\widehat{P}^{plin}_{b^l,\infty}(\mathbf{u};\mathbf{c}) = -\frac{1}{u_1(u_1c_1+u_2)}\exp\left\{-\mathrm{i}\left(u_1c_0+b^l(u_1c_1+u_2)\right)\right\}$$
$$\text{with } \varepsilon_1<0 \text{ and } \varepsilon_1c_1+\varepsilon_2<0. \tag{4.21}$$

If the boundary of the exercise set is convex, the transform of the piecewise linear approximation with M *straight-line segments can be written as*

$$\widehat{P}^{plin}(\mathbf{u};\mathbf{c}) = \begin{cases} \widehat{P}^{plin}_{-\infty,b_1^u}(\mathbf{u};\mathbf{c}) + \widehat{P}^{plin}_{b_M^l,\infty}(\mathbf{u};\mathbf{c}), & \text{if } M=2 \\ \widehat{P}^{plin}_{-\infty,b_1^u}(\mathbf{u};\mathbf{c}) + \sum_{j=2}^{M-1}\widehat{P}^{plin}_{b_j^l,b_j^u}(\mathbf{u};\mathbf{c}) + \widehat{P}^{plin}_{b_M^l,\infty}(\mathbf{u};\mathbf{c}), & \text{if } M>2 \end{cases} \tag{4.22}$$

by noting that the slope coefficients satisfy $0 \le c_{1,1} < c_{1,M}$*, such that the conflicting restrictions in* (4.19) *and* (4.21) *are both satisfied for all choices of* $\boldsymbol{\varepsilon}$ *with*

$$\varepsilon_1<0 \quad \text{and} \quad |\varepsilon_1c_{1,1}|<\varepsilon_2<|\varepsilon_1c_{1,M}|. \tag{4.23}$$

Proof: We start with the proof for the quadratic case. One directly observes that the payoff $I(y_1 > c_2y_2^2+c_1y_2+c_0)$ in (4.13) is not integrable, because it tends to one for large values of y_1. The payoff also tends to one for negative values of the coefficient c_2, if y_2 either approaches positive or negative infinity. In contrast, if $c_2>0$ the dampened payoff

$e^{\boldsymbol{\varepsilon}'\mathbf{y}}P^{quad}(\mathbf{y})$ for any $\varepsilon_1 < 0$ and $\varepsilon_2 \in \mathbb{R}$ converges. Note that the restriction $c_2 > 0$ is naturally satisfied in the case of a convex boundary. The dampened payoff is absolutely integrable and its Fourier transform exists. The discontinuous dampened payoff is also square integrable. This is easily seen by noting that the squared dampened digital payoff is simply $e^{2\boldsymbol{\varepsilon}'\mathbf{y}}P^{quad}(\mathbf{y})$. Taken together, it holds $e^{\boldsymbol{\varepsilon}'\mathbf{y}}P^{quad}(\mathbf{y}) \in L^1(\mathbb{R}^2) \cap L^2(\mathbb{R}^2)$, with $\boldsymbol{\varepsilon} = (\varepsilon_1,\varepsilon_2)',\ \varepsilon_1 < 0$ and $c_2 > 0$. The Fourier transform of the dampened payoff (following the standard notion of a Fourier transform with real argument $\mathbf{u}_r$) is given by

$$\widehat{P}^{quad}(\mathbf{u}_r;\mathbf{c}) = \iint_{\mathbb{R}^2} e^{(\mathrm{i}\mathbf{u}_r+\boldsymbol{\varepsilon})'\mathbf{y}}P^{quad}(\mathbf{y})d^2\mathbf{y}, \qquad \mathbf{u}_r \in \mathbb{R}^2.$$

Denoting $\mathbf{u} = -(\mathbf{u}_r - \mathrm{i}\boldsymbol{\varepsilon}) \in \mathbb{C}^2$, the transform can be rewritten as[10]

$$\widehat{P}^{quad}(\mathbf{u};\mathbf{c}) = \iint_{\mathbb{R}^2} e^{-\mathrm{i}\mathbf{u}'\mathbf{y}}P^{quad}(\mathbf{y})d^2\mathbf{y}, \qquad \mathbf{u} \in \mathbb{C}^2.$$

By the Parseval-Plancherel theorem $\widehat{P}^{quad}(\mathbf{u}) \in L^2(\mathbb{R}^2)$, and its inverse transform is given by (4.17). Applying Tonelli's theorem to the non-negative integrand $e^{-\mathrm{i}\mathbf{u}'\mathbf{y}}P^{quad}(\mathbf{y})$, we have

$$\begin{aligned}
\widehat{P}^{quad}(\mathbf{u};\mathbf{c}) &= \int_{-\infty}^{\infty} e^{-\mathrm{i}u_2y_2}\left[\int_{c_2y_2^2+c_1y_2+c_0}^{\infty} e^{-\mathrm{i}u_1y_1}dy_1\right]dy_2, \qquad c_0,c_1 \in \mathbb{R},\ c_2 \in \mathbb{R}_{>0},\\
&= \int_{-\infty}^{\infty} e^{-\mathrm{i}u_2y_2}\left[-\mathrm{i}(u_1)^{-1}e^{-\mathrm{i}u_1(c_2y_2^2+c_1y_2+c_0)}\right]dy_2\\
&= -\frac{\mathrm{i}\sqrt{\pi}}{u_1\sqrt{\mathrm{i}u_1c_2}}\exp\left\{\frac{\mathrm{i}\left(u_1^2(c_1^2-4c_0c_2)+2u_1u_2c_1+u_2^2\right)}{4u_1c_2}\right\},
\end{aligned}$$

completing the proof for the quadratic case.

Next, we turn to the three piecewise linear cases. It suffices to comment on appropriate choices of $\boldsymbol{\varepsilon}$, given any slope coefficient $c_1 \in \mathbb{R}$, such that $L^1(\mathbb{R}^2) \cap L^2(\mathbb{R}^2)$-integrability is provided for the dampened payoffs $e^{\boldsymbol{\varepsilon}'\mathbf{y}}P^{plin}(\mathbf{y})$. The final derivation of the transforms is very similar to the quadratic case. The case $P^{plin}_{b^l,b^u}(\mathbf{y}) = I(y_1 > c_1y_2 + c_0,\ y_2 \in (b^l,b^u))$ in (4.15) is particularly simple. Because of the bounded interval of y_2, it suffices to choose $\varepsilon_1 < 0$, such that the dampened payoff converges to zero if y_1 approaches positive infinity. With regard to the payoff $I(y_1 > c_1y_2 + c_0,\ y_2 \in (-\infty,b^u))$, $\varepsilon_1 < 0$ must also hold. The

10 The reason for the change of sign $\mathbf{u} = -(\mathbf{u}_r - \mathrm{i}\boldsymbol{\varepsilon})$ is visible in the proof of Proposition 1 and noting that the payoff transform here is specified according to initial values $\mathbf{y}_0$ (instead of $\bar{\mathbf{y}} = -\mathbf{y}_0$).

additional restriction $\varepsilon_1 c_1 + \varepsilon_2 > 0$ might be seen more directly by the following arguments. For all c_0,$c_1 \in \mathbb{R}$ we have

$$\begin{aligned}\widehat{P}^{plin}_{-\infty,b^u}(\mathbf{u};\mathbf{c}) &= \int_{-\infty}^{b^u} e^{-\mathrm{i}u_2 y_2}\left[\int_{c_1 y_2 + c_0}^{\infty} e^{-\mathrm{i}u_1 y_1} dy_1\right] dy_2, \\ &= \int_{-\infty}^{b^u} e^{-\mathrm{i}u_2 y_2}\left[-\mathrm{i}(u_1)^{-1} e^{-\mathrm{i}u_1(c_1 y_2 + c_0)}\right] dy_2.\end{aligned}$$

Inserting $\mathbf{u} = -(\mathbf{u}_r - \mathrm{i}\boldsymbol{\varepsilon})$, $\mathbf{u}_r = (u_{r,1},u_{r,2})' \in \mathbb{R}^2$, and splitting the integrand into its real and imaginary parts, it follows

$$\widehat{P}^{plin}_{-\infty,b^u}(\mathbf{u};\mathbf{c}) = (\varepsilon_1 + \mathrm{i}u_{r,1}) \int_{-\infty}^{b^u} e^{(\varepsilon_1 c_1 + \varepsilon_2) y_2} \times e^{\mathrm{i}(u_{r,1} c_1 + u_{r,2}) y_2} dy_2.$$

If y_2 approaches negative infinity, the real part $e^{(\varepsilon_1 c_1 + \varepsilon_2) y_2}$ of the integrand converges to zero if $\varepsilon_1 c_1 + \varepsilon_2 > 0$. The proof for the dampened payoff (4.16) follows with obvious variations. □

Remark 2 (Transform of the true exercise set) *Because of the simple structure of the exercise boundary, we can give the transform of the true boundary as well. For this, we write* $P(\mathbf{y}) = I(e^{y_1} - e^{y_2} - K)$, $K > 0$, *which resembles the payoff of a digital spread option. The Fourier transform of this payoff is very similar to the one of a normal spread option (cf. Lemma 2), and reads*

$$\widehat{P}(\mathbf{u};K) = K^{1-\mathrm{i}(u_1+u_2)} \frac{\Gamma(\mathrm{i}(u_1+u_2))\Gamma(-\mathrm{i}u_2)}{\Gamma(\mathrm{i}u_1+1)},$$

subject to the restrictions on $\Im(\mathbf{u}) = \boldsymbol{\varepsilon}$ *with* $\varepsilon_2 > 0$ *and* $\varepsilon_1 + \varepsilon_2 < 0$. *Notice, however, that we will use (at least some of) the coefficients* $\mathbf{c}$ *defined above in order to maximize the lower price bound. For the purpose of optimization, the above transform has only one free parameter,* K.[11] *The effect of varying* K *on the level and shape of the exercise boundary is illustrated in Figure 4.2. We propose to use the quadratic or piecewise linear approximation instead. In particular the quadratic approximation with three coefficients* (c_0,c_1,c_2), *all having a clear interpretation according to the level, slope and shape of the boundary, is typically found to give a sharper lower price bound than the above transform. Besides,*

11 Though another parameter could be introduced. Then, however, the transform yields a complicated structure based on generalized functions.

our simple transforms only involve the exponential function, i.e. it is not necessary to call the complex gamma function (three times). This makes it more efficient, even though appropriate coefficients $\mathbf{c}$ *must be found to initialize the optimization routine.*

With regard to converging approximations of the exercise boundary, it may however be desirable to look at approximations which converge faster to the true boundary than the piecewise linear one, while offering enough degrees of freedom. For instance, the transform of a piecewise quadratic approximation is also readily obtained in closed-form. To keep the exposition simple, we omit those results and focus on the simple transforms given above.

4.5 Moment matching basket distributions

In this section we detail a moment matching method for general models using the joint characteristic function of logarithmic asset prices. Throughout, we assume that the moments discussed beyond exist, cf. Section 4.2. We aim to find vectors of weights $\widetilde{\mathbf{w}}^+$ and $\widetilde{\mathbf{w}}^- \in \mathbb{R}^n_{\geq 0}$, replacing the original weights $\mathbf{w}^+$ and $\mathbf{w}^-$, to define modified log-geometric baskets $\widetilde{Y}^i = \widetilde{Y}^i(T) = (\widetilde{\mathbf{w}}^i)' \log \mathbf{S}(T)$, $i \in \{+,-\}$. The weights are chosen such that particular moments of $\widetilde{Y}^i$ match those of $\log A^i$. Using the moment generating or characteristic function, it is straightforward to compute the moments of $\widetilde{Y}^i$ and A^i in closed-form. The moments of $\log A^i$ are however generally unknown. We propose to take a detour by first posing a distributional assumption on A^i. Assuming a specific distribution, we can derive the moments of $\log A^i$ from those of the computed moments of A^i.[12] We detail each step of the moment matching procedure beyond. The relevant formulas are summarized at the end of this section.

1. *Moments of arithmetic sub-baskets.* Using the formulas in (4.27), the first and second moment (and the first cross-moment) of $A^i(T)$, $i \in \{+,-\}$ are computed analytically for general models.

2. *Approximate moments of* $\log A^i(T)$*.* The moments of $\log A^i(T)$ are generally unknown. Assuming that the joint distribution of the two sub-baskets $A^i(T)$ can be reasonably approximated by two correlated log-normal random variables, the formulas in (4.28) give closed-form expressions for $\mu_{\log A^i}$, $\sigma_{\log A^i}$ and $\rho^{ij}_{\log A}$. Other assumptions on the

12 Of course it is more simple to match the moments of a geometric basket G^i directly to those of the arithmetic basket A^i. However, the distributions of $\log G^i$ and $\log A^i$ can be very different, especially for higher number of assets involved. This follows by noting that $\log G^i$ is a sum of logarithms, while $\log A^i$ is the log of a sum. Numerical experiments reveal that our proposed method yields much better results.

distribution of the arithmetic sub-baskets, like a shifted log-normal (Borovkova et al. [Bor07]), or a log-extended skew normal (Zhou et al. [Zho08]), may also be reasonable choices. We however propose the simple log-normal assumption by two reasons. First, moment matching using the before-mentioned distributions involves solving a nonlinear system of three or more equations. Numerically, this can be quite unstable, as reported by Deelstra et al. [Dee10]. Second, the results of Borovkova et al. [Bor07] indicate that the simple log-normal assumption even provides a better fit if the basket distribution is positively skewed and the basket value cannot be negative. Note that through splitting the basket according to (4.10), we have $A^i(T) \geq 0$, $i \in \{+,-\}$, by construction. In typical practical applications (as well as in our examples), the distributions of sub-baskets A^i are also positively skewed.

3. *Matching $\sigma^i_{\log A}$ (and $\rho^{ij}_{\log A}$).* We aim to find weights $\widetilde{\mathbf{w}}^+$ and $\widetilde{\mathbf{w}}^-$, such that $\widetilde{Y}^i(T) = (\widetilde{\mathbf{w}}^i)' \log \mathbf{S}(T)$ share some of the (approximate) moments of $\log A^i$. Depending on the basket dimension n we propose to apply different methods. If the dimension is not too high, the numerical procedure detailed in 3.a attempts to match both $\sigma^i_{\log A}$ and $\rho^{ij}_{\log A}$ exactly. For higher-dimensional baskets we detail a simplified – but closed-form – approach in 3.b, which only matches $\sigma^i_{\log A}$.

   3.a *Moderate basket dimension.* If the dimension n is moderate, say $n = 3$ or $n = 4$, a numerical optimization routine can be efficiently applied to find weights $\widetilde{\mathbf{w}}^i$, such that the covariance matrices

$$\begin{pmatrix} \sigma^2_{\widetilde{Y}^+} & \rho^{+-}_{\widetilde{Y}} \sigma_{\widetilde{Y}^+} \sigma_{\widetilde{Y}^-} \\ \rho^{+-}_{\widetilde{Y}} \sigma_{\widetilde{Y}^+} \sigma_{\widetilde{Y}^-} & \sigma^2_{\widetilde{Y}^-} \end{pmatrix} \stackrel{!}{=} \begin{pmatrix} \sigma^2_{\log A^+} & \rho^{+-}_{\log A} \sigma_{\log A^+} \sigma_{\log A^-} \\ \rho^{+-}_{\log A} \sigma_{\log A^+} \sigma_{\log A^-} & \sigma^2_{\log A^-} \end{pmatrix}$$

   agree. The moments of $\log A^i$ are given in (4.28), and the ones of Y^i ($\widetilde{Y}^i$) in (4.31), respectively. In the numerical section we study one particular example of a basket spread option with $n = 3$ and payoff $(S_1 - S_2 - S_3 - K)^+$, i.e. the vectors of weights according to our definition in (4.9) are $\mathbf{w}^+ = (1,0,0)'$ and $\mathbf{w}^- = (0,1,1)'$. Since the positive sub-basket consists of only one weight, $\log A^+$ and Y^+ agree, and we directly set $\widetilde{\mathbf{w}}^+ = \mathbf{w}^+$. In this example the optimization routine is only applied to the two strictly positive weights contained in $\mathbf{w}^-$.

   3.b *Higher basket dimension.* If the dimension of the basket is high, numerical

optimization is too time-consuming. Instead, we only match $\sigma_{\widetilde{Y}^i}$ to $\sigma_{\log A^i}$ using

$$\widetilde{\mathbf{w}}^+ = \mathbf{w}^+ \frac{\sigma_{\log A^+}}{\sigma_{Y^+}}, \qquad \widetilde{\mathbf{w}}^- = \mathbf{w}^- \frac{\sigma_{\log A^-}}{\sigma_{Y^-}}, \tag{4.24}$$

which matches $\sigma_{\widetilde{Y}^i}$ exactly to the (approximate) $\sigma_{\log A^i}$, by noting that σ_{Y^i} is proportional to $\mathbf{w}^i$. The σ_{Y^i} are obtained using (4.31) with the original weights $\mathbf{w}^i$. We would like to emphasize that if one does not explicitly incorporate the correlations into the moment matching procedure, these quantities are nevertheless often found to be quite similar. In the example of Table 4.7 in Section 4.8.2 with $n = 20$ and a jump-diffusion specification for the asset prices, we find the true correlation to be $\rho^{+-}_{\log A} \approx 0.943$ (by simulation). Using the simple procedure (4.24) above, we have $\rho^{+-}_{\widetilde{Y}} = 0.933$, so the difference is rather small.

4. *Matching* $\mu_{\log A^i}$. In general, it is not possible to choose weights such that the first *and* the second moments are matched.[13] However, using the simple parametric form of the fitted exercise boundary based on either a quadratic or a piecewise linear approximation detailed in Section 4.4, we can shift (and spin) the boundary by adjusting the fitted coefficients $\mathbf{c}$. Define the difference of the first moments of $\log A^i$ and $\widetilde{Y}^i$ as $\mu^i_{\text{diff}} := \mu_{\log A^i} - \mu_{\widetilde{Y}^i}$. If the piecewise linear approximation (4.12) of the true exercise set is applied, the adjusted coefficients $\widetilde{\mathbf{c}} = (\widetilde{\mathbf{c}}_0, \widetilde{\mathbf{c}}_1)$ are obtained from the fitted coefficients $\mathbf{c}$ as

$$\begin{aligned} \widetilde{\mathbf{c}}_0 &= \mathbf{c}_0 + \mathbf{c}_1 \mu^-_{\text{diff}} - \mu^+_{\text{diff}}, \\ \widetilde{\mathbf{c}}_1 &= \mathbf{c}_1. \end{aligned} \tag{4.25}$$

If the quadratic approximation (4.11) with fitted scalar coefficients c_0, c_1 and c_2 is applied, the adjustment reads

$$\begin{aligned} \widetilde{c}_0 &= c_0 + c_2 (\mu^-_{\text{diff}})^2 + c_1 \mu^-_{\text{diff}} - \mu^+_{\text{diff}}, \\ \widetilde{c}_1 &= c_1 + 2 c_2 \mu^-_{\text{diff}}, \\ \widetilde{c}_2 &= c_2. \end{aligned} \tag{4.26}$$

13 This follows directly by noting that both μ_{Y^i} and σ_{Y^i} are proportional to the weights $\mathbf{w}^i$.

The formulas needed in steps 1–4 are summarized as follows. The first (two) (cross-)moments of the arithmetic sub-baskets are calculated from the characteristic function Φ_{X_T} of log-asset prices $\mathbf{X}_T = \log \mathbf{S}_T$ as

$$\begin{aligned}\mathbb{E}\left[A^i\right] &= \sum_{k=1}^{n} w_k^i \Phi_{X_T}(-\mathrm{i}\mathbf{e}_k)\\ \mathbb{E}\left[A^i A^j\right] &= \sum_{k,l=1}^{n} w_k^i w_l^j \Phi_{X_T}(-\mathrm{i}(\mathbf{e}_k + \mathbf{e}_l)), \quad i,j \in \{+,-\}.\end{aligned} \tag{4.27}$$

Under the log-normal assumption of the distribution of baskets A^i, the first two central moments as well as the first scaled cross-moment can be directly obtained using

$$\begin{aligned}\mu_{\log A^i} &= 2\log \mathbb{E}\left[A^i\right] - \frac{1}{2}\log \mathbb{E}\left[\left(A^i\right)^2\right]\\ \sigma_{\log A^i} &= \sqrt{\log \mathbb{E}\left[\left(A^i\right)^2\right] - 2\log \mathbb{E}\left[A^i\right]}\\ \rho^{ij}_{\log A} &= \frac{1}{\sigma_{\log A^i}\sigma_{\log A^j}} \log\left(\frac{\mathbb{E}\left[A^i A^j\right]}{\mathbb{E}\left[A^i\right]\mathbb{E}\left[A^j\right]}\right), \qquad i,j \in \{+,-\}.\end{aligned} \tag{4.28}$$

Next, we provide the formulas to compute the corresponding moments of the log-geometric baskets. To simplify the exposition (i.e. omitting sums) we define the joint characteristic function of $(w^+)'\mathbf{X}_T$ and $(w^-)'\mathbf{X}_T$ with two scalar arguments (u_1,u_2) as

$$\Phi_{(w^+X_T, w^-X_T)}(u_1,u_2) = \mathbb{E}\left[e^{\mathrm{i}u_1(\mathbf{w}^+)'\mathbf{X}_T + \mathrm{i}u_2(\mathbf{w}^-)'\mathbf{X}_T}\right]. \tag{4.29}$$

Using (4.29) we can compactly write the moments of the log-geometric baskets. We denote the log-geometric baskets defined by the original weights as $Y^i(T) = (\mathbf{w}^i)'\mathbf{X}_T$, and the corresponding ones with adjusted weights by $\widetilde{Y}^i(T) = (\widetilde{\mathbf{w}}^i)'\mathbf{X}_T$. To avoid redundant formulas, we only display the moments of Y^i. The moments of $\widetilde{Y}^i$ follow by just changing the weights. The general (k_1,k_2)-th (cross-)moment of the log-geometric baskets Y^i (and

$\widetilde{Y}^i$) can be recovered by differentiation:[14]

$$M_Y(k_1,k_2) := \mathbb{E}\left[\left(Y^+\right)^{k_1}\left(Y^-\right)^{k_2}\right] \tag{4.30}$$
$$= (-\mathrm{i})^{k_1+k_2}\left[\frac{\partial \Phi_{(w^+X_T,w^-X_T)}(u_1,u_2)}{\partial u_1^{k_1}\partial u_2^{k_2}}\right]_{(u_1,u_2)=(0,0)}.$$

The (scaled) central (cross-)moments of interest read

$$\begin{aligned}
\mu_{Y^+} &= M_Y(1,0), \quad \mu_{Y^-} = M_Y(0,1), \\
\sigma_{Y^+} &= \sqrt{M_Y(2,0) - (M_Y(1,0))^2}, \\
\sigma_{Y^-} &= \sqrt{M_Y(0,2) - (M_Y(0,1))^2}, \\
\rho_Y^{+-} &= \frac{1}{\sigma_{Y^+}\sigma_{Y^-}}\left(M_Y(1,1) - M_Y(1,0)M_Y(0,1)\right).
\end{aligned} \tag{4.31}$$

For the particular models applied in the numerical section, we provide closed-form expressions for the relevant moments of A^i and Y^i in Section 4.7.

4.6 An improved lower price bound

In Section 4.4 we defined the quadratic and piecewise linear approximating exercise sets $\mathcal{G}^x$, $x \in \{quad,plin\}$, cf. definitions (4.11) and (4.12), respectively. Following the notion of payoffs of digital options, we derived the Fourier transforms $\widehat{P}^x$ of $I(\mathcal{G}^x)$ in Theorem 1. Recall, for instance, the quadratic approximation $\mathcal{G}^{quad}(\mathbf{c}) = \{\omega : Y^+ > c_2(Y^-)^2 + c_1Y^- + c_0\}$ of the true exercise set $\mathcal{A} = \{\omega : \log A^+(T) > \log(A^-(T) + K)\}$. In a first step, we apply curve fitting to find a parameter vector $\mathbf{c} = (c_0,c_1,c_2)'$, such that $\mathcal{G}^{quad}(\mathbf{c})$ closely resembles the boundary of the true set $\mathcal{A}$ in a reasonable range of scales of $(\log A^+, \log A^-)$. The piecewise linear approximation, defined through an $M \times 2$-matrix of coefficients $\mathbf{c} = (\mathbf{c}_0,\mathbf{c}_1)$, can be chosen to fit the true convex boundary even over the whole domain of $\log A^+ \in \mathbb{R}$ and $\log A^- \in \mathbb{R}$. In a second step, appropriate variables Y^+ and Y^- must be found, which have a distribution close to the unknown one of the (log-)arithmetic sub-baskets, but a known joint characteristic function. A natural choice is to use the log-geometric baskets $Y^i(T) = \log G^i = (\mathbf{w}^i)' \log \mathbf{S}(T)$, $i \in \{+,-\}$, where $\mathbf{w}^i$ are defined in (4.9). However, this choice can be refined. In Section 4.5 an (approximate) moment matching

14 If the (k_1,k_2)-th moment exists, then the characteristic function is (k_1,k_2)-times continuously differentiable so we do not have to pose an extra assumption.

procedure is proposed to select modified weights $\widetilde{\mathbf{w}}^i$, such that the modified variables $\widetilde{Y}^i(T) = (\widetilde{\mathbf{w}}^i)' \log \mathbf{S}(T)$ share some first moments with $\log A^i$. As a part of this procedure, the coefficients $\mathbf{c}$ are also modified and denoted by $\widetilde{\mathbf{c}}$, cf. equations (4.26) and (4.25). Accordingly, we will denote the refined approximating set by $\widetilde{\mathcal{G}}^x$. The following proposition derives the value of the discounted expected payoff $(A(T) - K)I(\widetilde{\mathcal{G}}^x),\ x \in \{quad,plin\}$. To indicate the use of moment matching we denote the resulting lower price bound by LBMM. Similar to the method of CALDANA et al. [Cal14] recalled in Lemma 1, we propose a refinement of the lower bound by applying numerical maximization. The refined lower bound is denoted as LBMM*.

Proposition 2 *Assume that* $\mathbb{E}\left[e^{(\varepsilon_1 \widetilde{\mathbf{w}}^+ + \varepsilon_2 \widetilde{\mathbf{w}}^-)' \mathbf{X}(T)}\right] < \infty$ *and* $\mathbb{E}\left[e^{(\mathbf{e}_k + \varepsilon_1 \widetilde{\mathbf{w}}^+ + \varepsilon_2 \widetilde{\mathbf{w}}^-)' \mathbf{X}(T)}\right] < \infty$, $\forall k = 1,...,n$, *where* $\mathbf{e}_k$ *denotes the k-th element of the canonical basis in* $\mathbb{R}^n$. *A lower time-0 pricing bound to the basket spread call option according to a moment matched approximating exercise set* $\widetilde{\mathcal{G}}^x$ *is given by*

$$LBMM = C_K^{\widetilde{\mathcal{G}}^x}(\widetilde{\mathbf{c}}), \tag{4.32}$$

$$C_K^{\widetilde{\mathcal{G}}^x}(\widetilde{\mathbf{c}}) = \left(e^{-rT}(2\pi)^{-2} \iint_{\mathbb{R}^2 + \mathrm{i}\boldsymbol{\varepsilon}} \Psi_{(X_T, \widetilde{Y}_T)}(\mathbf{u}) \widehat{P}^x(\mathbf{u}; \widetilde{\mathbf{c}}) d^2\mathbf{u}\right)^+, \tag{4.33}$$

with $\widehat{P}^x(\mathbf{u}; \widetilde{\mathbf{c}})$, $\mathbf{u} \in \mathbb{C}^2$, *denoting the Fourier transform of* $I(\widetilde{\mathcal{G}}^x),\ x \in \{quad,plin\}$, *as defined in Theorem 1 for appropriately chosen values of* $\boldsymbol{\varepsilon}$ *given coefficients* $\widetilde{\mathbf{c}}$, *and*

$$\Psi_{(X_T, \widetilde{Y}_T)}(\mathbf{u}) = \sum_{k=1}^{n} w_k \Phi_{(X_T, \widetilde{Y}_T)}(-\mathrm{i}\mathbf{e}_k, \mathbf{u}) - K \Phi_{(X_T, \widetilde{Y}_T)}(\mathbf{0}, \mathbf{u}), \tag{4.34}$$

where w_k *denotes the k-th element of the original vector of basket weights* $\mathbf{w}$. *The lower price bound LBMM can be sharpened by maximizing over the coefficients* $\widetilde{\mathbf{c}}$ *as*

$$LBMM^* = \max_{\mathbf{c} \in [\widetilde{\mathbf{c}}(1 \pm \boldsymbol{\delta}_c)]} C_K^{\widetilde{\mathcal{G}}^x}(\mathbf{c}), \tag{4.35}$$

where the range for maximization specified by $\boldsymbol{\delta}_c$ *is chosen such that the conditions on* $\mathbf{c}$ *(given* $\boldsymbol{\varepsilon}$*) in Theorem 1 hold true. Fixing* $\boldsymbol{\varepsilon}$ *allows to precompute and reuse the computational costly part* $\Psi_{(X_T, \widetilde{Y}_T)}$ *throughout the maximization routine.*

PROOF: The line of proof is similar to that of Proposition 1. To avoid redundancy we omit some details already mentioned there. However, there is an important difference worthwhile to note. The basket option pricing formula in Proposition 1, as well as all other pricing formulas given so far are related to continuous payoff functions. Against, the payoff defined through $(A(T)-K)I(\widetilde{\mathcal{G}}^x),\ x \in \{quad,plin\}$ might be interpreted in terms of asset-or-nothing digital options, and a digital option. Since the true exercise set $\mathcal{A}$ and the approximating set $\widetilde{\mathcal{G}}^x$ do not completely agree, this is clearly a discontinuous payoff. Fortunately, Theorem 3.4 in EBERLEIN et al. [Ebe10] provides two conditions under which (4.33) is a valid pricing formula, even if asset prices are modeled as general exponential semimartingales. More precisely, if the payoff is discontinuous, but the semimartingale is continuous (in the sense of possessing a Lebesgue density), the inverse Fourier transform (4.33) is valid as a Lebesgue integral. If also the semimartingale is discontinuous, then EBERLEIN et al. [Ebe10] show that the inverse integral is still valid, but convergence of the integrand is proven as a L^2-limit. In the rest of the proof we show that the two conditions are satisfied.

The first condition is $L^1(\mathbb{R}^2) \cap L^2(\mathbb{R}^2)$-integrability of the payoff. Within the proof of Theorem 1, we already established that this condition holds for the digital payoffs $I(\widetilde{\mathcal{G}}^x)$ under some case-specific restrictions on $\boldsymbol{\varepsilon}$ and coefficients $\mathbf{c}$ (or $\widetilde{\mathbf{c}}$, respectively). Next, we show that the conditions still hold for $(A(T)-K)I(\widetilde{\mathcal{G}}^x)$. Consider the expected payoff under the (risk-neutral) pricing measure Q:

$$\mathbb{E}^Q\left[(A(T)-K)I(\widetilde{\mathcal{G}}^x)\right] = \sum_{k=1}^{n} w_k \mathbb{E}^Q\left[S_k(T)I(\widetilde{\mathcal{G}}^x)\right] - K\mathbb{E}^Q\left[I(\widetilde{\mathcal{G}}^x)\right].$$

$S_k(T)I(\widetilde{\mathcal{G}}^x)$ resembles the payoff of an asset-or-nothing digital option. For this payoff the conditions on damping factor $\boldsymbol{\varepsilon}$ are different to those for the digital payoff. However, using S_k as the numeraire, the expected payoff under measure Q_k is $\mathbb{E}^{Q_k}\left[I(\widetilde{\mathcal{G}}^x)\right]$. Thus, under measures Q_k, $k = 1,...,n$, we have again expected payoffs of pure digital options, and the conditions on $\boldsymbol{\varepsilon}$ and $\mathbf{c}$ in Theorem 1 are the same for all $n+1$ expectations. But importantly, changing measure does change the necessary assumptions on the existence of enough moments of $\log \mathbf{S}_T = \mathbf{X}_T$. The assumption of existence of enough moments is the second condition of Theorem 3.4 in EBERLEIN et al. [Ebe10]. In order to compute the expectations according to a moment matched approximating set $\widetilde{\mathcal{G}}^x$, we need the joint characteristic function of $\widetilde{Y}^+(T) = (\widetilde{\mathbf{w}}^+)'\mathbf{X}_T$ and $\widetilde{Y}^-(T) = (\widetilde{\mathbf{w}}^-)'\mathbf{X}_T$. Under measure Q,

the joint characteristic function with argument $\mathbf{u} = (u_1,u_2)' \in \mathbb{C}^2$ reads

$$\begin{aligned} \Phi^{Q}_{\widetilde{Y}_T}(\mathbf{u}) &= \mathbb{E}^{Q}\left[e^{\mathrm{i}u_1\widetilde{Y}^{+}(T)+\mathrm{i}u_2\widetilde{Y}^{-}(T)}\right] \\ &= \mathbb{E}^{Q}\left[e^{\mathrm{i}(u_1\widetilde{\mathbf{w}}^{+}+u_2\widetilde{\mathbf{w}}^{-})'\mathbf{X}_T}\right]. \end{aligned} \tag{4.36}$$

Under measure Q_k, $k = 1,...,n$, the characteristic function looks the same as the one above (because just the drift of X_k has changed). But changing measure back to Q, the expression of the characteristic function is different:

$$\begin{aligned} \Phi^{Q_k}_{\widetilde{Y}_T}(\mathbf{u}) &= \mathbb{E}^{Q_k}\left[e^{\mathrm{i}u_1\widetilde{Y}^{+}(T)+\mathrm{i}u_2\widetilde{Y}^{-}(T)}\right] \\ &= \mathbb{E}^{Q}\left[e^{X_k+\mathrm{i}u_1\widetilde{Y}^{+}(T)+\mathrm{i}u_2\widetilde{Y}^{-}(T)}\right] \\ &= \mathbb{E}^{Q}\left[e^{\mathrm{i}(-\mathrm{i}\mathbf{e}_k+u_1\widetilde{\mathbf{w}}^{+}+u_2\widetilde{\mathbf{w}}^{-})'\mathbf{X}_T}\right]. \end{aligned} \tag{4.37}$$

To unify notation, we denote the characteristic functions in (4.36) and (4.37) by $\Phi_{(X_T,\widetilde{Y}_T)}(.,\mathbf{u})$. According to (4.36), we write $\Phi_{(X_T,\widetilde{Y}_T)}(\mathbf{0},\mathbf{u})$. The characteristic functions in (4.37) are denoted by $\Phi_{(X_T,\widetilde{Y}_T)}(-\mathrm{i}\mathbf{e}_k,\mathbf{u})$, $k = 1,...,n$. Noting that the complex argument is $\mathbf{u} = \mathbf{u}_r - \mathrm{i}\boldsymbol{\varepsilon}$, splitting the real and the imaginary part of the exponent yields

$$\begin{aligned} \Phi_{(X_T,\widetilde{Y}_T)}(-\mathrm{i}\mathbf{e}_k,\mathbf{u}) &= \mathbb{E}^{Q}\left[e^{\mathrm{i}(-\mathrm{i}\mathbf{e}_k+(u_{r,1}-\mathrm{i}\varepsilon_1)\widetilde{\mathbf{w}}^{+}+(u_{r,2}-\mathrm{i}\varepsilon_2)\widetilde{\mathbf{w}}^{-})'\mathbf{X}_T}\right] \\ &= \mathbb{E}^{Q}\left[e^{(\mathbf{e}_k+\varepsilon_1\widetilde{\mathbf{w}}^{+}+\varepsilon_2\widetilde{\mathbf{w}}^{-})'\mathbf{X}_T} \times e^{\mathrm{i}(u_{r,1}\widetilde{\mathbf{w}}^{+}+u_{r,2}\widetilde{\mathbf{w}}^{-})'\mathbf{X}_T}\right], \end{aligned}$$

and the characteristic function exists if $\mathbb{E}^{Q}\left[e^{(\mathbf{e}_k+\varepsilon_1\widetilde{\mathbf{w}}^{+}+\varepsilon_2\widetilde{\mathbf{w}}^{-})'\mathbf{X}_T}\right]$ is finite. With regard to the definition of the moment generating function $M_{X_T}(\mathbf{u}) = \mathbb{E}[e^{\mathbf{u}'\mathbf{X}_T}]$, this is equivalent to assuming that the $(\mathbf{e}_k+\varepsilon_1\widetilde{\mathbf{w}}^{+}+\varepsilon_2\widetilde{\mathbf{w}}^{-})$-th moment of $\mathbf{X}_T$ exists, and the $(\varepsilon_1\widetilde{\mathbf{w}}^{+}+\varepsilon_2\widetilde{\mathbf{w}}^{-})$-th moment according to (4.36), respectively. To conclude, (4.33) is a valid pricing formula if both moment conditions are satisfied.

Taking Fourier transform with respect to all terms of $\sum_{k=1}^{n} w_k\mathbb{E}^{Q_k}\left[I(\widetilde{\mathcal{G}}^x)\right] - K\mathbb{E}^{Q}\left[I(\widetilde{\mathcal{G}}^x)\right]$, applying the convolution theorem, and factorizing the payoff transform $\widehat{P}^x(\mathbf{u};\widetilde{\mathbf{c}})$ yields

$$\left(\sum_{k=1}^{n} w_k\Phi_{(X_T,\widetilde{Y}_T)}(-\mathrm{i}\mathbf{e}_k,\mathbf{u}) - K\Phi_{(X_T,\widetilde{Y}_T)}(\mathbf{0},\mathbf{u})\right)\widehat{P}^x(\mathbf{u};\widetilde{\mathbf{c}})$$

The basket spread call price (4.33) follows by inverting the Fourier transform, and discounting. □

Remark 3 (Efficient implementation – measure correction) *The most costly part to compute the basket spread call price formula* (4.33) *is – by far – the sum of* $n+1$ *joint characteristic functions collected in* $\Psi_{(X_T,\widetilde{Y}_T)}$*, cf. equation* (4.34)*. It is precisely the calculation of* Ψ *that causes quadratic increase of computational afford in the basket dimension* n*, i.e. linear increasing complexity of each joint characteristic function* $\Phi_{(X_T,\widetilde{Y}_T)}$*, and linear increase in the dimension of the sum in* Ψ*.*[15] *Even in moderate dimensions* n *and in models with quite simple joint characteristic functions (like the multivariate GBM model detailed in Section 4.7.1), computing* Ψ *takes much more than 90% of the total run-time. We mention that it is however possible and very effective to rewrite* Ψ*, such that only the characteristic function* $\Phi_{(X_T,\widetilde{Y}_T)}(\mathbf{0},\mathbf{u})$ *(which is the one where no change of measure was applied) has to be computed. All other characteristic functions* $\Phi_{(X_T,\widetilde{Y}_T)}(-\mathrm{i}\mathbf{e}_k,\mathbf{u})$*,* $k=1,...,n$*, follow by multiplying it with a correction factor* $corr_k$*, i.e.*

$$\Phi_{(X_T,\widetilde{Y}_T)}(-\mathrm{i}\mathbf{e}_k,\mathbf{u}) = corr_k(\mathbf{u}) \times \Phi_{(X_T,\widetilde{Y}_T)}(\mathbf{0},\mathbf{u}).$$

Using this, we can restate Ψ *as*

$$\Psi_{(X_T,\widetilde{Y}_T)}(\mathbf{u}) = \left(\sum_{k=1}^{n} w_k \times corr_k(\mathbf{u}) - K\right) \Phi_{(X_T,\widetilde{Y}_T)}(\mathbf{0},\mathbf{u}). \tag{4.38}$$

We refer to the correction factors as measure corrections. Of course, applying (4.38) *does only make sense if the effort to compute a correction factor is less than the effort to compute the respective characteristic function. At least for those models we study in the numerical section, the difference is striking. This is precisely because the characteristic functions involve (repeated) matrix multiplications which are rather costly for higher dimensions* n*. Against, the correction factors only require some vector-vector multiplications. Therefore, applying* (4.38) *is about* n*-times faster than computing* Ψ *using the original version* (4.34)*. Our numerical experiments reveal that the overall computational time to calculate LBMM (and similar LBMM***) using* (4.38) *is actually (at most) linearly increasing in* n*.*[16] *Efficient implementation allows calculate the price of a basket spread option comprising* $n = 200$ *assets in a jump diffusion model with an* $n \times n$ *diffusive covariance matrix and an* $n \times n$

15 Against, both versions of the payoff transform $\widehat{P}^x(\mathbf{u};\widetilde{\mathbf{c}})$, $x \in \{quad,plin\}$, in Theorem 1 are independent of the basket dimension $n \geq 2$. Furthermore, both versions just comprise some basic computations involving the exponential function.

16 However, we cannot state linear increasing complexity for general pricing models.

(covariance) matrix for jump sizes in just about 2 seconds, cf. Table 4.9. We state the formulas for the model dependent correction factors in Section 4.7.

Sensitivities of the basket option price with respect to initial prices $S_k(0)$, strike level K, or the model parameters can be obtained similarly. For instance, provided that the lower price bound LBMM itself is positive, the first-order sensitivity with respect to the k-th initial asset price $S_k(0)$, $k = 1,...,n$, is given by

$$\frac{\partial LBMM}{\partial S_k(0)} = e^{-rT}(2\pi)^{-2} \iint_{\mathbb{R}^2+\mathrm{i}\varepsilon} \frac{\partial \Psi_{(X_T,\widetilde{Y}_T)}(\mathbf{u})}{\partial S_k(0)} \widehat{P}^x(\mathbf{u};\widetilde{\mathbf{c}}) d^2\mathbf{u},$$

where we assume that differentiation and integration can be exchanged. For details about this assumption we refer to Eberlein et al. [Ebe10]. As a consequence of the envelope theorem, the greeks with respect to the maximized lower price bound LBMM* are obtained in the same way, cf. Caldana et al. [Cal14].

4.7 Particular pricing models

We proofed the basket spread option pricing formulas in Proposition 2 to be valid for general continuous-time models, i.e. if asset prices are modeled as exponential semimartingales. With regard to the numerical examples in Section 4.8, we restrict ourselves to just two different models. Caldana et al. [Cal14] give examples for a strand of further models, also comprising mean reverting price processes, or a stochastic correlation model. Since the characteristic functions needed in Proposition 2 are very similar to those needed for the pricing formula of Caldana et al. [Cal14] recalled in Lemma 1, we refer the reader to their paper. We first study the accuracy of our lower price bound in the multivariate geometric Brownian motion (GBM) model. We choose this particular model because it allows us to compare our results not only to the method of Caldana et al. [Cal14], but also to the results according to four analytical basket spread option pricing approximations of Deelstra et al. [Dee10]. Amongst methods applying comonotonicity theory, the authors also study a hybrid method combining moment matching with a basket spread option pricing formula of Li et al. [Li08]. The basic idea underlying the Li et al. formula is to approximate the exercise boundary by a quadratic function. The coefficients of the quadratic function are obtained by a Taylor expansion of the exercise bound. Summing up, there are some common features with our method, and comparing the relative accuracy is of special interest.

The second model is a jump diffusion model. In particular it is an n-dimensional extension of a model introduced by HUANG et al. [Hua06]. The extension is due to CALDANA et al. [Cal14]. Besides correlated diffusive parts, the model accounts for idiosyncratic jumps as well as macroeconomic jumps. Asset-specific jump sizes according to a macroeconomic jump are correlated. We study the performance of our method in this model because it generates basket distributions which are severely skewed and leptokurtic. Explicitly, our moment matching procedure only accounts for moments up to the second order. Also, we have to pose an assumption on the distribution of arithmetic sub-baskets A^i, $i \in \{+,-\}$, to arrive at closed-form expressions for the moments of $\log A^i$, given those of A^i. As discussed in Section 4.5, we pose the simple log-normal assumption. Therefore, it is interesting to study the sharpness of our lower price bound if the assumption is severely violated. In the following, we state the formulas to apply our method in the GBM and the jump diffusion model, respectively. Except the formulas related to moments and the characteristic functions as well as the correction factors required to compute our pricing formula, the exposition is taken from CALDANA et al. [Cal14].

4.7.1 The multivariate geometric Brownian motion model

Denoting r a constant risk-free interest rate, $\mathbf{q}$ an $n \times 1$ vector of dividend yields, $\boldsymbol{\Sigma}$ the $n \times n$ covariance matrix with elements $\rho_{kl}\sigma_k\sigma_l$, for $k \neq l = 1,...,n$, where $|\rho_{kl}| \leq 1$, and $\boldsymbol{\Sigma}_{kk} = \sigma_k^2$. $\mathbf{W}$ is an n-dimensional Brownian motion. The risk-neutral stock price dynamics is specified by

$$d\mathbf{S}_t = \mathbf{S}_t \circ \left((r - \mathbf{q})dt + \sqrt{\boldsymbol{\Sigma}} d\mathbf{W}_t \right).$$

The characteristic function of $\mathbf{X}_T = \log \mathbf{S}_T$ with argument $\mathbf{u} = (u_1,...,u_n)'$ reads

$$\Phi_{X_T}(\mathbf{u}) = e^{\mathrm{i}\mathbf{u}'(\mathbf{X}_0 + \mathbf{m}T) - \frac{1}{2}\mathbf{u}'\boldsymbol{\Sigma}\mathbf{u}T}, \qquad \mathbf{m} = r - \mathbf{q} - \frac{1}{2} diag(\boldsymbol{\Sigma}).$$

The characteristic function of log-returns $\mathbf{X}_T^R = \log \mathbf{S}_T - \log \mathbf{S}_0$ is very similarly given by $\Phi_{X_T^R}(\mathbf{u}) = e^{\mathrm{i}\mathbf{u}'\mathbf{m}T - \frac{1}{2}\mathbf{u}'\boldsymbol{\Sigma}\mathbf{u}}$. The joint characteristic function of the log-geometric basket and the log-returns in equation (4.2), required to apply the formula of CALDANA et al. [Cal14] (cf. Lemma 1), reads

$$\Phi_{(X_T^R, Y_T)}(\mathbf{u}, u_0) = e^{\mathrm{i}u_0 Y_n(t)} \Phi_{X_T^R}(\mathbf{u} + u_0\mathbf{w}) = e^{\mathrm{i}u_0 Y(0) + \mathrm{i}(\mathbf{u} + u_0\mathbf{w})'\mathbf{m}T - \frac{1}{2}(\mathbf{u} + u_0\mathbf{w})'\boldsymbol{\Sigma}(\mathbf{u} + u_0\mathbf{w})T},$$

where $\mathbf{u} = (u_1,...,u_n)'$, while u_0 is a scalar argument. In order to apply our main pricing formula in Proposition 2 we require the joint characteristic functions of the k-th log-asset price, $k = 1,...,n$, and the moment matched log-geometric sub-baskets $\widetilde{Y}^i = \mathbf{w}^i \log \mathbf{S}_T$, $i \in \{+,-\}$. Additionally, we require the characteristic function of just the $\widetilde{Y}^i$. As discussed in Remark 3, it is more efficient to just compute the latter characteristic function, and then to correct it by a factor to obtain the other n characteristic functions, cf. equation (4.38). For the GBM model we have

$$\begin{aligned}\Phi_{(X_T,\widetilde{Y}_T)}(\mathbf{0},\mathbf{u}) = e^{\mathrm{i}u_1(\widetilde{\mathbf{w}}^+)'(\mathbf{X}_0+mT)+\mathrm{i}u_2(\widetilde{\mathbf{w}}^-)'(\mathbf{X}_0+mT)} \\ \times e^{-\frac{1}{2}\left(u_1^2(\widetilde{\mathbf{w}}^+)'\boldsymbol{\Sigma}\widetilde{\mathbf{w}}^+ + u_2^2(\widetilde{\mathbf{w}}^-)'\boldsymbol{\Sigma}\widetilde{\mathbf{w}}^- + 2u_1u_2(\widetilde{\mathbf{w}}^+)'\boldsymbol{\Sigma}\widetilde{\mathbf{w}}^-\right)T},\end{aligned}$$

where $\mathbf{u} = (u_1,u_2)'$. The correction factor according to equation (4.38) simply reads

$$corr_k(\mathbf{u}) = e^{X_k(0)+(r-q_k)T+\mathrm{i}\left(u_1\boldsymbol{\Sigma}_{k,\cdot}\widetilde{\mathbf{w}}^+ + u_2\boldsymbol{\Sigma}_{k,\cdot}\widetilde{\mathbf{w}}^-\right)T},$$

with $\boldsymbol{\Sigma}_{k,\cdot}$ denoting the k-th row of the covariance matrix. We now summarize the relevant moments of the arithmetic sub-baskets and the log-geometric sub-baskets, respectively. According to equation (4.27), we denote the vector of forward prices by $\mathbf{F}_T = \mathbf{S}_0 \circ e^{(r-\mathbf{q})T}$, and obtain for $i,j \in \{+,-\}$:

$$\begin{aligned}\mathbb{E}\left[A^i\right] &= (\mathbf{w}^i)'\mathbf{F}_T \\ \mathbb{E}\left[A^iA^j\right] &= (\mathbf{w}^i \circ \mathbf{F}_T)'e^{\boldsymbol{\Sigma}T}(\mathbf{w}^j \circ \mathbf{F}_T).\end{aligned}$$

The moments of the log-geometric sub-baskets $Y^i(T)$ (and analogously the moments of $\widetilde{Y}^i(T)$) follow by differentiation, cf. equation (4.30). The GBM-specific (scaled) central (cross-)moments read

$$\begin{aligned}\mu_{Y^i} &= (\mathbf{w}^i)'(\mathbf{X}_0 + \mathbf{m}T) \\ \sigma_{Y^i} &= \sqrt{(\mathbf{w}^i)'\boldsymbol{\Sigma}(\mathbf{w}^i)T} \\ \rho_Y^{ij} &= \frac{1}{\sigma_{Y^i}\sigma_{Y^j}}(\mathbf{w}^i)'\boldsymbol{\Sigma}(\mathbf{w}^j)T.\end{aligned}$$

4.7.2 A multivariate jump diffusion model

In the extended jump diffusion model of HUANG et al. [Hua06], the k-th terminal stock price, $k = 1,...,n$, is given by[17]

$$S_k(T) = S_k(0) \exp\left[\left(r - q_k - \frac{\sigma_k^2}{2} - \lambda^m \varkappa_k^m - \lambda_k^{id} \varkappa_k^{id}\right) T + \sigma_k W_k(t) + \sum_{i=1}^{N^m(T)} Z_k^m(i) + \sum_{j=1}^{N_k^{id}(T)} Z_k^{id}(j)\right],$$

where the super-index 'm' is regarded to macroeconomic jumps, while 'id' refers to idiosyncratic jumps. More precisely, the macroeconomic jumps are specified by an n-dimensional compound Poisson process

$$\sum_{i=1}^{N^m(T)} \mathbf{Z}^m(i) = \left(\sum_{i=1}^{N^m(T)} Z_1^m(i),..., \sum_{i=1}^{N^m(T)} Z_n^m(i)\right)',$$

driven by the Poisson process N^m. The intensity of N^m is assumed to be constant and denoted by λ^m. Under measure Q, the iid-jumps $\mathbf{Z}^m$ are distributed as multivariate asymmetric Laplace $\mathcal{MAL}(\boldsymbol{\alpha}^m, \boldsymbol{\Sigma}^m)$-random variables, where $\boldsymbol{\alpha}^m \in R^n$, $\boldsymbol{\alpha}^m \neq \mathbf{0}$, and $\boldsymbol{\Sigma}^m$ is an $n \times n$ non-negative definite symmetric matrix with elements[18]

$$\boldsymbol{\Sigma}_{k,l}^m = \xi_k \xi_l \rho_{k,l}^m, \qquad \boldsymbol{\Sigma}_{k,k}^m = (\xi_k)^2.$$

Idiosyncratic jumps of the assets S_k, $k = 1,...,n$, are modeled by n independent, univariate compound Poisson processes $\sum_{j=1}^{N_k^{id}(T)} Z_k^{id}(j)$, driven by the Poisson processes N_k^{id}. The constant jump intensities λ_k^{id} are collected in the vector $\boldsymbol{\lambda}^{id} = (\lambda_1^{id},...,\lambda_n^{id})'$. The iid-jumps Z_k^{id} are distributed as (univariate) asymmetric Laplace $\mathcal{AL}(\alpha_k^{id}, \xi_k^{id})$-random variables, where parameters α_k^{id} and ξ_k^{id} are merged in vectors $\boldsymbol{\alpha}^{id} = (\alpha_1^{id},...,\alpha_n^{id})'$ and $\boldsymbol{\xi}^{id} = (\xi_1^{id},...,\xi_n^{id})'$. The expected macroeconomic and idiosyncratic jump sizes under measure Q both have

17 For further details on the model we refer to CALDANA et al. [Cal14].
18 Details on the multivariate asymmetric Laplace distribution can be found in KOTZ et al. [Kot01].

closed-form solutions (cf. CALDANA et al. [Cal14]):

$$\varkappa_k^m = \left(1 - \alpha_k^m - \frac{1}{2}(\xi_k^m)^2\right)^{-1} - 1$$
$$\varkappa_k^{id} = \left(1 - \alpha_k^{id} - \frac{1}{2}(\xi_k^{id})^2\right)^{-1} - 1.$$

The joint characteristic function of log-asset prices $\mathbf{X}_T$ reads

$$\Phi_{X_T}(\mathbf{u}) = \exp\left[\mathbf{X}_0 + \left(\mathrm{i}\mathbf{u}'\boldsymbol{\eta} - \frac{1}{2}\mathbf{u}'\boldsymbol{\Sigma}\mathbf{u} + \lambda^m\left(\left[1 - \mathrm{i}\mathbf{u}'\boldsymbol{\alpha}^m + \frac{1}{2}\mathbf{u}'\boldsymbol{\Sigma}^m\mathbf{u}\right]^{-1} - 1\right)\right.\right.$$
$$\left.\left. + \boldsymbol{\lambda}^{id}\left(\left[1 - \mathrm{i}\mathbf{u}'\boldsymbol{\alpha}^{id} + \frac{1}{2}(\mathbf{u}^2)'(\boldsymbol{\xi}^{id})^2\right]^{-1} - 1\right)'\right)T\right],$$

where $\mathbf{u} = (u_1,...,u_n)'$, and $\boldsymbol{\eta}$ is defined as $\boldsymbol{\eta} = r - \mathbf{q} - \frac{1}{2}diag(\boldsymbol{\Sigma}) - \lambda^m\varkappa^m - \boldsymbol{\lambda}^{id}\varkappa^{id}$.[19] With regard to Remark 3, we require

$$\begin{aligned}\Phi_{(X_T,\widetilde{Y}_T)}(\mathbf{0},\mathbf{u}) = {} & e^{\mathrm{i}u_1(\widetilde{\mathbf{w}}^+)'(\mathbf{X}_0+\eta T)+\mathrm{i}u_2(\widetilde{\mathbf{w}}^-)'(\mathbf{X}_0+\eta T)} \\ & \times e^{-\frac{1}{2}\left(u_1^2(\widetilde{\mathbf{w}}^+)'\boldsymbol{\Sigma}\widetilde{\mathbf{w}}^+ + u_2^2(\widetilde{\mathbf{w}}^-)'\boldsymbol{\Sigma}\widetilde{\mathbf{w}}^- + 2u_1u_2(\widetilde{\mathbf{w}}^+)'\boldsymbol{\Sigma}\widetilde{\mathbf{w}}^-\right)T - (\lambda^m + \boldsymbol{\lambda}^{id})T} \\ & \times e^{\lambda^m T\left[1 - \mathrm{i}\left(u_1(\widetilde{\mathbf{w}}^+)'\boldsymbol{\alpha}^m + u_2(\widetilde{\mathbf{w}}^-)'\boldsymbol{\alpha}^m\right) + \frac{1}{2}a_1^m(\mathbf{u})\right]^{-1}} \\ & \times e^{\sum_{k=1}^n \lambda_k^{id}T\left[1 - \mathrm{i}\alpha_k^{id}\left(u_1\widetilde{w}_k^+ + u_2\widetilde{w}_k^-\right) + \frac{1}{2}(\xi_k^{id})^2\left(u_1\widetilde{w}_k^+ + u_2\widetilde{w}_k^-\right)\right]^{-1}},\end{aligned}$$

where $a_1^m(\mathbf{u})$ is an auxiliary function defined beyond. The correction factors according to equation (4.38) only involve a couple of efficient-to-compute vector multiplications:

$$\begin{aligned}corr_k(\mathbf{u}) = {} & e^{X_k(0) + (r-q_k)T + \mathrm{i}\left(u_1\boldsymbol{\Sigma}_{k,\cdot}\widetilde{\mathbf{w}}^+ + u_2\boldsymbol{\Sigma}_{k,\cdot}\widetilde{\mathbf{w}}^-\right)T} \\ & \times e^{-\lambda^m T\left[1 - a_2^m(\mathbf{u}) + \frac{1}{2}a_1^m(\mathbf{u})\right]^{-1}} \\ & \times e^{\lambda^m T\left[1 - a_2^m(\mathbf{u}) + \frac{1}{2}a_1^m(\mathbf{u}) - \frac{1}{2}\boldsymbol{\Sigma}_{k,k}^m - \mathrm{i}\left(u_1\boldsymbol{\Sigma}_{k,\cdot}^m\widetilde{\mathbf{w}}^+ + u_2\boldsymbol{\Sigma}_{k,\cdot}^m\widetilde{\mathbf{w}}^-\right)\right]^{-1}} \\ & \times e^{-\lambda_k^{id}T\left[1 - c_k^{id}\right]^{-1} + \lambda_k^{id}T\left[1 - c_k^{id} - \alpha^{id} - \frac{1}{2}(\xi_k^{id})^2 - \mathrm{i}(\xi_k^{id})^2\right]^{-1}},\end{aligned}$$

19 The covariance matrix according to the diffusive part, $\boldsymbol{\Sigma}$, is defined analogously to the one of the GMB model. Choosing jump intensities $\lambda^m = \boldsymbol{\lambda}^{id} = 0$, the jump diffusion model comprises the GBM model as a special case.

where $\boldsymbol{\Sigma}^m_{k,\cdot}$ denotes the k-th row of $\boldsymbol{\Sigma}^m$. We define the auxiliary functions, as

$$\begin{aligned}
a_1^m(\mathbf{u}) &= \left(u_1^2(\widetilde{\mathbf{w}}^+)'\boldsymbol{\Sigma}^m\widetilde{\mathbf{w}}^+ + u_2^2(\widetilde{\mathbf{w}}^-)'\boldsymbol{\Sigma}^m\widetilde{\mathbf{w}}^- + 2u_1u_2(\widetilde{\mathbf{w}}^+)'\boldsymbol{\Sigma}^m\widetilde{\mathbf{w}}^-\right)\\
a_2^m(\mathbf{u}) &= \mathrm{i}\left(u_1(\widetilde{\mathbf{w}}^+)'\boldsymbol{\alpha}^m + u_2(\widetilde{\mathbf{w}}^-)'\boldsymbol{\alpha}^m\right)\\
a_k^{id}(\mathbf{u}) &= \mathrm{i}\alpha_k^{id}\left(u_1\widetilde{w}_k^+ + u_2\widetilde{w}_k^-\right) + \frac{1}{2}(\xi_k^{id})^2\left((u_1\widetilde{w}_k^+)^2 + (u_2\widetilde{w}_k^-)^2\right).
\end{aligned}$$

Notice that the functions have to be computed only once for all the n corrections. Finally, we summarize the required moments of the arithmetic and log-geometric sub-baskets under the jump diffusion model. Refering to equation (4.27), we obtain the first moment of arithmetic basket A^i, i,$j \in \{+,-\}$, as

$$\mathbb{E}\left[A^i\right] = (\mathbf{w}^i)'e^{\mathbf{X}_0+\left(\boldsymbol{\eta}+\frac{1}{2}diag(\boldsymbol{\Sigma})+\lambda^m\left[1-(\boldsymbol{\alpha}^m+\frac{1}{2}diag(\boldsymbol{\Sigma}^m))\right]^{-1}-\lambda^m+\boldsymbol{\lambda}^{id}\circ\left[1-(\boldsymbol{\alpha}^{id}-\frac{1}{2}(\boldsymbol{\xi}^{id})^2)\right]^{-1}-\boldsymbol{\lambda}^{id}\right)T}.$$

The second moment (or first cross-moment, respectively), $\mathbb{E}\left[A^iA^j\right]$, is also easily obtained, but too lengthy to present it here. We refer the reader to the characteristic function-version in equation (4.27) instead. The moments of the log-geometric sub-baskets $Y^i(T)$ (and analogously the moments of $\widetilde{Y}^i(T)$), are given by

$$\begin{aligned}
\mu_{Y^i} &= (\mathbf{w}^i)'\left(\mathbf{X}_0 + (\boldsymbol{\eta} + \lambda^m\boldsymbol{\alpha}^m + \boldsymbol{\lambda}^{id}\circ\boldsymbol{\alpha}^{id})T\right)\\
\sigma_{Y^i} &= \sqrt{(\mathbf{w}^i)'\mathbf{C}_{mat}(\mathbf{w}^i)T + ((\mathbf{w}^i)^2)'(\boldsymbol{\lambda}^{id}\circ(2(\boldsymbol{\alpha}^{id})^2 + (\boldsymbol{\xi}^{id})^2))T}\\
\rho_Y^{ij} &= \frac{1}{\sigma_{Y^i}\sigma_{Y^j}}(\mathbf{w}^i)'\mathbf{C}_{mat}(\mathbf{w}^j)T,
\end{aligned}$$

where $\mathbf{C}_{mat} = \boldsymbol{\Sigma} + \lambda^m\boldsymbol{\Sigma}^m + 2\lambda^m\boldsymbol{\alpha}^m(\boldsymbol{\alpha}^m)'$ is an auxiliary $n \times n$ matrix.

4.8 Numerical results

4.8.1 Implementation preliminaries

Before we start to compare the accuracy of the proposed lower price bounds LBMM and LBMM* to other methods, some preliminaries and implementation details should be mentioned. First of all, we need to fit the coefficients $\mathbf{c}$, regarding to either the quadratic or the piecewise linear boundary approximation, to the true exercise boundary. Recall the quadratic approximation $\mathcal{G}^{quad}(\mathbf{c}) = \{\omega \ : \ Y^+ > c_2(Y^-)^2 + c_1 Y^- + c_0\}$, where the $Y^i = Y^i(T)$ denote the approximating variables for the log-arithmetic sub-baskets $\log A^i$. Since the simple 2nd-degree polynomial cannot capture the shape of the true boundary along the whole real line (i.e. the domain of $Y^-(T)$ or $\log A^-(T)$), curve fitting is be applied according to scales of Y^- within an appropriately chosen interval $[y^-_{low},y^-_{up}]$. Figures 4.1 and 4.2 illustrate the true boundary, combined with a contour plot of the bivariate density of $(\log A^+, \log A^-)$. We propose a simple and illustrative method to select y^-_{low} and y^-_{up} based on bivariate (cross-)moments of $(\log A^+, \log A^-)$. Assuming that the arithmetic sub-baskets are jointly log-normal distributed, the parameters $\mu_{\log A^i}$, $\sigma_{\log A^i}$, and $\rho^{ij}_{\log A}$ follow from equation (4.28). Denote by $\mathbf{C}_{Chol}$ the Cholesky decomposition of the 2×2 covariance matrix of $\log A^i$, $i \in \{+,-\}$. Selecting $N_\sigma \in \mathbb{R}_{>0}$, and $\theta \in [0,2\pi]$, the tuples

$$(\bar{y}^+,\bar{y}^-) = N_\sigma(\cos\theta, \sin\theta)\mathbf{C}_{Chol} + (\mu_{\log A^+},\mu_{\log A^-}),$$

correspond to points on an N_σ-ellipse. The ellipse is located around $(\mu_{\log A^+},\mu_{\log A^-})$. N_σ has an interpretation as the number of standard deviations in an univariate Gaussian sense. It controls for the radius of the ellipse, while $\rho^{ij}_{\log A}$ controls for the slope. The ellipse is basically obtained by shifting and stretching the unit circle. The unit circle consists of points $(\cos\theta, \sin\theta)$. We typically chose $N_\sigma = 4$. The two intersections of the true boundary and the ellipse provide us reasonable choices for y^-_{low} and y^-_{up}.[20] We apply OLS-regression to find the coefficients $\mathbf{c}$. We finally use a small number (say 10 to 20) of equally spaced scales of $y^- \in [y^-_{low},y^-_{up}]$, and regress the true boundary $y^+ = \log(y^- - K)$ against the scales.

20 The intersection points are simply solved for. If there are no intersections – which can be the case for extremely out of the money options – N_σ should be increased to expand the radius of the ellipse. Also, if the distribution of $(\log A^+, \log A^-)$ is very far from jointly normal, one might favor the piecewise linear approximation instead. This approximation can be fitted to match the boundary along the whole real line.

Experiments are implemented in Matlab version 8.3.0, and conducted on an Intel Xeon 8×3.5 GHz machine running under Windows with 32 GB RAM. The (bivariate) inverse Fourier integrals are approximated using non-adaptive Gauss-Legendre quadrature with $M = 2^8$ points in each dimension. The infinite integration region is truncated at $\{[-80,80],[-80,80]\}$ for the bivariate integration formulas in Proposition 2, and at [0,80] for the univariate Caldana et al. formula in Lemma 1. All results were back-tested using a higher number of integration points as well as a wider integration region. We detect no deviations at a level 10^{-4}, i.e. the level of precision reported in the tables of Section 4.8.2. Notice that using non-equally spaced Gaussian quadrature (instead of equally-spaced FFT integration schemes, see Remark 1 for a discussion), a number of $M = 2^8$ integration points is already quite high. Experiments show that all results can be obtained using just 2^7 points, with a loss of precision of maximum order 10^{-2}. With regard to the bivariate integrals, cutting the number of points by halve corresponds to saving about 75% of total run-time.[21]

With regard to the approximation of the exercise set, our experiments revealed that the quadratic and the piecewise linear approximations perform almost identically.[22] Applying numerical maximization to compute the lower price bound LBMM*, the piecewise linear approximation with a higher number of sub-intervals offers more coefficients $\mathbf{c}$ to maximize about. However, the small gain in sharpening the lower price bound was found to not outweigh the increase in computational cost. Applying the quadratic approximation throughout, we shift the integration contour using $\varepsilon_1 = -2.3$ and $\varepsilon_2 = 2$. As proposed by the authors, we compute the Caldana et al. formula using a dampening factor $\delta = 0.7$. Caldana et al. [Cal14] give a formula to compute a starting value for $\varkappa$. The starting value is used to initialize the maximization routine.[23] We found that the computed initial value can be quite far from the resulting optimal $\varkappa^*$ which maximizes the lower price bound. In consequence, the maximization routine must consider a wide range around the starting value, and the number of scales of $\varkappa$ must be chosen sufficiently high to obtain precise results. We choose a number of 500 scales throughout. The situation for our proposed method using curve fitting and moment matching is substantially different. The coefficients

21 We mention that M is not restricted to be a power of two.

22 Though, for extremely low strike levels K, the piecewise linear approximation must be used instead. This follows because if K approaches zero (i.e. the exercise boundary becomes a straight line), the leading order coefficient c_2 of the 2nd-order polynomial approaches zero. This conflicts with the restriction on c_2 in equation (4.18).

23 The formula to compute initial values of $\varkappa$ is developed for the GBM model. However, it can also be applied in other setups.

$\widetilde{\mathbf{c}} = (\widetilde{c}_0, \widetilde{c}_1, \widetilde{c}_2)'$ (i.e. the coefficients which are used to compute LBMM directly), are found to be excellent starting values for the maximization routine in equation (4.35). Further, we find that maximization over all three coefficients is actually not necessary (at least in our examples). Instead, we only maximize the lower bound with respect to the level coefficient c_0 of the approximate boundary. We search for LBMM* using just a small number of scales of c_0 in a narrow region around $\widetilde{c}_0$. Precisely, we use just 31 equally-spaced scales in a region $\widetilde{c}_0(1 \pm 0.05)$.[24]

Finally, we would like to mention that supplementary tables and QQ-plots regarding the accuracy of the proposed moment matching procedure according to the different models and dimensions n are omitted to save space. Rather, we directly focus on the relative performance of the resulting pricing formulas. The most important findings on the moment matching performance are, however, discussed within the text.

4.8.2 Relative pricing accuracy

Tables 4.1 – 4.4 compare the relative accuracy of the proposed lower price bounds LBMM and LBMM* to the lower price bound of Caldana et al. [Cal14]. The underlying pricing model is the multivariate geometric Brownian motion model. Further, the relative performance is compared to four analytical pricing approximations proposed and studied by Deelstra et al. [Dee10].[25] The following box summarizes the short labels.

24 Using an odd number of scales and a symmetric region around $\widetilde{c}_0$ ensures that LBMM$^* \geq$ LBMM.

25 The authors actually compare the performance of even 8 methods designed to price basket spread options. The preselected 4 competitors presented in Tables 4.1 – 4.4 are already the best performing approximations.

LBMM*	=	Proposed lower price bound based on moment matching, Fourier transform inversion, and numerical maximization, cf. eq. (4.35)
LBMM	=	Proposed lower price bound based on moment matching and Fourier transform inversion, cf. eq. (4.32)
Caldana	=	Caldana et al. [Cal14] lower price bound based on Fourier transform inversion and numerical maximization, cf. Lemma 1
Deel1	=	Deelstra et al. [Dee10] improved comonotonic upper bound (ICUB)
Deel2	=	Deelstra et al. [Dee10] shifted log-normal approximation (SLN)
Deel3	=	Deelstra et al. [Dee10] hybrid moment matching with Li et al. [Li08] spread option approximation (HybMMLi)
Deel4	=	Deelstra et al. [Dee10] hybrid moment matching with improved comonotonic upper bound (HybMMICUB)

The hybrid price approximations labeled as Deel3 and Deel4 are based on splitting the basket spread into two sub-baskets. Moment matching is applied to each sub-basket, and the price approximation finally follows by using an appropriate 2-asset spread option pricing formula. Splitting the basket to obtain more homogeneous sub-baskets is analog to our approach. Against, the methods labeled by Deel1 and Deel2 do not separate the basket, which relates them to the Caldana-method.

Strike	MC	LBMM*	LBMM	Caldana	Deel1	Deel2	Deel3	Deel4
15	19.6849	19.6835	19.6831	17.2435	19.9819	19.6925	19.5251	19.5231
20	16.7051	16.7043	16.7032	13.4984	17.0143	16.7345	16.5693	16.5673
25	14.1010	14.1007	14.0991	10.1956	14.4105	14.1460	13.9964	13.9944
30	11.8519	11.8518	11.8501	7.4024	12.1523	11.9059	11.7811	11.7790
35	9.9281	9.9280	9.9263	5.1493	10.2123	9.9851	9.8898	9.8876
40	8.2951	8.2949	8.2935	3.4228	8.5588	8.3506	8.2860	8.2837
45	6.9174	6.9170	6.9159	2.1697	7.1581	6.9683	6.9330	6.9305

Table 4.1: Basket spread call option prices in the geometric Brownian motion model detailed in Section 4.7.1. The basket dimension is $n = 3$. Parameters are chosen according to a positively skewed basket distribution. The (relative) accuracy of our proposed lower price bounds LBMM* and LBMM is compared to the accuracy of 5 (semi-)analytical approximation methods. Benchmark prices are obtained by Monte Carlo simulations (MC) with 300 millions of trials. Standard errors of the MC-prices are all of order 10^{-5}. Except the results for LBMM*, LBMM and 'Caldana', the prices are taken from Deelstra et al. [Dee10], Table 4. According to their setup, basket weights and parameters are set to $\mathbf{w} = (1, -1, -1)'$, $T = 1$, $r = 0.05$, $\mathbf{q} = \mathbf{0}$, $\mathbf{S}_0 = (100,24,46)'$, $\boldsymbol{\sigma} = (0.4,0.22,0.3)'$, $\rho_{12} = 0.17, \rho_{13} = 0.91$ and $\rho_{23} = 0.41$.

Table 4.1 contains basket spread option prices for different strike levels K. The basket dimension $n = 3$ is low. Basket weights, parameters and strike levels are identical to those of Table 4 in Deelstra et al. [Dee10]. Benchmark prices are obtained through a large scale Monte Carlo simulation. We observe that our proposed methods LBMM* and LBMM outperform all competing approaches. Both lower price bounds are very sharp. The relative price differences (or pricing errors) subject to the MC-benchmark prices are displayed in Table 4.2. With regard to our methods, the maximum pricing error is -0.02%. We also observe that the gain from numerically maximizing over the lower price bound is quite small. Though, we observe an improvement for LBMM* over LBMM for all strike levels. With regard to the lower price bound of Caldana et al., pricing differences are substantially higher. For a lower (higher) strike level $K = 15$ ($K = 45$), the relative price difference is -12.4% (-68.63%). Notice that their approach treats the basket spread as a whole. As explained above, the analytical approximations labeled Deel1 and Deel2 also proceed this way, but their performance is distinctly better. Our numerical experiments revealed that the method of Caldana et al. suffers mostly from the heterogeneity of the covariance matrix. Against, our method splits the basket into two more homogeneous sub-baskets. Then, the moment matching procedure (precisely the version detailed in 3.a, Section 4.5, i.e. the numerical optimization for low-dimensional baskets) accounts for the means as well as the covariances of the sub-baskets. In this particular example, the original vector of basket weights $\mathbf{w} = (1, -1, -1)'$ results in moment matched weights $\widetilde{\mathbf{w}}^+ = (1,0,0)'$ and $\widetilde{\mathbf{w}}^-(0,0.3267,0.6684)'$ for the positive and the negative sub-baskets, respectively.

Strike	LBMM*	LBMM	Caldana	Deel1	Deel2	Deel3	Deel4
15	-0.0001	-0.0001	-0.1240	0.0151	0.0004	-0.0081	-0.0082
20	-0.0000	-0.0001	-0.1920	0.0185	0.0018	-0.0081	-0.0082
25	-0.0000	-0.0001	-0.2770	0.0219	0.0032	-0.0074	-0.0076
30	-0.0000	-0.0002	-0.3754	0.0253	0.0046	-0.0060	-0.0062
35	-0.0000	-0.0002	-0.4813	0.0286	0.0057	-0.0039	-0.0041
40	-0.0000	-0.0002	-0.5874	0.0318	0.0067	-0.0011	-0.0014
45	-0.0001	-0.0002	-0.6863	0.0348	0.0074	0.0023	0.0019

Table 4.2: Relative price differences according to Table 4.1. The benchmark prices are the prices obtained by Monte Carlo simulations.

The parameters in Table 4.1 are chosen such that the distribution of the basket is positively skewed. Against, Table 4.3 refers to a negative skewness. As discussed in the section on moment matching, we expect that the performance of our method is somewhat impaired by negative skewness. Though, through splitting the basket into sub-baskets which each

exhibit positive skewness, the effect is assumed to be moderate.

Strike	MC	LBMM*	LBMM	Caldana	Deel1	Deel2	Deel3	Deel4
2.5	23.5925	23.5533	23.5531	23.3605	24.6617	23.1681	23.5137	23.5138
10	17.2049	17.1648	17.1638	16.7954	18.5944	16.8591	17.1363	17.1373
17.5	11.4099	11.3721	11.3695	10.7091	13.0945	11.3394	11.3854	11.3873
25	6.6009	6.5639	6.5612	5.5017	8.4135	6.9203	6.6579	6.6584
32.5	3.1872	3.1465	3.1458	1.7965	4.8064	3.7629	3.3226	3.3147
40	1.2518	1.2140	1.2126	0.1622	2.3929	1.7925	1.3950	1.3853
47.5	0.4026	0.3789	0.3726	0.0000	1.0323	0.7369	0.4861	0.4913

Table 4.3: Basic setup as in Table 4.1, but parameters are chosen according to a negatively skewed arithmetic basket distribution. The setup is the same as in Deelstra et al. [Dee10], Table 7. Monte Carlo simulation is applied with 15 millions of trials. Standard errors are of order 10^{-4} for all strike levels K. The basket weights and parameters are $\mathbf{w} = (1, -1, -1)'$, $T = 1$, $r = 0.05$, $\mathbf{q} = \mathbf{0}$, $\mathbf{S}_0 = (100,63,12)'$, $\boldsymbol{\sigma} = (0.21,0.34,0.63)'$, $\rho_{12} = 0.87, \rho_{13} = 0.3$ and $\rho_{23} = 0.43$.

The results in Table 4.3 basically confirm our conjectures. Our pricing bounds LBMM* and LBMM are less accurate than in the positive skewness case, Table 4.1. However, the performance is still good. With one exception, our lower bounds again outperform all other methods. The exeption is not really an exeption, though. This can be best seen from the relative price differences in Table 4.4.

Strike	LBMM*	LBMM	Caldana	Deel1	Deel2	Deel3	Deel4
2.5	-0.0017	-0.0017	-0.0098	0.0453	-0.0180	-0.0033	-0.0033
10	-0.0023	-0.0024	-0.0238	0.0808	-0.0201	-0.0040	-0.0039
17.5	-0.0033	-0.0035	-0.0614	0.1476	-0.0062	-0.0021	-0.0020
25	-0.0056	-0.0060	-0.1665	0.2746	0.0484	0.0086	0.0087
32.5	-0.0128	-0.0130	-0.4363	0.5080	0.1806	0.0425	0.0400
40	-0.0302	-0.0313	-0.8704	0.9116	0.4319	0.1144	0.1066
47.5	-0.0588	-0.0745	-1.0000	1.5641	0.8304	0.2074	0.2203

Table 4.4: Relative price differences according to Table 4.3. Benchmark prices are the prices obtained by Monte Carlo simulations.

At the strike level $K = 17.5$ only, the hybrid methods Deel3 and Deel4 exhibit little smaller price differences. However, all methods Deel2, Deel3 and Deel4 are neither lower nor upper price bounds.[26] This is revealed by inspection, noting the change of sign of

26 The original naming *hybrid moment matching with improved comonotonic upper bound (HybMMICUB)* for Deel4 is thus a bit misleading. Only Deel1 (ICUB) is a valid upper price bound.

the price differences across strike levels. For lower (higher) strike levels, these methods underprice (overprice) the option. Given this, there will be a certain strike for which each method is actually exact. Tables 4.3 and 4.4 also reveal the importance of splitting the basket spread. The subset of methods allowing for a split, (LBMM*,LBMM,Deel3 & Deel4), perform better than the other methods, especially at higher strike levels. According to the method of Caldana et al., we even observe a zero-option price for the strike level $K = 47.5$. Precisely, the maximization routine does not yield a positive price, and the maximum operator comes into play. Similarly, the upper price bound labeled Deel1 yields a price which is more than twice the true price. Regarding to the GBM model and a low dimension n, we conclude that our proposed method is very accurate for a wide range of strikes.

Next, we turn our attention to the jump diffusion model detailed in Section 4.7.2. We also focus on higher dimensions n. The methods proposed by Deelstra et al. [Dee10] are specific to the GBM model and do not apply here. Similar to the exposition in Caldana et al. [Cal14], we further study the gain of using our lower price bound as a control variate for Monte Carlo simulations. We report results for *crude* Monte Carlo simulations (MC^{cr}), as well as for Monte Carlo using our lower bound LBMM as the control variate (MC).[27] To this end, we define

$$\begin{aligned} \text{MC} &= \text{LBMM} + e^{-rT}\tilde{\mathbb{E}}\left[(A(T)-K)^+ \;-\; (A(T)-K)I(\mathcal{G}^{quad})\right] \\ \text{MC}^{cr} &= e^{-rT}\tilde{\mathbb{E}}\left[(A(T)-K)^+\right], \end{aligned} \tag{4.39}$$

where $\tilde{\mathbb{E}}$ denotes the usual Monte Carlo-expectation operator (under measure Q), i.e. the arithmetic mean over paths. Surely, the gain from using the control variate is the higher, the sharper the lower bound price bound is. If it is exact, then the expectation above will be zero. Even though LBMM cannot be exact for $n > 2$, at least $(A(T)-K)^+$ and $(A(T)-K)I(\mathcal{G}^{quad})$ are highly correlated, reducing the Monte Carlo standard error.

Table 4.5 presents basket spread call option prices according to a basket dimension $n = 20$. Parameters are chosen according to a moderate risky market phase. As in the GBM case, LBMM* and LBMM yield accurate prices for a wide range of strikes. Relative price differences in Table 4.6 reveal that the lower bounds understate the true prices within a range of 0.33% to 5.37%. We observe that the gain stemming from numerical maximization increases with increasing strike levels. For low strikes the gain is almost zero, but for

27 Of course, LBMM* can serve as a control variate in almost the same manner.

Strike	MC	SE	MC^{cr}	SE^{cr}	LBMM*	LBMM	Caldana
50	60.2339	0.0021	60.2793	0.0666	60.0368	60.0319	59.7381
100	29.0777	0.0021	29.1122	0.0541	28.8586	28.8579	28.7861
150	12.5802	0.0022	12.5758	0.0407	12.3951	12.3919	12.1067
200	5.6567	0.0021	5.6370	0.0306	5.5245	5.5129	5.0554
250	2.8441	0.0020	2.8218	0.0236	2.7551	2.7410	2.2830
300	1.5794	0.0018	1.5605	0.0188	1.5207	1.5073	1.1168
350	0.9418	0.0015	0.9231	0.0154	0.9029	0.8912	0.5781

Table 4.5: Basket spread call option prices in the jump diffusion model detailed in Section 4.7.2. The basket dimension is $n = 20$. Basket weights and parameters are as in CALDANA et al. [Cal14], Table 8. Denoting $\mathbf{1}_k$ a $k \times 1$ vector of ones, we set $\mathbf{w} = (\mathbf{1}'_{10}, -0.9 \times \mathbf{1}'_{10})'$, $T = 1$, $r = 0.01$, $\mathbf{q} = \mathbf{0}_{20}$, $\mathbf{S}_0 = 100 \times \mathbf{1}_{20}$, $\boldsymbol{\sigma} = 0.2 \times \mathbf{1}_{20}$, $\boldsymbol{\xi}^m = 0.25 \times \mathbf{1}_{20}$, $\boldsymbol{\xi}^{id} = 0.15 \times \mathbf{1}_{20}$, $\boldsymbol{\alpha}^m = \boldsymbol{\alpha}^{id} = -0.05 \times \mathbf{1}_{20}$, $\lambda^m = 1$, $\boldsymbol{\lambda}^{id} = 0.1 \times \mathbf{1}_{20}$, $\rho_{kj} = 0.75$, $\rho^m_{kj} = 0.75$, for $k \neq j$, $k,j = 1,...,20$. Column MC^{cr} denotes crude Monte Carlo simulation with 1 million trials. MC refers to Monte Carlo simulations using LBMM as a control variate. Standard errors are labeled as SE^{cr} and SE, respectively.

$K = 350$ the relative price difference is 124 bp lower for LBMM* than for LBMM. Though, both bounds clearly outperform the bound proposed by Caldana et al. Again, we observe that difference in accuracy inclines with the strike level. For $K = 350$, we find the Caldana et al. pricing error more than 9 times higher than the error of LBMM*.

Strike	LBMM*	LBMM	Caldana
50	-0.0033	-0.0034	-0.0082
100	-0.0075	-0.0076	-0.0100
150	-0.0147	-0.0150	-0.0376
200	-0.0234	-0.0254	-0.1063
250	-0.0313	-0.0362	-0.1973
300	-0.0372	-0.0457	-0.2929
350	-0.0413	-0.0537	-0.3862

Table 4.6: Relative price differences according to Table 4.5. Benchmark prices are the prices in column MC.

Regarding to the decline of Monte Carlo standard errors using LBMM as a control variate, we observe quite striking improvements. At a low strike of $K = 50$, where LBMM is a very sharp lower bound, the standard error of the crude Monte Carlo price SE^{cr} is more than 30 times higher than the standard error SE. For the high strike level $K = 350$, SE^{cr} is still reduced by a factor of 10.

Strike	MC	SE	MC^{cr}	SE^{cr}	LBMM*	LBMM	Caldana
50	115.3433	0.0339	115.5576	0.1763	106.8247	106.5216	106.5834
100	90.5178	0.0339	90.6965	0.1614	81.9893	81.9148	81.1719
150	70.4499	0.0341	70.5392	0.1461	62.2185	62.2038	60.0366
200	54.3363	0.0343	54.4203	0.1312	46.7159	46.4369	42.9213
250	41.6282	0.0348	41.7152	0.1171	34.7505	33.9657	29.4819
300	31.6911	0.0353	31.8155	0.1040	25.6525	24.3031	19.3063
350	24.1052	0.0362	24.1970	0.0921	18.8275	17.0139	11.9328

Table 4.7: Basket spread option prices in the jump diffusion model detailed in Section 4.7.2. Basically, the setup is the same as in Table 4.5. But asset weights and parameters cause a distinctly more heterogeneous basket distribution. Also, (sub-)baskets are heavily skewed and leptokurtic. Denoting $\mathbf{1}_k$ a $k \times 1$ vector of ones, we set $\mathbf{w} = (\mathbf{1}'_{10},\ -0.5 \times \mathbf{1}'_2,\ -\mathbf{1}'_8)'$, $T = 1$, $r = 0.01$, $\mathbf{q} = \mathbf{0}_{20}$, $\mathbf{S}_0 = 100 \times \mathbf{1}_{20}$, $\boldsymbol{\sigma} = 0.4 \times \mathbf{1}_{20}$, $\boldsymbol{\xi}^m = 0.5 \times \mathbf{1}_{20}$, $\boldsymbol{\xi}^{id} = 0.3 \times \mathbf{1}_{20}$, $\boldsymbol{\alpha}^m = \boldsymbol{\alpha}^{id} = -0.5 \times \mathbf{1}_{20}$, $\lambda^m = 1$, $\boldsymbol{\lambda}^{id} = 0.5 \times \mathbf{1}_{20}$, $\rho_{kj} = 0.5$, $\rho^m_{kj} = 0.5$, for $k \neq j$, k,j = 1,...,20.

Strike	LBMM*	LBMM	Caldana
50	-0.0739	-0.0765	-0.0759
100	-0.0942	-0.0950	-0.1032
150	-0.1168	-0.1170	-0.1478
200	-0.1402	-0.1454	-0.2101
250	-0.1652	-0.1841	-0.2918
300	-0.1905	-0.2331	-0.3908
350	-0.2189	-0.2942	-0.5050

Table 4.8: Relative price differences according to Table 4.7. Benchmark prices are the prices in column MC.

The setup of Table 4.7 corresponds to a very turbulent market phase. The diffusive volatility is higher than the one assumed in Table 4.5. But most importantly, the jump parameters are changed. The parameter set implies substantial downside risk. For this particular model and parameter setup, the contour plot in Figure 4.1 depicts (an approximation of) the bivariate density of the log-arithmetic sub-baskets. The pricing results in Table 4.7 show that our method suffers from the intensification. Relative price differences in Table 4.8 are severely higher than those in Table 4.6. In the turbulent setting, we now observe that the difference between the maximized lower bound LBMM* and the non-maximized lower bound LBMM is more pronounced. But as before, the difference depends on the strike level. Additional numerical experiments revealed that the loss of precision of our methods stems from less accurate moment matching. In step 2. of the moment matching procedure we posed the assumption that the joint distribution of the arithmetic sub-baskets can be

reasonably approximated by two correlated log-normal random variables. This assumption allows to directly compute the moments of $\log A^i$ from the moments of A^i. Applying simulations, we found that the obtained parameters $\mu_{\log A^i}$, $\sigma_{\log A^i}$ and $\rho^{ij}_{\log A}$ are not close enough to the true moments of the log-arithmetic sub-baskets. We conclude that for model setups with far from log-normal asset price dynamics, a more advanced moment matching approach is advisable. This is left for further research. Though, using the lower price bound as a control variate still improves the accuracy of Monte Carlo simulations considerably. For the low (high) strike level $K = 50$ ($K = 350$), the standard error is reduced by a factor of 5 (2.5).

n	MC^{cr}	MC	LBMM*	LBMM	Caldana
2	0.770	0.848	0.112	0.033	0.004
4	1.290	1.420	0.134	0.054	0.006
6	1.823	2.009	0.155	0.078	0.007
8	2.428	2.667	0.181	0.099	0.008
10	2.939	3.235	0.203	0.123	0.010
20	5.555	6.123	0.313	0.237	0.024
40	10.877	11.968	0.534	0.455	0.065
50	13.380	14.752	0.648	0.565	0.084
60	16.161	17.796	0.765	0.684	0.107
80	21.458	23.624	0.980	0.907	0.195
100	26.829	29.466	1.197	1.110	0.272
200	54.030	59.325	2.284	2.202	0.999

Table 4.9: CPU time (in seconds) for different basket dimensions n. Parameters are as in Table 4.5. Basket weights are defined as $\mathbf{w} = (\mathbf{1}'_{n/2}, \ -0.9 \times \mathbf{1}'_{n/2})'$, and strike levels as $K = 10 \times n$. Monte Carlo simulations is applied with 1 million trials. Again, MC refers to Monte Carlo simulation using LBMM as a control variate. The difference in CPU time between MC and MC^{cr} consists of the time to compute LBMM plus the time for additional operations in equation (4.39). With regard to LBMM and LBMM*, the CPU time for boundary fitting (OLS regression) and closed-form moment matching is very small. In total, these operations take 5×10^{-4} seconds for $n = 2$, up to 1.4×10^{-3} seconds for $n = 200$.

Table 4.9 presents CPU times according to basket spread options in the jump diffusion model. The basket dimension is increased from $n = 2$ (i.e. a normal spread option) to a large number of $n = 200$ assets. The prices obtained within the timing experiment are presented in Table 4.10. We observe that the difference in CPU times between LBMM* and LBMM is rather small. Further, the difference due to numerical maximization is almost independent of the basket dimension. This becomes clear by noting that maximization according to eq. (4.35) just requires to re-compute the payoff (or boundary) transform

$\widehat{P}^x(\mathbf{u},\mathbf{c})$, $x \in \{quad,plin\}$, which does not depend on n. Against, the computationally intensive calculation of $\Psi(\mathbf{u})$ is not part of the maximization routine. Further, our proposed quadratic or piecewise linear approximations of the true boundary do not require (more or less costly) calculations of special functions (like the complex gamma function). Before, we observed that the relative improvement of LBMM* over LBMM depends on the option's moneyness. As revealed by the pricing results in Table 4.10, it also depends on the basket dimension. The decision of whether to apply maximization or not should take these findings into account.

n	MC^{cr}	SE^{cr}	MC	SE	LBMM*	LBMM	Caldana
2	4.6260	0.0000	4.6279	0.0127	4.6256	4.6252	4.5514
4	5.2823	0.0010	5.3130	0.0169	5.2385	5.2374	5.0874
6	5.5265	0.0010	5.5438	0.0196	5.4590	5.4570	5.2377
8	5.6320	0.0012	5.6153	0.0218	5.5448	5.5419	5.2637
10	5.6736	0.0015	5.6553	0.0235	5.5737	5.5698	5.2432
20	5.6554	0.0023	5.6632	0.0312	5.5245	5.5129	5.0554
40	5.6164	0.0028	5.6420	0.0406	5.4762	5.4546	4.9595
50	5.6558	0.0031	5.6261	0.0441	5.5090	5.4821	5.0043
60	5.7148	0.0035	5.6557	0.0479	5.5650	5.5331	5.0793
80	5.8704	0.0040	5.8594	0.0570	5.7199	5.6795	5.2790
100	6.0622	0.0045	6.0606	0.0607	5.9084	5.8614	5.5124
200	7.2234	0.0075	7.2616	0.0908	7.0283	6.9642	0.0296

Table 4.10: Pricing results for different basket dimensions n. The setup is the one described in Table 4.9. Accordingly, CPU times to compute the prices can be found in Table 4.9. Notice that the price 0.0296 in column Caldana at dimension $n = 200$ is not a typo. We back-tested it in different ways. It seems to be a structural problem of the pricing formula in high dimensions, not an implementation issue.

For the particular model used within the timing experiments we observe an almost exact linear increase of the CPU times for LBMM* and LBMM. This is due to an efficient implementation of the collection of joint characteristic functions detailed in Remark 3. Against, we implemented the formula of Caldana et al. according to its original version, cf. Lemma 1. The Caldana et al. formula comes with a single integral. Therefore, it is surely more efficient to compute than our formulas. But, using the standard implementation as proposed by the authors, we observe a near-to quadratic increase of CPU times at higher dimensions. We conclude that methods applying bivariate Fourier transform inversion can also be very efficient, even in high dimensions. Accordingly, the timing difference between MC and MC^{cr} is found to be small. To obtain the same level of accuracy applying crude Monte Carlo, the number of trials must be drastically increased. Regarding to the CPU

times of Monte Carlo simulations it is worthwhile to notice that in the jump diffusion model studied here, no time discretization (like an Euler scheme) is required. In models like stochastic volatility models, where time discretization is necessary, the relative efficiency of integral transform methods is even more pronounced, especially for long maturities.

4.9 Conclusion

In this chapter we introduced a new valuation method for basket options. The method can be applied to pricing and hedging problems in general semimartingale models, comprising general diffusions, affine models, or (time-changed) Levy models. As opposed to the method of Caldana et al. [Cal14], we propose a hybrid approach which combines regressions, moment matching and Fourier transform inversion. To improve the quality of moment matching, we split the basket into two more homogeneous sub-baskets. A second improvement stems from accounting for the convexity of the exercise boundary between sub-baskets. Numerical experiments revealed that our refinements significantly sharpen the lower price bound of Caldana et al. The difference in accuracy is found to be the more pronounced, the more curved the boundary of the exercise set is. The curvature of the boundary is intimately related to the strike level. The improvement stemming from moment matching comes at almost no additional computational effort. Accounting for non-linearity raises the dimension of the inverse Fourier transform from one to two. However, the computational complexity remains quadratic in the number of assets. Efficiently implemented using a measure correction, it is even reduced to a linear increase in the computational time. This is the same order of complexity as it is known for Monte Carlo simulations, which is often regarded as the only method applicable to general pricing models in general dimensions. Besides interpreting it as a stand-alone pricing method, we also examine the use of the lower price bound as a control variate to increase the efficiency of Monte Carlo simulations. In our experiments the control variate technique reduced the Monte Carlo standard error by a factor of typically about 10.

In the influencing paper of Caldana et al. [Cal14], the authors also present an upper price bound for the basket option. Though, their results imply that the upper bound can be quite inaccurate. Improving on the upper price bound by applying a hybrid method is left for future research. Finally, we mention that our proposed method is not restricted to basket options. Though not presented here to save space, we also examined the pricing of compound options under stochastic volatility. In this example, the option value is non-linearly related to the log-asset price and the assets' local volatility. Adapting our

approach, the piecewise linear approximation of the exercise set leads to a very accurate and efficient pricing formula. In a recent survey, Chiarella et al. [Chi13] study efficient methods to price compound options under stochastic volatility. Experiments revealed that our approach outperforms all methods presented in this paper. Extending the work of Deelstra et al. [Dee10] to general semimartingale models, we also plan to adapt our method to pricing and hedging problems in the context of Asian and Asian basket spread options.

CHAPTER 5

Summary and Outlook

The present thesis consists of three chapters. The chapters contribute to the literature on pricing, hedging and optimal investments in stochastic environments exposed to volatility and jump risk. A main aspect of the thesis is regarded to the interplay of market volatility and the risk premium. If there is a stable interplay between these quantities, short-term volatility projections can be used to optimize investment strategies. Under the assumption of diffusive asset price dynamics, stable volatility strategies are indeed optimal strategies if the risk premium is proportional to the square root of the local variance. In the context of portfolio insurance, stable volatility proportional portfolio insurance (PPI) are optimal for an investor with hyperbolic absolute risk aversion (HARA). The multiple is inversely proportional to the local volatility. For the special case of an investor without subsistence level, i.e an investor with constant relative risk aversion (CRRA), the optimal strategy is also a stable volatility strategy. Here, the portfolio weight of the risky asset is inversely proportional to its local volatility. Using S&P 500 index return data we conduct an empirical performance evaluation. We find that stable volatility strategies outperform strategies with a constant multiple as well as strategies with a multiple inversely proportional to the local variance. The out-performance is robust with respect to alternative performance measures and levels of risk aversion. We apply quasi maximum likelihood to estimate parameters of a Markov regime switching EGARCH-in-Mean model. Due to numerical feasibility, the model is restricted to account for two regimes. According to the interplay between volatility and risk premium, our results indicate that the risk premium consists of a constant part and a part which is proportional to the square root of the variance.

In the presence of model risk, the question of robustness of investment strategies is highly relevant. Presuming that mother nature plays against the investor, the thesis studies robust strategies in market environments exposed to volatility and jump risk. We first find that the investor can or even should ignore the hedging demand. While utility losses from investing myopically are small if the true model is known, ignoring the hedging demand may even be beneficial under model risk. According to a given set of models and risk premium specifications, stable volatility strategies are indeed the robust strategies. However, this hold only true if the strategy accounts for a constant jump intensity. Against, all strategies which neglect jump risk perform prohibitively bad.

Stochastic volatility and jumps are also very important in the field of option pricing. The thesis contributes to the option pricing literature by introducing a pricing and hedging method for high-dimensional basket options. The method can be applied to pricing and hedging problems in general semimartingale models, comprising general diffusions, affine models, or time-changed Levy models. We propose a hybrid approach which combines regressions, moment matching and Fourier transform inversion. The resulting lower bound is found to be very precise for a wide range of strike levels. Benchmarking the accuracy of our method with five competing (semi-)analytical pricing approaches in a geometric Brownian motion framework, it yields the closest approximation. Our method also performs well in a jump diffusion framework.

With regard to the empirical performance of stable volatility and related strategies it is interesting to study more general underlying assets. The present thesis deals with an equity market index as a surrogate for the underlying asset. The index is treated as a single asset. A performance evaluation and robustness check of stable volatility strategies based on assets of fixed income, foreign exchange, commodity or energy markets is left for further research. Combining ideas of Chapters 2 and 4, we also plan to study stable volatility strategies based on baskets or basket spreads comprising several assets. Our work on the robustness of stable volatility strategies can be further improved by taking a more advanced criterion for robustness into account. It is also interesting to study stable volatility strategies in the presence of ambiguity aversion.

Future research on basket option pricing and hedging is first and foremost dedicated to a sharp upper price bound. A precise upper bound is important to complement the lower

price bound introduced in this thesis. The size of the spread between lower and upper bound directly enables to assess the quality of the approximation. Using an approximating exercise set which is optimized by moment matching, we plan to generalize the upper price bounds proposed by Rogers et al. [Rog95b] and Nielsen et al. [Nie02] to a semimartingale framework. Numerical experiments with respect to the jump diffusion model revealed that the proposed moment matching procedure can be inaccurate if the model is parametrized according to a very turbulent market phase. Within the procedure we posed a certain distributional assumption. Studying other distributional assumptions to refine the procedure is left for further research. Finally, our hybrid approach is not restricted to basket options. We also plan to generalize the work of Deelstra et al. [Dee10] on pricing and hedging of Asian and related options to a broader class of models.

Bibliography

[Alo11] Alos, E., A. Eydeland, and P. Laurence: 'A Kirks and a Bacheliers formula for three asset spread options'. *Energy risk* (2011), vol. 9(2011): pp. 52–57 (cit. on p. 70).

[Ann09] Annaert, J., S. Van Osselaer, and B. Verstraete: 'Performance evaluation of portfolio insurance strategies using stochastic dominance criteria'. *Journal of Banking & Finance* (2009), vol. 33: pp. 272–280 (cit. on p. 8).

[Asc13] Ascheberg, M., N. Branger, and H. Kraft: *When Do Jumps Matter for Portfolio Optimization?* Tech. rep. *Available at SSRN 2257689*, 2013 (cit. on p. 52).

[Bae10] Baele, L., G. Bekaert, and K. Inghelbrecht: 'The determinants of stock and bond return comovements'. *Review of Financial Studies* (2010), vol. 23(6): pp. 2374–2428 (cit. on p. 39).

[Bak97] Bakshi, G., C. Cao, and Z. Chen: 'Empirical performance of alternative option pricing models'. *Journal of Finance* (1997), vol. 52(5): pp. 2003–2049 (cit. on pp. 40, 47).

[Bal09] Balder, S., M. Brandl, and A. Mahayni: 'Effectiveness of CPPI Strategies under Discrete–Time Trading'. *Journal of Economic Dynamics and Control* (2009), vol. 33: pp. 204–220 (cit. on pp. 8, 16–18).

[Bal12] Balder, S., R. Feldman, and A. Mahayni: *Optimizing Proportional Portfolio Insurance Strategies – From Theory to Practice*. Tech. rep. Mercator School of Management, University of Duisburg–Essen, 2012 (cit. on pp. 8, 36).

[Bar00] Barberis, N.: 'Investing for the long run when returns are predictable'. *Journal of Finance* (2000), vol. 55: pp. 225–264 (cit. on pp. 9, 42).

[Bar15] Barroso, P. and P. Santa-Clara: 'Momentum has its moments'. *Journal of Financial Economics* (2015), vol. 116: pp. 111–120 (cit. on pp. 39, 40, 42, 46).

[Bas02] Basak, S.: 'A Comparative Study of Portfolio Insurance'. *Journal of Economic Dynamics and Control* (2002), vol. 26(7-8): pp. 1217–1241 (cit. on pp. 5, 9, 12).

[Bat00] Bates, D.S.: 'Post-'87 crash fears in the S&P 500 futures option market'. *Journal of Econometrics* (2000), vol. 94(1-2): pp. 181–238 (cit. on pp. 40, 47).

[Beb09] Beber, A., M.W. Brandt, and K.A. Kavajecz: 'Flight-to-quality or flight-to-liquidity? Evidence from the Euro-area bond market'. *Review of Financial Studies* (2009), vol. 22(3): pp. 925–957 (cit. on p. 39).

[BA11] Ben Ameur, H. and J-L. Prigent: 'CPPI Method with a Conditional Floor'. *International Journal of Business* (2011), vol. 16: pp. 218–229 (cit. on p. 8).

[BA13] Ben Ameur, H. and J-L. Prigent: 'Optimal portfolio positioning under ambiguity'. *Economic Modelling* (2013), vol. 34: pp. 89–97 (cit. on p. 43).

[BA14] Ben Ameur, H. and J-L. Prigent: 'Portfolio insurance: Gap risk under conditional multiples'. *European Journal of Operational Research* (2014), vol. 236(1): pp. 238–253 (cit. on p. 42).

[BT13] Ben-Tal, A., D. Den Hertog, A. De Waegenaere, B. Melenberg, and G. Rennen: 'Robust solutions of optimization problems affected by uncertain probabilities'. *Management Science* (2013), vol. 59(2): pp. 341–357 (cit. on p. 43).

[Ber11] Bertrand, P. and J-L. Prigent: 'Omega performance measure and portfolio insurance'. *Journal of Banking & Finance* (2011), vol. 35: pp. 1811–1823 (cit. on pp. 8, 18).

[Ber03] Bertrand, P. and J-L. Prigent: 'Portfolio Insurance Strategies: A Comparison of Standard Methods when the Volatility of the Stock is Stochastic'. *International Journal of Business* (2003), vol. 8(4): pp. 15–31.

[Ber02a] Bertrand, P. and J-L. Prigent: *Portfolio Insurance Strategies: OBPI versus CPPI*. Tech. rep. GREQAM and Université Montpellier1, 2002 (cit. on p. 8).

[Ber02b] Bertrand, P. and J-L. Prigent: 'Portfolio insurance: The extreme value to the CPPI method'. *Finance* (2002), vol. 23: pp. 69–86.

[Bin07] Binsbergen, J.H. van and M.W. Brandt: 'Solving dynamic portfolio choice problems by recursing on optimized portfolio weights or on the value function?' *Computational Economics* (2007), vol. 29(3-4): pp. 355–367 (cit. on p. 141).

[Bla87] Black, F. and R. Jones: 'Simplifying Portfolio Insurance'. *Journal of Portfolio Management* (1987), vol. 14: pp. 48–51 (cit. on p. 6).

[Bla92] Black, F. and A.R. Perold: 'Theory of Constant Proportion Portfolio Insurance'. *Journal of Economic Dynamics and Control* (1992), vol. 16(3-4): pp. 403–426 (cit. on pp. 8, 17).

[Bol11] Bollerslev, T. and V. Todorov: 'Tails, fears, and risk premia'. *Journal of Finance* (2011), vol. 66(6): pp. 2165–2211 (cit. on p. 39).

[Boo00] Bookstaber, R. and J.A. Langsam: 'Portfolio Insurance Trading Rules'. *Journal of Futures Markets* (2000), vol. 8: pp. 15–31 (cit. on p. 8).

[Bor07] Borovkova S.and Permana, F.J. and H. van der Weide: 'A closed form approach to the valuation and hedging of basket and spread option'. *Journal of Derivatives* (2007), vol. 14(4): pp. 8–24 (cit. on pp. 71, 84, 93).

[Bou95] Boulier, J.F. and A. Kanniganti: 'Expected performance and risks of various portfolio insurance strategies'. *5th AFIR International Colloquium.* 1995: pp. 1093–1124 (cit. on p. 8).

[Bra05] Brandt, M.W., A. Goyal, P. Santa-Clara, and J.R. Stroud: 'A simulation approach to dynamic portfolio choice with an application to learning about return predictability'. *Review of Financial Studies* (2005), vol. 18(3): pp. 831–873 (cit. on p. 141).

[Bra08] Branger, N., C. Schlag, and E. Schneider: 'Optimal portfolios when volatility can jump'. *Journal of Banking & Finance* (2008), vol. 32: pp. 1087–1097 (cit. on pp. 9, 42).

[Bra15] Branger, N., A. Mahayni, and D. Zieling: 'Robustness of stable volatility strategies'. *Journal of Economic Dynamics and Control* (2015), vol. 60: pp. 134–151 (cit. on p. 2).

[Bre76] Brennan, M.J. and E.S. Schwartz: 'The Pricing of Equity–Linked Life Insurance Policies with an Asset Value Guarantee'. *Journal of Financial Economics* (1976), vol. 3: pp. 195–213.

[Bri04] Brigo, D., F. Mercurio, F. Rapisarda, and R. Scotti: 'Approximated moment-matching dynamics for basket-options pricing'. *Quantitative Finance* (2004), vol. 4(1): pp. 1–16 (cit. on pp. 71, 72, 75, 84).

[Bur10] Buraschi, A., P. Porchia, and F. Trojani: 'Correlation risk and optimal portfolio choice'. *Journal of Finance* (2010), vol. 65(1): pp. 393–420 (cit. on p. 43).

[Cag02] Cagetti, M., L.P. Hansen, T. Sargent, and N. Williams: 'Robustness and pricing with uncertain growth'. *Review of Financial Studies* (2002), vol. 15(2): pp. 363–404 (cit. on p. 43).

[Cal14] Caldana, R., G. Fusai, A. Gnoatto, and M. Grasselli: *General closed-form basket option pricing bounds*. Tech. rep. *Available at SSRN 2376134*, 2014 (cit. on pp. 3, 69–73, 75–78, 97, 101, 102, 104, 105, 108–110, 113, 114, 118).

[Cam92] Campbell, J.Y. and L. Hentschel: 'No news is good news: An asymmetric model of changing volatility in stock returns'. *Journal of Financial Economics* (1992), vol. 31(3): pp. 281–318 (cit. on p. 39).

[Cam02] Campbell, J.Y. and L.M. Viceira: *Strategic Asset Allocation – Portfolio Choice for Long-Term Investors*. Oxford University Press, 2002 (cit. on pp. 13, 45).

[Car03] Carmona, R. and V. Durrleman: 'Pricing and hedging spread options'. *Siam Review* (2003), vol. 45(4): pp. 627–685 (cit. on pp. 70, 75).

[Car99] Carr, P. and D. Madan: 'Option valuation using the fast Fourier transform'. *Journal of computational finance* (1999), vol. 2(4): pp. 61–73 (cit. on p. 78).

[Ces03] Cesari, R. and D. Cremonini: 'Benchmarking, portfolio insurance and technical analysis: a Monte Carlo comparison of dynamic strategies of asset allocation'. *Journal of Economic Dynamics and Control* (2003), vol. 27: pp. 987–1011 (cit. on p. 8).

[Cha05] Chacko, G. and L.M. Viceira: 'Dynamic consumption and portfolio choice with stochastic volatility in incomplete markets'. *Review of Financial Studies* (2005), vol. 18(4): pp. 1369–1402 (cit. on p. 46).

[Che02] Chen, Z. and L.G. Epstein: 'Ambiguity, risk, and asset returns in continuous time'. *Econometrica* (2002), vol. 70(4): pp. 1403–1443 (cit. on p. 43).

[Chi11] Chiappori, P.-A. and M. Paiella: 'Relative risk aversion is constant: Evidence from panel data'. *Journal of the European Economic Association* (2011), vol. 9(6): pp. 1021–1052 (cit. on p. 10).

[Chi13] Chiarella, C., S. Griebsch, and B. Kang: *Investigating Time-Efficient Methods to Price Compound Options in the Heston Model*. Tech. rep. *Available at SSRN 2224387*, 2013 (cit. on p. 119).

[Chi09] Chiarella, C., B. Kang, G.H. Meyer, and A. Ziogas: 'The evaluation of American option prices under stochastic volatility and jump-diffusion dynamics using the method of lines'. *International Journal of Theoretical and Applied Finance* (2009), vol. 12(03): pp. 393–425 (cit. on p. 140).

[Con05] Connolly, R., C. Stivers, and L. Sun: 'Stock market uncertainty and the stock-bond return relation'. *Journal of Financial and Quantitative Analysis* (2005), vol. 40(01): pp. 161–194 (cit. on p. 39).

[Con09] Cont, R. and P. Tankov: 'Constant proportion portfolio insurance in the presence of jumps in asset prices'. *Mathematical Finance* (2009), vol. 19: pp. 379–401 (cit. on p. 8).

[Cur94] Curran, M.: 'Valuing Asian and portfolio options by conditioning on the geometric mean price'. *Management science* (1994), vol. 40(12): pp. 1705–1711 (cit. on p. 69).

[Dee10] Deelstra, G., A. Petkovic, and M. Vanmaele: 'Pricing and hedging Asian basket spread options'. *Journal of computational and applied mathematics* (2010), vol. 233(11): pp. 2814–2830 (cit. on pp. 71, 72, 93, 101, 109–113, 119, 123).

[DeM09] DeMiguel, V. and F.J. Nogales: 'Portfolio selection with robust estimation'. *Operations Research* (2009), vol. 57(3): pp. 560–577 (cit. on p. 40).

[Dic10] Dichtl, H. and W. Drobetz: 'Portfolio insurance and prospect theory investors: Popularity and optimal design of capital protected financial products'. *Journal of Banking & Finance* (2010), vol. 35: pp. 1683–1697 (cit. on p. 8).

[Die10] Dierkes, M., C. Erner, and S. Zeisberger: 'Investment horizon and the attractiveness of investment strategies: A behavioral approach'. *Journal of Banking and Finance* (2010), vol. 34(5): pp. 1032–1046 (cit. on p. 8).

[Dir14] Diris, B.F., F.C. Palm, and P.C. Schotman: 'Long-Term Strategic Asset Allocation: An Out-of-Sample Evaluation'. *forthcoming Management Science* (2014), vol. (cit. on pp. 14, 41).

[Do04] Do, B.H. and R.W. Faff: 'Do futures-based strategies enhance dynamic portfolio insurance?' *Journal of Futures Markets* (2004), vol. 24: pp. 591–608 (cit. on p. 8).

[Duf00] Duffie, D., J. Pan, and K. Singleton: 'Transform analysis and asset pricing for affine jump-diffusions'. *Econometrica* (2000), vol. 68(6): pp. 1343–1376 (cit. on p. 47).

[Ebe10] Eberlein, E., K. Glau, and A. Papapantoleon: 'Analysis of Fourier transform valuation formulas and applications'. *Applied Mathematical Finance* (2010), vol. 17(3): pp. 211–240 (cit. on pp. 82, 98, 101).

[Ebe09] Eberlein, E., A. Papapantoleon, A.N. Shiryaev, et al.: 'Esscher transform and the duality principle for multidimensional semimartingales'. *The Annals of Applied Probability* (2009), vol. 19(5): pp. 1944–1971 (cit. on p. 74).

[Elk14] Elkamhi, R. and D. Stefanova: 'Dynamic Hedging and Extreme Asset Co-movements'. *forthcoming Review of Financial Studies* (2014), vol. (cit. on p. 42).

[Eng87] Engle, R.F., D.M. Lilien, and R.P. Robins: 'Estimating time varying risk premia in the term structure: the ARCH-M model'. *Econometrica: Journal of the Econometric Society* (1987), vol. 55: pp. 391–407 (cit. on p. 25).

[Eps03] Epstein, L.G. and J. Miao: 'A two-person dynamic equilibrium under ambiguity'. *Journal of Economic Dynamics and Control* (2003), vol. 27(7): pp. 1253–1288 (cit. on p. 43).

[Era03] Eraker, B., M. Johannes, and N. Polson: 'The impact of jumps in volatility and returns'. *Journal of Finance* (2003), vol. 58(3): pp. 1269–1300 (cit. on pp. 40, 47, 53, 54).

[Fab10] Fabozzi, F.J., D. Huang, and G. Zhou: 'Robust portfolios: contributions from operations research and finance'. *Annals of Operations Research* (2010), vol. 176(1): pp. 191–220 (cit. on p. 43).

[Fel12] Feldhütter, P., L.S. Larsen, C. Munk, and A.B. Trolle: *Keep it simple: Dynamic bond portfolios under parameter uncertainty.* Tech. rep. *Available at SSRN 2018844*, 2012 (cit. on p. 41).

[Fra01] Framstad, N.C., B. Øksendal, and A. Sulem: 'Optimal consumption and portfolio in a jump diffusion market with proportional transaction costs'. *Journal of Mathematical Economics* (2001), vol. 35(2): pp. 233–257 (cit. on p. 42).

[Gab14] Gabrel, V., C. Murat, and A. Thiele: 'Recent advances in robust optimization: An overview'. *European Journal of Operational Research* (2014), vol. 235(3): pp. 471–483 (cit. on p. 43).

[Gar07] Garlappi, L., R. Uppal, and T. Wang: 'Portfolio selection with parameter and model uncertainty: A multi-prior approach'. *Review of Financial Studies* (2007), vol. 20(1): pp. 41–81 (cit. on p. 45).

[Gen93] Gentle, D.: 'Basket weaving'. *Risk* (1993), vol. 6(6): pp. 51–52 (cit. on p. 75).

[Gil89] Gilboa, I. and D. Schmeidler: 'Maxmin expected utility with non-unique prior'. *Journal of Mathematical Economics* (1989), vol. 18(2): pp. 141–153 (cit. on pp. 43, 45).

[Gol03] Goldfarb, D. and G. Iyengar: 'Robust portfolio selection problems'. *Mathematics of Operations Research* (2003), vol. 28(1): pp. 1–38 (cit. on p. 43).

[Gra96] Gray, S.F.: 'Modeling the conditional distribution of interest rates as a regime-switching process'. *Journal of Financial Economics* (1996), vol. 42(1): pp. 27–62 (cit. on p. 24).

[Gro93] Grossman, S.J. and Z. Zhou: 'Optimal investment strategies for controlling drawdowns'. *Mathematical Finance* (1993), vol. 3: pp. 241–276 (cit. on p. 9).

[Gro89] Grossman, S.J. and J. Villa: 'Portfolio Insurance in Complete Markets: A Note'. *Journal of Business* (1989), vol. 62: pp. 473–476 (cit. on p. 5).

[Hai12] Hainaut, D. and R. MacGilchrist: 'Strategic asset allocation with switching dependence'. *Annals of Finance* (2012), vol. 8(1): pp. 75–96 (cit. on p. 28).

[Ham09a] Hamidi, B., E. Jurczenko, and B. Maillet: 'A CAViaR Modelling for a Simple Time-Varying Proportion Portfolio Insurance Strategy'. *Bankers, Markets & Investors* (2009), vol. (cit. on pp. 8, 9, 35).

[Ham14] Hamidi, B., B. Maillet, and J.-L. Prigent: 'A dynamic autoregressive expectile for time-invariant portfolio protection strategies'. *Journal of Economic Dynamics and Control* (2014), vol. 46: pp. 1–29 (cit. on pp. 17, 42).

[Ham09b] Hamidi, B., B. Maillet, and J.L. Prigent: *A Risk Management Approach for Portfolio Insurance Strategies*. Tech. rep. Université Panthéon-Sorbonne (Paris 1), Centre d'Economie de la Sorbonne, 2009 (cit. on p. 8).

[Han06] Hansen, L.-P., T.J. Sargent, G. Turmuhambetova, and N. Williams: 'Robust control and model misspecification'. *Journal of Economic Theory* (2006), vol. 128(1): pp. 45–90.

[Han01] Hansen, L.-P. and T.J. Sargent: 'Robust control and model uncertainty'. *American Economic Review* (2001), vol. 91(2): pp. 60–66.

[Han08] Hansen, L.-P. and T.J. Sargent: *Robustness*. Princeton University Press, 2008 (cit. on p. 43).

[Han10] Hansen, L.P. and T.J. Sargent: 'Fragile beliefs and the price of uncertainty'. *Quantitative Economics* (2010), vol. 1(1): pp. 129–162.

[Hen09] Henry, O.T.: 'Regime switching in the relationship between equity returns and short-term interest rates in the UK'. *Journal of Banking & Finance* (2009), vol. 33(2): pp. 405–414 (cit. on pp. 7, 24).

[Her05] Herold, U., R. Maurer, and N. Purschaker: 'Total Return Fixed-Income Portfolio Management'. *Journal of Portfolio Management* (2005), vol. 31: pp. 32–43 (cit. on p. 8).

[Hes93] Heston, S.L.: 'A closed-form solution for options with stochastic volatility with applications to bond and currency options'. *Review of Financial Studies* (1993), vol. 6(2): pp. 327–343 (cit. on p. 49).

[Ho11] Ho, L., J. Cadle, and M. Theobald: 'An analysis of risk-based asset allocation and portfolio insurance strategies'. *Review of Quantitative Finance and Accounting* (2011), vol. 36: pp. 247–267 (cit. on p. 8).

[Hua06] Huang, Z. and S.G. Kou: *First passage times and analytical solutions for options on two assets with jump risk*. Tech. rep. 2006 (cit. on pp. 102, 104).

[Hur10] Hurd, T.R. and Z. Zhou: 'A Fourier transform method for spread option pricing'. *SIAM Journal on Financial Mathematics* (2010), vol. 1(1): pp. 142–157 (cit. on pp. 71–73, 76, 79, 80, 83).

[Jac03] Jacod, J. and A.N. Shiryaev: *Limit theorems for stochastic processes.* Springer, 2003 (cit. on p. 74).

[Jes09] Jessen, C.: *Constant proportion portfolio insurance: Discrete-time trading and gap risk coverage.* Tech. rep. University of Copenhagen, 2009 (cit. on pp. 9, 35).

[Jia09] Jiang, C., Y. Ma, and Y. An: 'The effectiveness of the VaR-based portfolio insurance strategy: An empirical analysis'. *International Review of Financial Analysis* (2009), vol. 18: pp. 185–197 (cit. on pp. 8, 36).

[Jur11] Jurek, J.W. and L.M. Viceira: 'Optimal Value and Growth Tilts in Long-Horizon Portfolios'. *Review of Finance* (2011), vol. 15(1): pp. 29–74 (cit. on p. 41).

[Kar99] Karatzas, I. and S.E. Shreve: *Methods of Mathematical Finance.* Springer Verlag, 1999 (cit. on p. 14).

[Kaz04] Kazemi, H., T. Schneeweis, and B. Gupta: 'Omega as a performance measure'. *Journal of Performance Measurement* (2004), vol. 8: pp. 16–25 (cit. on p. 23).

[Kea02] Keating, C. and W.F. Shadwick: 'A universal performance measure'. *Journal of Performance Measurement* (2002), vol. 6: pp. 59–84 (cit. on p. 21).

[Khu09] Khuman, A. and N. Constantinou: *How does CPPI perform against the simplest guarantee strategies?* Tech. rep. Working Paper WP035-09, University of Essex, 2009 (cit. on pp. 9, 35).

[Kil06] Kilin, F.: *Accelerating the calibration of stochastic volatility models.* Tech. rep. Frankfurt School of Finance & Management, 2006 (cit. on p. 80).

[Kim96] Kim, T.S. and E. Omberg: 'Dynamic nonmyopic portfolio behavior'. *Review of Financial Studies* (1996), vol. 9: pp. 141–161 (cit. on pp. 9, 42).

[Kir95] Kirk, E.: 'Correlation in the energy markets'. *Managing energy price risk* (1995), vol. 1: pp. 71–78 (cit. on p. 76).

[Kla02] Klaassen, F.: 'Improving GARCH volatility forecasts with regime-switching GARCH'. *Empirical Economics* (2002), vol. 27(2): pp. 363–394 (cit. on pp. 24, 26).

[Kor13] Korn, R. and S. Zeytun: 'Efficient basket Monte Carlo option pricing via a simple analytical approximation'. *Journal of Computational and Applied Mathematics* (2013), vol. 243: pp. 48–59 (cit. on p. 75).

[Kot01] Kotz, Sa., T.J. Kozubowski, and K. Podgórski: 'Asymmetric Multivariate Laplace Distribution'. *The Laplace Distribution and Generalizations*. Springer, 2001: pp. 239–272 (cit. on p. 104).

[Kra05] Kraft, H.: 'Optimal portfolios and Heston's stochastic volatility model: an explicit solution for power utility'. *Quantitative Finance* (2005), vol. 5(3): pp. 303–313 (cit. on pp. 139, 141).

[Lar12] Larsen, L.S. and C. Munk: 'The costs of suboptimal dynamic asset allocation: General results and applications to interest rate risk, stock volatility risk, and growth/value tilts'. *Journal of Economic Dynamics and Control* (2012), vol. 36(2): pp. 266–293 (cit. on p. 41).

[Lel76] Leland, H.E. and M. Rubinstein: *The Evolution of Portfolio Insurance*. in: D.L. Luskin (Ed.), Portfolio Insurance: A guide to Dynamic Hedging, Wiley, 1976.

[Li08] Li, M., S.-J. Deng, and J. Zhou: 'Closed-Form Approximations for Spread Option Prices and Greeks.' *Journal of Derivatives* (2008), vol. 15(3): pp. 58 –80 (cit. on pp. 71, 76, 101, 110).

[Li10] Li, M., J. Zhou, and S.-J. Deng: 'Multi-asset spread option pricing and hedging'. *Quantitative Finance* (2010), vol. 10(3): pp. 305–324 (cit. on pp. 70, 76).

[Lin14] Linders, D. and W. Schoutens: *Basket option pricing and implied correlation in a Lévy copula model*. Tech. rep. *Available at SSRN 2468778*, 2014 (cit. on p. 75).

[Liu13] Liu, H. and M. Loewenstein: 'Market Crashes, Correlated Illiquidity, and Portfolio Choice'. *Management Science* (2013), vol. 59(3): pp. 715–732 (cit. on p. 42).

[Liu07] Liu, J.: 'Portfolio selection in stochastic environments'. *Review of Financial Studies* (2007), vol. 20(1): pp. 1–39 (cit. on pp. 42, 46, 53, 139, 141).

[Liu03a] Liu, J., F.A. Longstaff, and J. Pan: 'Dynamic asset allocation with event risk'. *Journal of Finance* (2003), vol. 58: pp. 231–259 (cit. on p. 9).

[Liu03b] Liu, J., F.A. Longstaff, and J. Pan: 'Dynamic asset allocation with event risk'. *Journal of Finance* (2003), vol. 58(1): pp. 231–259 (cit. on pp. 41, 42, 50, 51, 53, 139).

[Lor08] Lord, R., F. Fang, F. Bervoets, and C.W. Oosterlee: 'A fast and accurate FFT-based method for pricing early-exercise options under Lévy processes'. *SIAM Journal on Scientific Computing* (2008), vol. 30(4): pp. 1678–1705 (cit. on p. 80).

[Mac06] Maccheroni, F., M. Marinacci, and A. Rustichini: 'Ambiguity aversion, robustness, and the variational representation of preferences'. *Econometrica* (2006), vol. 74(6): pp. 1447–1498 (cit. on pp. 43, 45).

[Mae04] Maenhout, P.J.: 'Robust portfolio rules and asset pricing'. *Review of Financial Studies* (2004), vol. 17(4): pp. 951–983 (cit. on p. 43).

[Mar05] Marcucci, J.: 'Forecasting stock market volatility with regime-switching GARCH models'. *Studies in Nonlinear Dynamics & Econometrics* (2005), vol. 9(4) (cit. on p. 24).

[Mer73] Merton, R.C.: 'An Intertemporal Capital Asset Pricing Model'. *Econometrica* (1973), vol. 41: pp. 867–887 (cit. on pp. 13, 46).

[Mer71] Merton, R.C.: 'Optimal Consumption and Portfolio Rules in a Continuous Time Model'. *Journal of Economic Theory* (1971), vol. 3: pp. 373–413 (cit. on pp. 6, 9, 12, 42, 50).

[MKa07] MKaouar, F. and J-L. Prigent: *Portfolio Insurance with transaction costs: The case of the CPPI method.* Tech. rep. Technical report Université Montesquieu Bordeaux IV, 2007 (cit. on pp. 9, 35).

[Muc10] Muck, M.: 'Trading strategies with partial access to the derivatives market'. *Journal of Banking & Finance* (2010), vol. 34: pp. 1288–1298 (cit. on pp. 9, 42).

[Nel91] Nelson, D.B.: 'Conditional heteroskedasticity in asset returns: A new approach'. *Econometrica* (1991), vol. 59: pp. 347–370 (cit. on p. 25).

[Nie02] Nielsen, J.-A. and K. Sandmann: 'Pricing Bounds on Asian Options'. *Journal of Financial and Quantitative Analysis* (2002), vol. 38(2): pp. 449–473 (cit. on p. 123).

[Øks05] Øksendal, B. and A. Sulem: *Applied stochastic control of jump diffusions*. Vol. 498. Springer, 2005 (cit. on p. 42).

[Pal14] Paletta, T., A. Leccadito, and R. Tunaru: *Pricing and Hedging Basket Options with Exact Moment Matching*. Tech. rep. *Available at SSRN 2368316*, 2014 (cit. on p. 76).

[Pan02] Pan, J.: 'The jump-risk premia implicit in options: Evidence from an integrated time-series study'. *Journal of Financial Economics* (2002), vol. 63(1): pp. 3–50 (cit. on pp. 40, 47).

[Pau09] Paulot, L. and X. Lacroze: 'Efficient pricing of CPPI using Markov operators'. *Quantitative Finance Papers* (2009), vol. (cit. on pp. 9, 35).

[Ped02] Pedersen, C.S. and S.E. Satchell: 'On the foundation of performance measures under asymmetric returns'. *Quantitative Finance* (2002), vol. 2: pp. 217–223 (cit. on p. 23).

[Reh11] Reher, G. and B. Wilfling: 'Markov-switching GARCH models in finance: a unifying framework with an application to the German stock market'. *Center for Quantitative Economics (CQE), University of Muenster* (2011), vol. (cit. on pp. 24, 25).

[Rog13] Rogers, L.C.G.: *Optimal investment*. Springer, 2013 (cit. on p. 51).

[Rog95a] Rogers, L.C.G. and Z. Shi: 'The value of an Asian option'. *Journal of Applied Probability* (1995), vol.: pp. 1077–1088 (cit. on p. 69).

[Rog95b] Rogers, L.C.G. and Z. Shi: 'The Value of an Asian Option'. *Journal of Applied Probability* (1995), vol. 32: pp. 1077–1088 (cit. on p. 123).

[San05] Sangvinatsos, A. and J.A. Wachter: 'Does the Failure of the Expectations Hypothesis Matter for Long-Term Investors?' *Journal of Finance* (2005), vol. 60(1): pp. 179–230 (cit. on p. 41).

[Sch13] Schied, A.: *Model-free CPPI*. Tech. rep. arXiv preprint arXiv:1305.5915, 2013 (cit. on pp. 14, 15).

[Sch89] Schwert, W.G.: 'Why does stock market volatility change over time?' *Journal of Finance* (1989), vol. 44(5): pp. 1115–1153 (cit. on p. 39).

[Sha66] Sharpe, W.F.: 'Mutual fund performance'. *Journal of Business* (1966), vol. 39: pp. 119–138 (cit. on p. 21).

[Sor94] Sortino, F.A. and L.N. Price: 'Performance measurement in a downside risk framework'. *Journal of Investing* (1994), vol. 3: pp. 59–64 (cit. on p. 21).

[Str11] Strzalecki, T.: 'Axiomatic foundations of multiplier preferences'. *Econometrica* (2011), vol. 79(1): pp. 47–73 (cit. on pp. 43, 45).

[Upp03] Uppal, R. and T. Wang: 'Model misspecification and underdiversification'. *Journal of Finance* (2003), vol. 58(6): pp. 2465–2486 (cit. on p. 43).

[Vor92] Vorst, T.: 'Prices and hedge ratios of average exchange rate options'. *International Review of Financial Analysis* (1992), vol. 1(3): pp. 179–193 (cit. on p. 70).

[Wac13] Wachter, J.A.: 'Can Time-Varying Risk of Rare Disasters Explain Aggregate Stock Market Volatility?' *Journal of Finance* (2013), vol. 68(3): pp. 987–1035 (cit. on p. 39).

[Whi00] Whitelaw, R.F.: 'Stock market risk and return: An equilibrium approach'. *Review of Financial Studies* (2000), vol. 13(3): pp. 521–547 (cit. on p. 24).

[Zag11] Zagst, R. and J. Kraus: 'Stochastic dominance of portfolio insurance strategies'. *Annals of Operations Research* (2011), vol. 185: pp. 75–103 (cit. on p. 8).

[Zak09] Zakamouline, V. and S. Koekebakker: 'Portfolio performance evaluation with generalized Sharpe ratios: Beyond the mean and variance'. *Journal of Banking & Finance* (2009), vol. 33: pp. 1242–1254 (cit. on p. 21).

[Zho08] Zhou, J. and X. Wang: 'Accurate closed-form approximation for pricing Asian and basket options'. *Applied Stochastic Models in Business and Industry* (2008), vol. 24(4): pp. 343–358 (cit. on p. 93).

[Zie14] Zieling, D., A. Mahayni, and S. Balder: 'Performance evaluation of optimized portfolio insurance strategies'. *Journal of Banking & Finance* (2014), vol. 43: pp. 212–225 (cit. on pp. 2, 40, 42, 46, 55).

APPENDIX A

Appendix to Chapter 3: Implementation of model-dependent optimal strategies

In the following, we propose a numerical approach to solve the portfolio planning problem for a general specification of the risk premium $\mu_t - r = \mu_0 + \mu_v V_t + \mu_\sigma \sqrt{V_t}$ and the jump intensity $l_t = l_0 + l_v V_t + l_h h_t$. The resulting jump-diffusion model nests all models of the set $\mathcal{M}$ summarized in Table 3.1 as special cases. The first-order condition (FOC) (3.9) becomes

$$\mu_0 + \mu_v V_t + \mu_\sigma \sqrt{V_t} - \gamma \phi_t^* V_t + \frac{g_v}{g} \rho \sigma_v V_t + \left(M_t^{*,(1)} - m_t\right)\left(l_0 + l_v V_t + l_h h_t\right) = 0.$$

Notice that the myopic demand can easily be solved for by setting $g_v = 0$. In general, the optimal portfolio weight ϕ_t^* depends on time t (through $\frac{g_v}{g}$) and on the state variables V_t and h_t. For the special case of models RPV/LV and RPV/NJ, the dependence on the state variables vanishes, and ϕ_t^* depends on time t only. The guess $g(t,V) = e^{A(t)+B(t)V}$ replaces the 2-dimensional HJB-equation by two ordinary differential equations (ODEs) for A and B. These ODEs can be solved analytically for the model RPV/NJ (see Liu [Liu07] and [Kra05]) and quasi-analytically, using standard finite difference techniques, for the model RPV/LV (see Liu et al. [Liu03b]).[1]

In the general case, however, ϕ_t^* depends on the state variables V and/or h, and the HJB-equation must be solved numerically. Instead of discretizing the state space and solving the 3-dimensional HJB-equation directly, we adopt the basic idea of the so-called method of lines and replace the PDE by a system of differential equations which are treated

1 The sufficient condition for an optimal solution derived by [Kra05] is satisfied in our setup.

as ODEs.[2] We first conjecture an approximate solution for g of the form

$$g(t,V,h) \approx e^{A(t)+B(t)V+C(t)\sqrt{V}+H(t)h}.$$

For $\mu_\sigma = 0$ (risk premium specifications except RPσ), we set $C(t) = 0$, and for $l_h = 0$ (jump intensity specifications except Lh), we set $H(t) = 0$ for all $t \in [0,T]$. In a second step, we plug the guess for g into the HJB-equation (3.8). Defining

$$\tilde{M}_t^* := M_t^{*,(2)} - (1-\gamma)m_t\phi_t^* - 1,$$

we split the equation into four differential equations as follows

$$\begin{aligned}
0 &= A_t + B\kappa_v\theta_v + \frac{1}{8}\sigma_v^2 C^2 + H\kappa_h\theta_h + (1-\gamma)r + (1-\gamma)\phi_t^*\mu_0 + \tilde{M}_t^* l_0 \\
0 &= B_t + B\left[-\kappa_v + (1-\gamma)\phi_t^*\rho\sigma_v\right] + 0.5\sigma_v^2 B^2 - 0.5\gamma(1-\gamma)(\phi_t^*)^2 + (1-\gamma)\phi_t^*\mu_v + \tilde{M}_t^* l_v \\
0 &= C_t + 0.5C\left[-\kappa_v + (1-\gamma)\phi_t^*\rho_{vs}\sigma_v + \sigma_v^2 B - \frac{4\kappa_v\theta_v - \sigma_v^2}{4V_t}\right] + (1-\gamma)\phi_t^*\mu_\sigma \\
0 &= H_t - \kappa_h H + 0.5\sigma_h^2 H^2 + \tilde{M}_t^* l_h
\end{aligned}$$

with boundary conditions $A(T) = B(T) = C(T) = H(T) = 0$. Plugging the approximation for g into the FOC for the portfolio weight ϕ_t^* gives

$$\begin{aligned}
\mu_0 + \mu_v V_t + \mu_\sigma\sqrt{V_t} - \gamma\phi_t^* V_t + B(t)\rho\sigma_v V_t + 0.5C(t)\rho\sigma_v\sqrt{V_t} \\
+ \left(M_t^{*,(1)} - m_t\right)\left(l_0 + l_v V_t + l_h h_t\right) = 0.
\end{aligned} \tag{A.1}$$

Solving the above system gives A, B, C, H, and ϕ_t^* as functions of time t and of the state variables V and h. This dependence on the state variables has been ignored in the calculation of the partial derivatives of g w.r.t. V and h. Therefore, the resulting solution is an approximate one.

The numerical implementation starts at time T with the terminal conditions $B(T) = C(T) = 0$. We then solve for the optimal portfolio weights on a grid of space variables (V,h). Proceeding backward in time in small steps Δt, we solve for ϕ_t^*, $B(t)$, and $C(t)$ on each point of the discretized state space and store the results. Note that at time t, $B(t)$ and $C(t)$

2 An application of the method of lines for pricing American options under stochastic volatility and jumps is given in [Chi09].

depend on $B(t+\Delta t)$ and $C(t+\Delta t)$. Unless for the special cases with a state independent myopic demand, it is important to account for transitions of the state variables between successive points in time. In repeated numerical experiments, it turned out that the most efficient and stable way is to calculate $E[(V_{t+\Delta t},h_{t+\Delta t})|(V_t,h_t)]$ and then to determine the corresponding values of $B(t+\Delta t)$ and $C(t+\Delta t)$ by interpolation.

A numerical back-test was conducted along the lines of [Bin07] who propose a generic simulation-based method.[3] The method basically applies across-path regressions to approximate conditional expectations, which are then used to find optimal portfolio weights along each path. In our context, the myopic demand is given in (quasi-)closed form. Based on this observation, we refine the method and solve for the hedging demand, given the optimal myopic demand. The back-test results can be summarized as follows. Evaluating the CE growth rates on the same set of paths used to apply the regressions, the gains from including the hedging demand are positively biased. This can be verified, at least for the two models with (quasi-)closed form solutions.[4] This finding also holds for a large number of paths. When we repeat the simulation and use another set of paths with the fitted values of the regression, we obtain gains from including the hedging demand which are smaller than those using the proposed method for all 12 models. For some models, the gains are even negative. On the one hand, these observations highlight the difficulties of approximating hedging demands – even if the true model is known. On the other hand, we rely on the proposed ODE-approximation as a robust choice to obtain near-optimal portfolio weights.

3 The method of [Bin07] is a modification of the method given in [Bra05].

4 Liu [Liu07] states and [Kra05] shows that in the model RPσ/NJ the hedging demand is zero. This gives another indication to back-test the results. Our ODE-approximation yields almost exactly zero hedging demands for this model, with small distortions at very low levels of V.

APPENDIX B

Appendix to Chapter 4: Strictly positive baskets

Figure B.1: Exercise boundary of strictly positive baskets

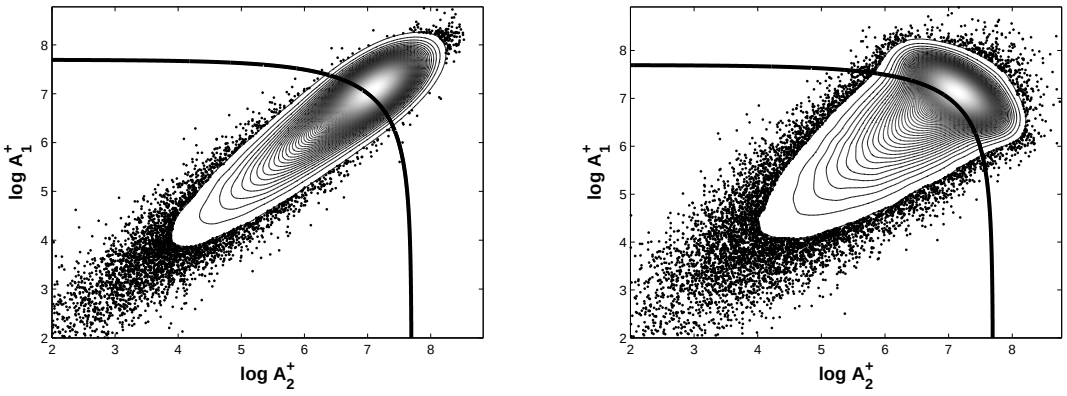

(a) Positive correlation of sub-baskets

(b) Negative correlation of the diffusive part

Setup of (a) as in Figure 4.1, but all assets have strictly positive weights. The basket is decomposed into two positive sub-baskets A_1^+ and A_2^+, each consisting of 10 assets. The strike level is $K = 2200$ ($\log K \approx 7.7$). The basket option payoff can be rewritten as $(A_1^+ + A_2^+ - K)^+ = (A_1^+ + A_2^+ - K) - (A_1^+ + A_2^+ - K)^-$. The presented concave boundary corresponds to the exercise set of the negative part (in logarithmic variables) $\mathcal{A} = \{\omega : \log A_2^+ < \log K, \log A_1^+ < \log(K - A_2^+)\}$. In (b) we changed the correlation matrix of the diffusive part of the joint dynamics. Assets in either sub-basket have positively correlated diffusive parts, while diffusive correlation is negative between A_1^+ and A_2^+. The joint distribution of jumps is left unchanged.